Design and Development of a web Roll-to-Roll testing system with lateral dynamics control of Displacement guide.

By

Sung-Yu Tsai

A thesis in partial fulfilment of the requirement for the degree of

Masters of Engineering

In

Mechatronics

Massey University

Palmerston North

New Zealand

2012

Abstract

Roll-to-Roll (R2R) systems have been widely used in the traditional paper printing and packaging industry. In addition, Roll-to-Roll systems are also considered as a cost effective mass production solution for printed electronics, such as RFID and Solar cells in the recent years [1]. In a Roll-to-Roll system, web material often experiences lateral motion during the transportation to processes [1]. This project presents the lateral dynamics control system integration using centered pivoted displacement guide for Roll-to-Roll application. An initial literature review of the project is carried out with supporting theory and web handling mechanism. The complete system design consists of four units, namely unwinder unit, load cell unit, guide unit and rewinder unit. In this project, two microcontrollers are proposed to control the four units with additional instrumentation and signal conditioning between sensors/actuators, and the controller. The Guide system dynamics are simulated using first order single degree-of-freedom oscillator model controlled with classical PID servo designs. Finally, the complete system is tested with different disturbances input to the system. The system lateral response is compared with and without the guide system. Results are shown to have reduced the lateral motion when media transport speeds are at 20m/min, 40m/min and 60m/min.

Acknowledgements

I would like to express my deepest appreciation to the following people and department for their support during the course of this research:

Firstly, I would like to thank Prof. Jen-Yuan (James) Chang for his full support and guidance throughout this research. It has been a wonderful experience being a member of Mechatronics and Vibrations Research Laboratory.

I would like to thank Prof. Subhas Mukhopadhyay for his support during this research, and made a visit to Taiwan.

I would like to acknowledge Prof Don Cleland for allowing me to do my research with Prof. Chang at National Tsing Hua University in Taiwan.

I thank all my colleagues from Mechatronics and Vibrations Research Laboratory for productive discussions and assistance during this research.

Finally, I would like to thank the Power Mechanical Department from National Tsing Hua University for having me during my entire research period.

Table of Contents

List of Figures

List of Tables

Chapter 1. Introduction

In this section, the Roll-to-Roll processing technology is introduced. In addition, the history and a demonstration of a conventional processing flowchart are also demonstrated. The printing technology in terms of flexible electronics is also addressed. The problem of the lateral motion is presented. Finally, the objectives of the project are introduced.

1.1. Roll-to-Roll Processing technology

Web Roll-to-Roll (R2R) processing has been widely used in many of the mass production manufacturing industries. These include the traditional printing and packing or electronics industries as shown in Figure 1-1. A typical Roll-to-Roll (R2R) system involves a continuous strip of flexible medium which is transported and processed; that is the flexible medium is transported through rollers which bring the web material to different processes. Although there are many different processes in those industries, Roll-to-Roll processing is still commonly used among them. The flexible medium which used in Roll-to-Roll systems is often called web. The web materials which are commonly used in applications include paper, metal and plastics.

Figure 1-1: Roll-to-Roll processing on newspaper industry [2]

In the recent years, R2R systems have been identified as a cost effective mass production method for flexible electronics printing [2]-[3]. According to market research firm iSuppli Corp [4], the flexible display market is expected to grow from 5 million in 2006 to 339 million in 2013, or 83.5 percent per year. Due to the continuous manufacturing of R2R system, R2R processing is expected to significantly increase the efficiency and productivity, as well as reduce the cost of processes. A typical manufacturing flexible electronics is demonstrated in Figure 1-2, where the raw material (web) coil is unwind and go through a series of processes. The processes involves are different in each case, due to the applications required on process. Figure 1-2 only illustrates a typical manufacturing process flow on R2R processing. After each process, the finished product is rewind back to the coil.

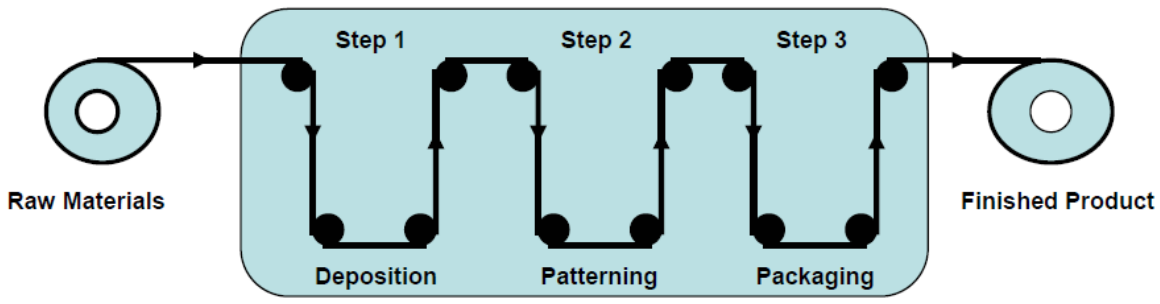

Figure 1-2: Roll-to-Roll manufacturing process flow [5]

1.2. Flexible electronics and Printing technology

1.2.1. Flexible electronics

Due to the possibility of current electronics manufacturing replacement on some of the electronics application, flexible electronics has become a very popular research area between many companies and researchers. Flexible electronics is used on manufacturing electronics circuit where the circuit is assembled on flexible substrates. As opposed to having electronics components being picked and placed onto printed circuit boards (PCB); electronics components are printed onto flexible substrates layer by layer of electronics materials. The commonly used substrate material is Poly (ethylene terephthalate)-foil (PET) due to the low cost and high temperature stability. As shown on Figure 1-3 [6], researchers from Aneeve Nanotechnology (UCLA) have developed back-gated and top-gated carbon nanotube–based electronics for use with OLED displays with R2R technology. Each layer of electronics, such as, Polymer dielectric and silver (Ag) is printed onto the plastic flexible substrate.

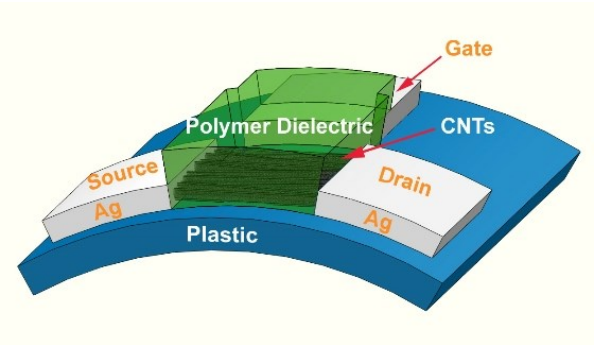

Figure 1-3: Roll-to-Roll printed electronics schematics [6]

There are many different flexible electronics application which is used on R2R technology. The R2R printed electronics include RFID, solar cells, Thin Film Transistors (TFT) and displays (LEDs and LCDs) [7] - [8]. Some of the applications are demonstrated in the following. An example of displays, Hewlett-Packard has developed the first affordable, flexible electronics displays at the Arizona State University as illustrated in Figure 1-4 [9]. In addition, thin film transistors are also able to be printed on the flexible plastic substrate as illustrated on Figure 1-5. Finally, Solar Solutions manufactured Flexible Solar cells to consumers are also shown on Figure 1-6.

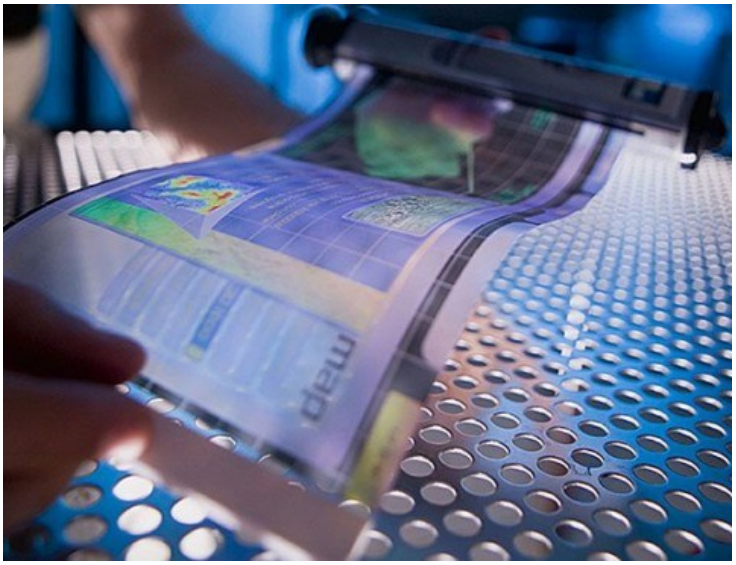

Figure 1-4: Flexible display [9]

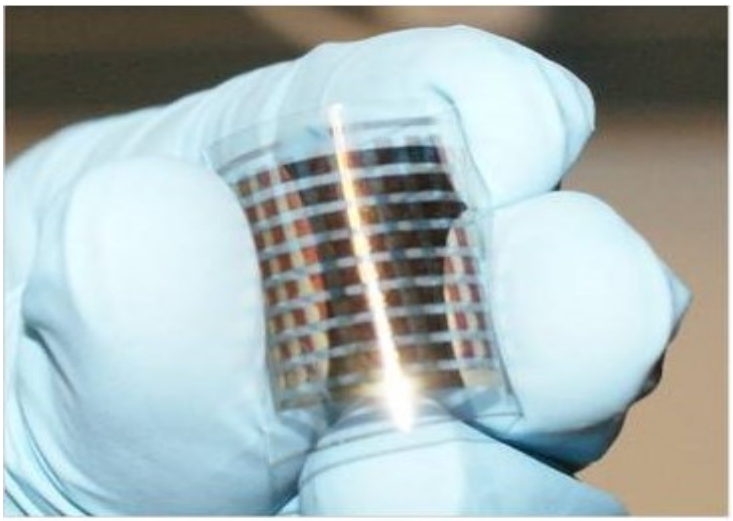

Figure 1-5: Roll-to-Roll printed TFT [10]

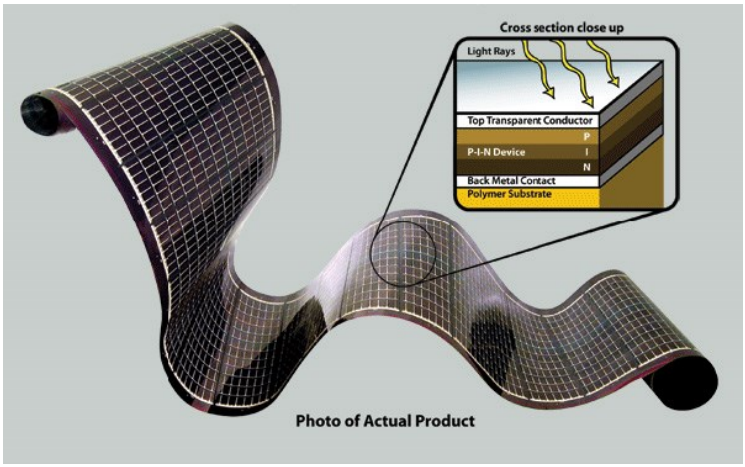

Figure 1-6: Roll-to-Roll printed solar cell [11]

1.2.2. Electronics printing technology

There are many printing technologies used in printed electronics. A general printing technologies block diagram is shown on Figure 1-7. Printing technologies mainly divided into two main categories, which are Sheet based and Roll-to-Roll based. Sheet based methods are generally used where the production volume is low but high precision work is required. Two examples of this method are inkjet and screen printing, where printing process is taken place on the scale of separate sheets at the time. On the other hand, Roll-to-Roll printing method requires continuous high volume production process as the web coil is unwind and series of printing processes

are applied. There are three commonly used printing methods for Roll-to-Roll processing, which are Gravure, offset and flexographic. The principle of Gravure printing method is demonstrated in Figure 1-8. This method generally consists of impressions cylinder, plate cylinder, ink and blade. The engraved plate cylinder is used to transfer the printed image to the paper [12]. The plate cylinder cells image are filled with ink, as the cylinder is rotated. The blade controls the amount of the ink which can be filled by wiping the excess ink from the cylinder surface. By doing this, the excess ink are removed which leaves the ink within the engraved cells. The plate cylinder then transfers the image to the substrate with the help of rubber impression cylinder.

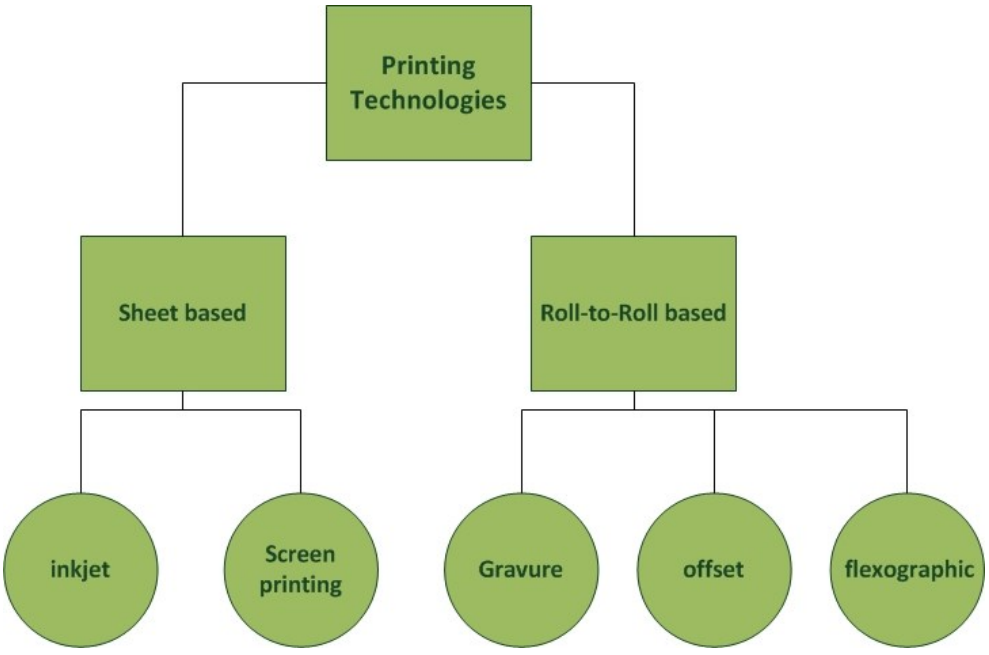

Figure 1-7: printing technology block diagram

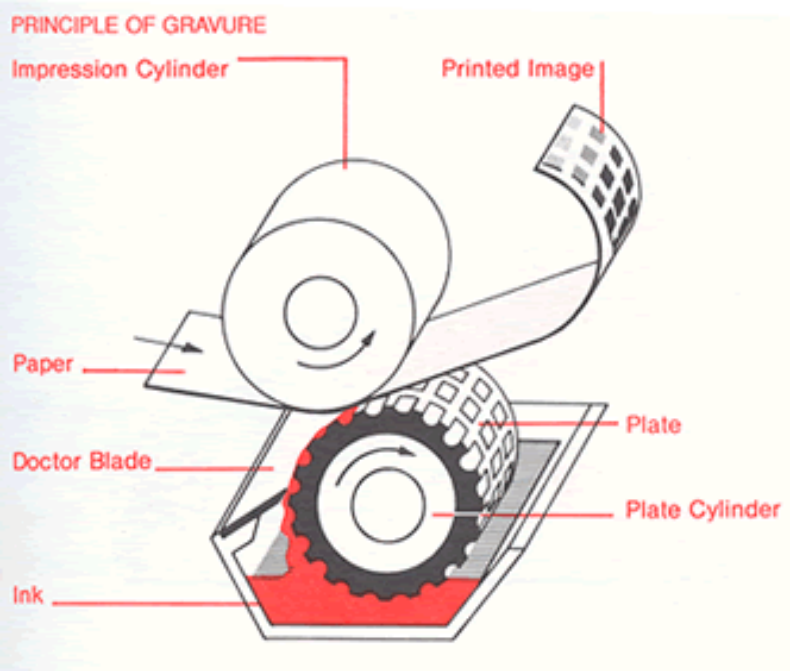

Figure 1-8: Principle of Gravure printing [12]

1.3. Lateral motion problem

As mentioned in the previous section (1.2), Roll-to-Roll processing is a continuous manufacturing process. This is due to the web travel through a series of rollers for processes until the final printed product is finished. In addition, each layers of ink or electronics solution is deposited onto the substrate. However, during the web transportation between rollers, the web also experiences motion perpendicular to the direction of feeding. This motion is often referred to as lateral motion. Lateral motion can affect the location where the electronics is printed. Due to this fact, the alignment of the printing between each layer can be affected. Hence lateral motion significantly affects the performance of the electronics or the image quality. The contrast between ideal web alignment and web experiences lateral motion can be seen in Figure 1-9. When the web is perfectly aligned, the material is perpendicular to the rotating axis. Whereas when the web experiences lateral motion, the web is moved away from the centre position which can affect the final printed product.

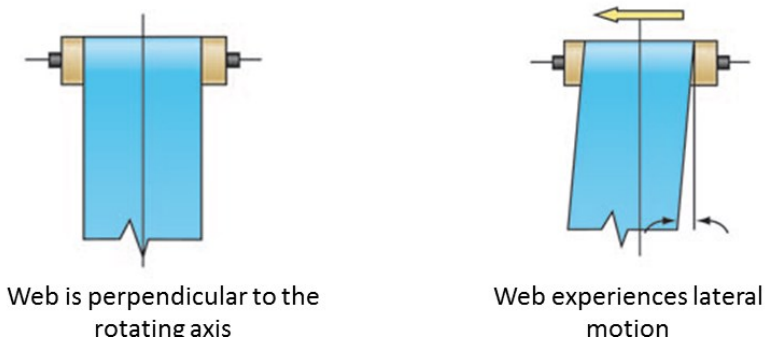

Figure 1-9: Web perpendicular to axis vs. lateral motion [13]

1.4. Objectives

The Objectives of this project is: To design and develop a web Roll-to-Roll testing system with lateral dynamics control of displacement guide.

These include:

- Design a mechatronics system for lateral dynamics control in order to minimize the lateral motion of the web.
- Integrate an Roll-to-Roll production testing system which have:
    - Winder unit
    - Load cell unit
    - Guide system unit
    - Rewinder unit

Chapter 2. Literature review

In this section, the initial literature review of important information is obtained in order to design and develop the system required in this project. It is divided into two main categories; basic web handling principles and web lateral motion control. Basic Web Handling Principles is especially helpful in terms of hardware system design as it is trivial for design consideration. Conversely, web lateral motion control is useful for controller design and simulation because web and actuator dynamics.

2.1. Basic Web Handling Principles

Web handling is often referred to the art and science of moving a web [14]. During transportation between processes, web may experience problems, such as, lateral motion, wrinkling, and breakage. Therefore, Precision web handling is required for smooth web operations. In this section, basic web handling principle is addressed with a typical R2R application. Precision web handling is used across many different industries, from the traditional printing industry to flexible electronics manufacturer and more. This project consist many different areas which will need to be researched in order to have a complete Web Handling mechatronics system. The areas include roller, unwind method, rewind method, lateral-guiding method, web tension control and traction. This section covers the areas where it is found to be the most useful to the design of our R2R testing system.

2.1.1. Rollers

Rollers are the main components used in a Roll-to-Roll system. They are used to handle web material transportation between processes. The shape of a roller can be

a standard cylindrical type or even camber to have different web behaviors. Rollers affect machine's performance and printing quality. Some of the factors which can be affected by rollers are: change the path, tension or even cause wrinkles.

The number of rollers which required is often subjective. One of the key factors on the number of roller required is to do with the unsupported span of material in between rollers [14]. The best web span is dependent on the width and thickness of the web. If the span is too long, the web will tend to sag, or vibrate which can affect the tension of the web. On the other hand, if the web is too short, the alignment of the web can be over sensitive due to the perpendicular entry rule (see details in Section 2.2).

2.1.2. Unwind and Rewind

The raw/unprinted web (printed electronics substrate) can be purchased in a coil form. In order to do Roll-to-Roll processing, the web coil is required to be unwind and threading through rollers. After all of the process, the web is usually rewind back to the coil form and keeps in inventory. However, if the web is required to be used right after the processing, cutting process is also allowed to be used. In this project, it is concentrated on identifying the web lateral motion control. Therefore, cutting process which the web is cut will be neglected.

There are three main winding types, such as, Centerwind, surface wind or turret wind. The Centerwind machine is shown on Figure 2-1. It unwinds and rewinds the web material onto a central shaft. It is done by controlling the speed of the center of the coil.

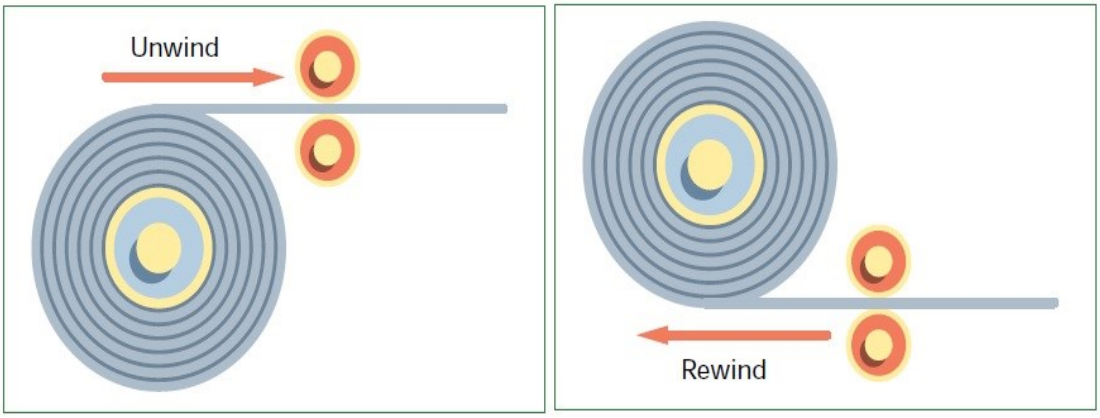

Figure 2-1: Centerwind with unwind and rewind [15]

Surface wind and turret wind is illustrated on Figure 2-2. Surface wind is similar to Centerwind which the material is winded onto a centre shaft (Core). However, the winding process is controlled by the Motor Driven Surface Winder Roll. On the other hand, the Turret wind consists of 2 Centerwinds which have a pivot in between as shown. When the Centerwind #1is finished, the Centerwind #2 is rotated about the pivot point and ready to start a new roll without stopping the process.

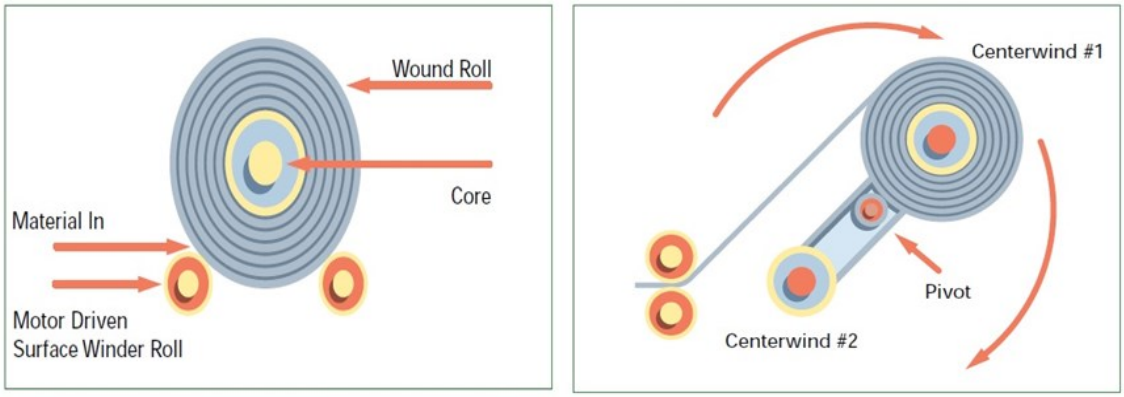

Figure 2-2: Surface wind (left) and turret wind (right) [15].

2.1.3. Web guides

As mentioned in the earlier section, lateral motion affects the performance of the electronics during printing process. The lateral motion can often be controlled using web guides. It is used to center and maintain the alignment of the web and rollers [14]. The lateral guides block diagram can be seen in Figure 2-3. There are two

main types of lateral guides, such as, passive guide and active guides. The passive guides control the lateral motion by mechanical isolation [16]. These include the use of edge and surface guide which constrain the lateral path of the web. Conversely, the active guides control the lateral motion by servo actuator system. This is achieved using displacement guide and steering guide which actively guide the web back to the centre line of the axis.

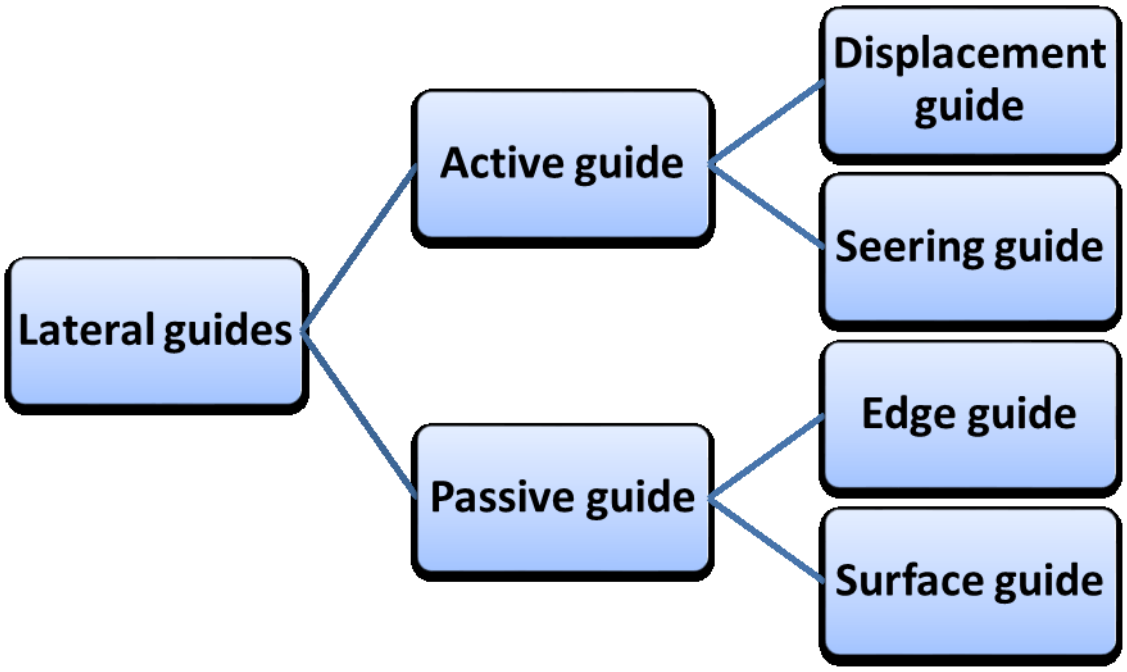

Figure 2-3: Lateral guides block diagram

2.1.3.1. Passive guide

Passive guide controls the lateral motion by restricting the path of lateral movement using either, edge guide or surface guide. In terms of edge guide, rigid or compliant flanges are used to apply force to the edge of the web which can constrain the lateral motion [16]. However, the edge of the web can be damaged and introduce Lateral motion due to flange-edge contacts. On the other hand, Surface friction guides can apply distributed lateral forces on wider web surface [16]. These include grooved, roughened rollers and none-rotating cylindrical rollers. The advantages of

using surface guiding are the elimination of possibility of edge damage and also reduce high frequency lateral motion. The disadvantages of surface winder are that the method is highly depended on contact pressure, and the friction between the web and surface guide. In this project, the passive edge guide is only proposed to be used to minimize the initial lateral movement produced by unwind and rewind operation.

2.1.3.2. Active guide

Active guide uses actuator to change the position of the web in order to reduce lateral motion. The lateral motion information is transferred to the controller by sensors which feedback the lateral position. Sensors can vary from mechanical switches to photo eyes, such as, ultrasonic sensors and infrared sensors. The web lateral motion can be adjusted by changing the axis of rotation of the web guide.

There are two main kinds of web guides category, which are steering guide and displacement guide, respectively. A steering guide is used in areas where distance between processes is long. Whereas, Displacement guide is used in areas where distance between processes is short. The main actuation methods used in the two web guides are pneumatics. A typical steering guide is illustrated in Figure 2-4. Steering guide consists of three web spans; that are Entry Span, Exit Span and Guide Span. It is used in situation where the position of a long span is required to be controlled. The Guide Span can range from 5 to 50 web widths long depending on the lateral stiffness of the web [13].The majority of the steering guides have only one actuated roller. In contrast, a typical displacement guide is shown in Figure 2-5. A displacement guide is often place closely before the printing process or even upstream of winder to reduce the lateral motion. Similarly to steering guide, the displacement guide cover 3 web spans; Entry Span, Guide Span and Exit Span. It is

common to have Entry Span, Guide Span and Exit Span all larger than one web width [13].

Although the two main categories have been researched, there are still continuously improved design methods in order to reduce the lateral motion between rolls. The more detail guides are addressed in section 2.2

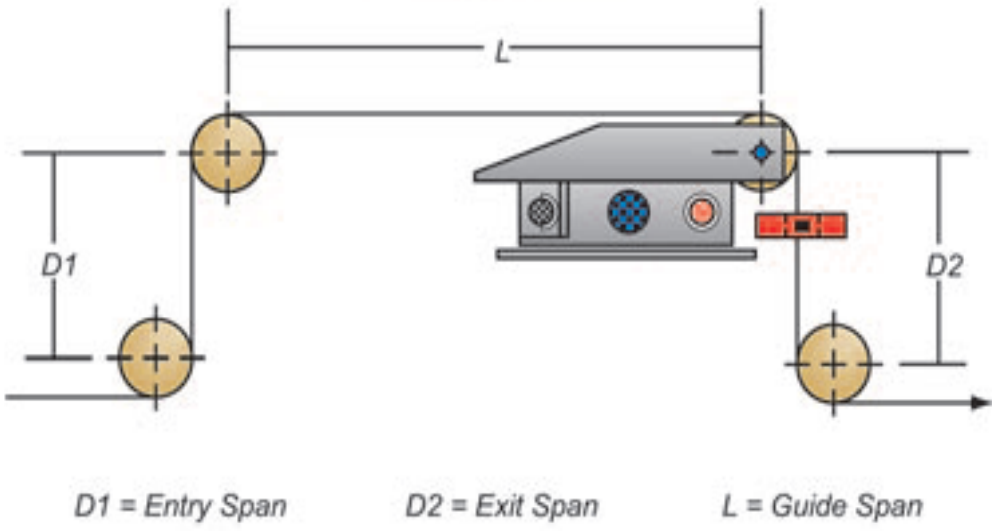

Figure 2-4: Steering guide [13]

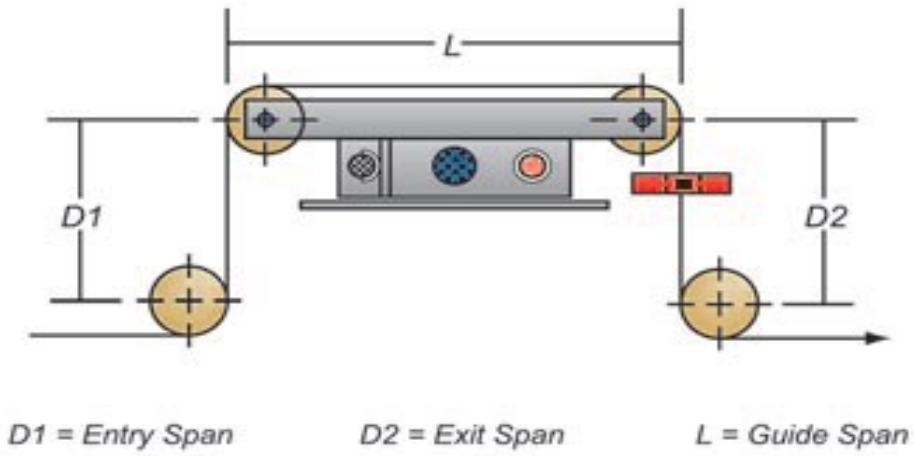

Figure 2-5: Displacement guide [13]

2.1.4. Web Tension

Web tension is often considered as the longitudinal force being exerted on a process material, or may be defined as the average machine direction web force expressed in force per unit web width [14]. The objective of web handling is to

transport the web material with tension below the elastic limit which will not cause damage to the web [11]. In Figure 2-6, a typical stress/strain curve is illustrated with its elastic limit. The tension is required to be set well below the elastic limit which the web extension will return to its normal zero extension state or length. As mentioned by Ponjanda-Madappa [11] and Rothwell [17], it is recommended to set the web tension at level of 10 to 30 percent of the web's ultimate tensile which will have factors of 10 to 1 and 2.5 to 1.

In web handling systems, tension is usually required to be kept constant. This is kept constant in order to minimize web breakage and wrinkling; maintain web path and registration; achieve good print quality [18]. However, web tension can be affected by many different factors, such as, roller eccentricity, substrate quality, and roller drag due to friction on bearing.

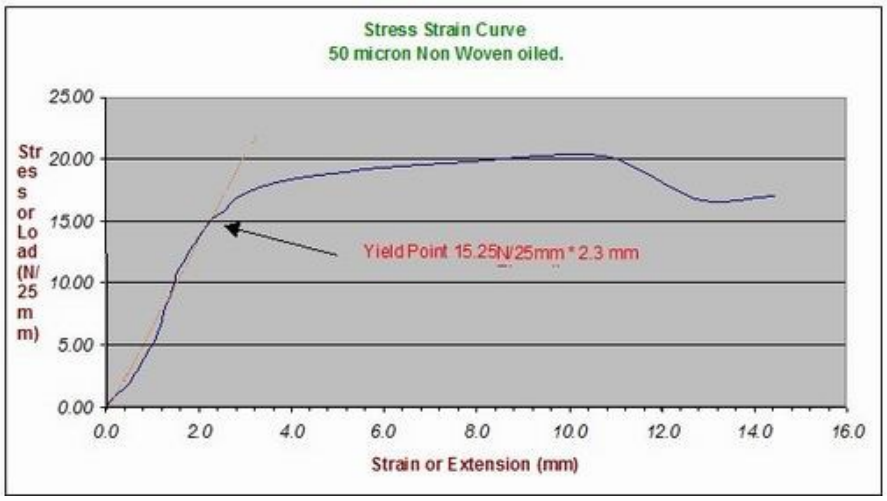

Figure 2-6: Stress/Strain reference curve [17]

2.1.4.1. Web tension control methods

In order to control and maintain the web tension, it is often required to measure the web tension. There are three main types of sensors to sense the tension of the web; that are dancer, load cell and accumulator. Each of these three sensors has

different methods of controlling the web tension and different performance characteristics.

Dancer is a simple and commonly used method to control tension. A dancer schematic is shown in Figure 2-7. It is a mechanical roll or wheel that sits on material. When the production is running, dancer position is feedback to the controller which automatically adjusts the winder speed. When the tension is high, the dancer roll will move up to the minimum position. Whereas when the tension is low, the dancer roll will move to the maximum position. The dancer position moves up and down during the operation. It is used where the tension control precision is not high. Tension error around 50% is considered as normal [14].

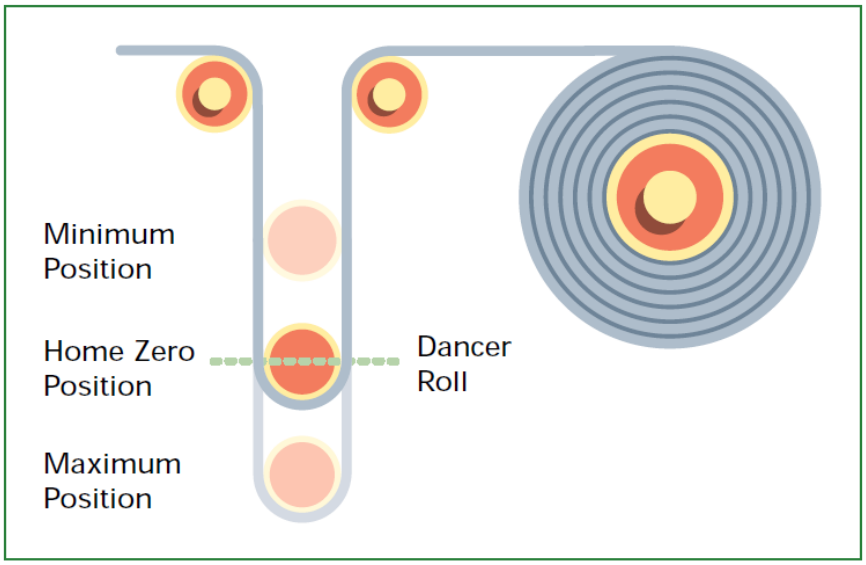

Figure 2-7: Dancer tension control schematics [15]

Load cell is an electromechanical sensor which converts tension/force to an electrical signal. The load cell tension control schematic is shown in Figure 2-8. Strain gauge is often used on load cell, which consists of Wheatstone bridge configurations. The strain gauge inside a load cell is deformed when a force is applied. The resistance change of the wire can be measured through Wheatstone bridge and output an electrical signal. After the signal is converted to electrical signal, it is feedback to the

controller which adjusts the winding speed in order to keep the tension constant. It is able to control within 10% of the set point where tension is high enough to be measured [14].

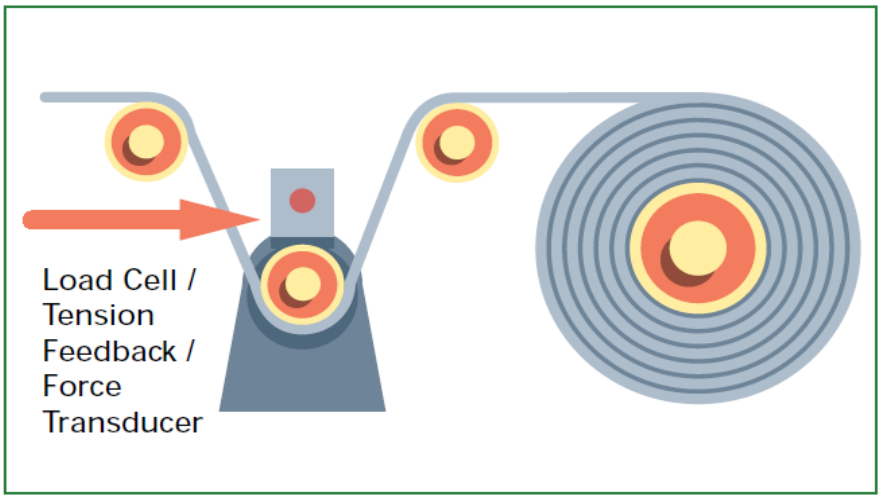

Figure 2-8: Load cell tension control schematics [15]

Accumulator Schematic is illustrated in Figure 2-9. It is also known as loop control which similar technique as the dancer. The position feedback of the web can be detected through photosensor, ultrasonic sensor and other devices [15]. Similarly to the dancer, when the tension is large, the web will move to the Minimum position. Whereas when the tension is small, the web will move to the Maximum Position.

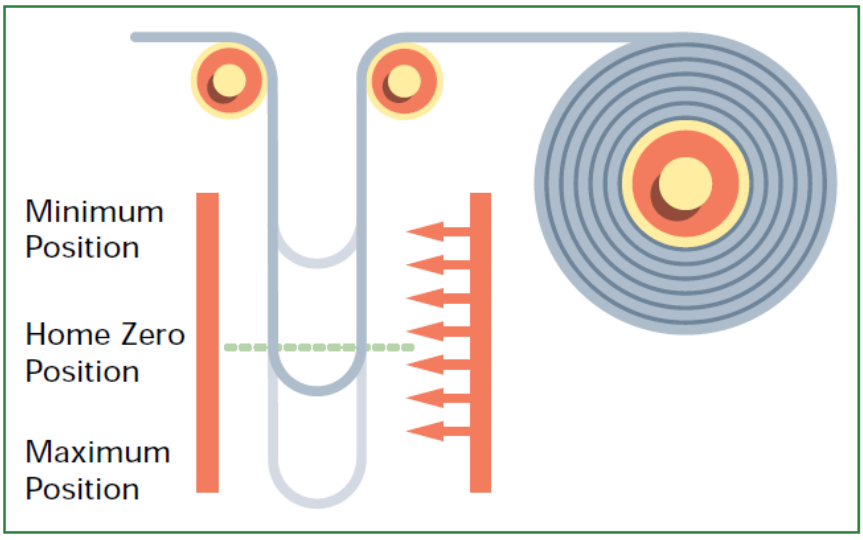

Figure 2-9: Accumulator schematic [15]

The three main types of tension control methods are summarized in

Table 2-1.They are not the only methods of achieving tension control, but are the more useful and common ways. There are many other solutions or methods of controlling tension beyond the scope of this project.

Table 2-1: Basic tension control table (modified from [14])

Type	Suited Application	Description Detail
Dancer	• Used in tension where tension is not required be controlled precisely • Tension error of 50%	• The Dancer roll is mounted on a stage and counterbalanced by an adjustable air cylinder. • Position is detected by an encoder or potentiometer which feedback to the controller to adjust the winding torque.
Load-cell	• Used in application where tension is high enough to be measured using load cell. • Tension error of 10%.	• The tension is measured when the web is pressing down on the load cell. • The web is required to thread through the load cell which it cover around the load cell.
Accumulator	• An improved version of dancer. • Used in situation where the mechanical dancer does not allowed.	• Light, sound or any contactless sensor is used to feedback the position to the controller.

2.1.4.2. Winding control methods

The winding process (include unwind and rewind) is an essential factor which can influence the production speed. This is because it controls the pulling and

resistance to the web material as well as the line-speed. The line-speed is referred to the speed of web being processed in meters per minute. However, the line-speed of the material is not equal to the winding motor's RPM speed. Consider a winding motor that is running at a constant RPM to wind web material. As the material is winding, the diameter of the web coil increases. If the winding motor keeps the RPM constant, the surface-speed/line-speed will also increase. The relationship between angular winding velocity and surface web velocity is shown in Figure 2-10. The actual line-displacement is equal to the radius of the coil times by the rotation position/angle. The surface velocity of the coil is equal to the radius of the velocity times the winding angular velocity. Therefore, the in order to keep the line-speed constant, the winding motor is required to change the speed as the diameter of the coil is changing. It is shown to have an inverse proportional relationship between the winding motor RPM and coil radius. Most of the processes require constant line-speed during steady state running; increase in line-speed is required to be compensated for [15]. Therefore, the winding controller is required to have the functionality for linear velocity matching.

On the other hand, it is required to maintain constant tension in a web. The relationship between coil's tension, torque and radius is demonstrated in Figure 2-11. As shown in the Figure, tension is equal to torque divide by the radius of the coil. If the tension is kept constant, torque and radius will have a proportional relationship between the two variables. Therefore, during the winding process (increase of coil radius), the torque of the must also increase in order to have constant tension.

The winder motor can also be controlled by a motor controller which can regulate a fixed motor current and provide sufficient toque as the radius of the coil is increased. Therefore, it enables us to control the torque and also keep the tension constant.

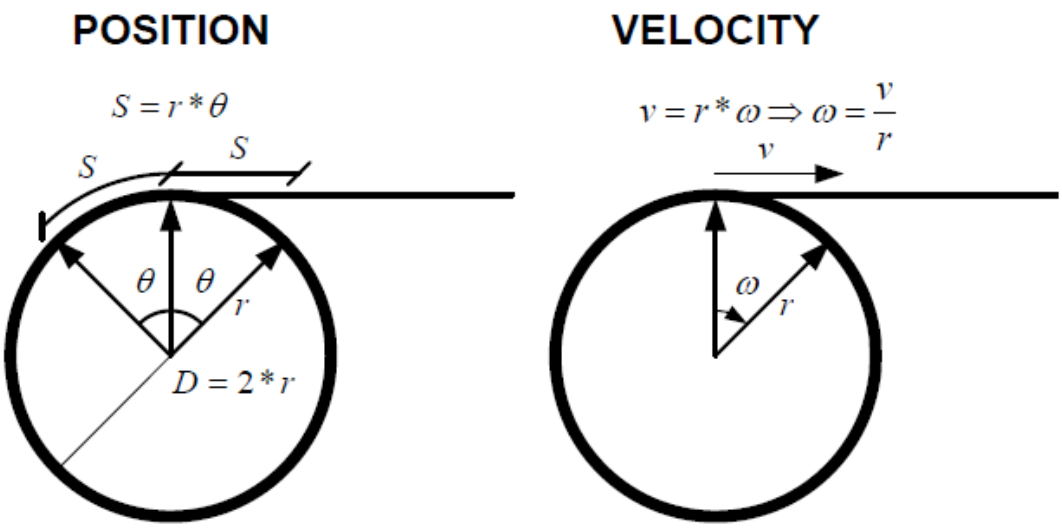

Figure 2-10: Surface and Rotational Velocity [19]

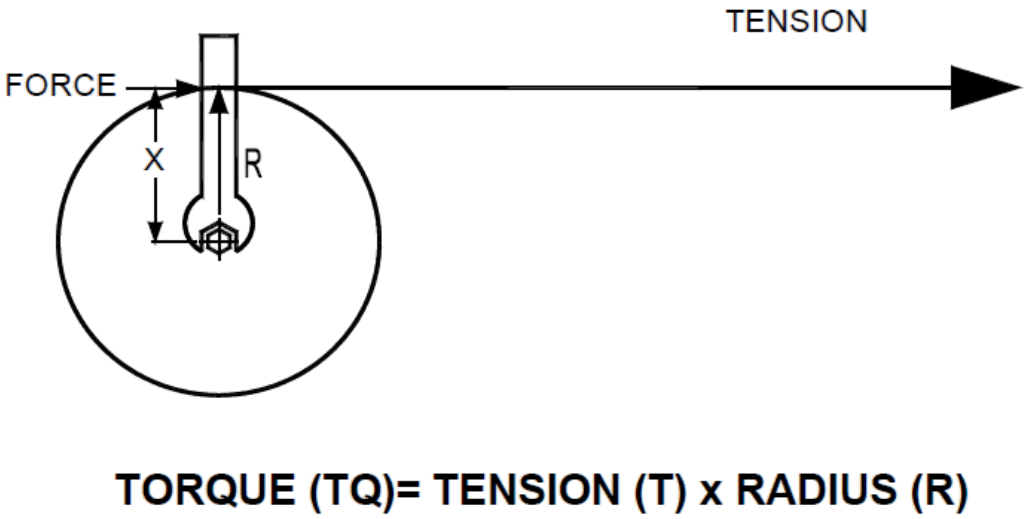

Figure 2-11: Torque, tension and radius diagram [20]

2.1.5. Traction

In terms of web Handling, Traction is the friction force which the roller is applied on the web. Frictional force is an important factor in Roll-to-Roll because the web will start to slip over the roller without enough traction. There are many different methods to increase traction between roller and web. These methods include, apply rough surface coating to the roller, add annular grooves or increase wrap angle [18].

It is identified that rough surface coating requires additional costs and also adds more cost to maintenance. In addition, apply annular grooves may only have effect at low speed. The most suitable methods in web handling application is to increase the wrap angle as it does not have many bad side effects and is able to produce large increase in traction [18]. The friction force in web handling application can be illustrated using The Capstan Friction Equation as illustrated in Figure 2-12. As the web bends over a small segment of the roller, the tension will increase from T to T+dT with angle dθ. The normal force is DN and the frictional force is μdN which acts to oppose slippage.

If we apply the Equilibrium in the x direction, the sum of forces in x direction equal to zero.

$$\sum F_x = 0 \tag{2-1}$$

$$T\cos\frac{d\theta}{2} + \mu(dN) - (T + dT)\cos\frac{d\theta}{2} = 0 \tag{2-2}$$

This is then reduced to

$$\mu dN = dT \tag{2-3}$$

Since the cosine of a differential is unity and product of two differentials can be neglected. Therefore, an equation in y direction is:

$$dN - (T + dT)\sin\frac{d\theta}{2} + T\sin\frac{d\theta}{2} = 0, \tag{2-4}$$

This is able to be reduced to

$$dN = Td\theta \tag{2-5}$$

The normal force can be eliminated from equation (2-3) and (2-5) to give the differential equation, and then integrate over the total contact angle:

$$\frac{dT}{T} = \mu d\theta \rightarrow \int_{T_1}^{T_2} \frac{dT}{T} = \int_0^{\beta} \mu d\theta \tag{2-6}$$

After this is reduce to capstan equation:

$$T_2 = T_1 e^{\mu\beta} \tag{2-7}$$

The equation (7) can be illustrated in Figure 2-13. Therefore, is can be seen that traction is a function of wrap angle, web tension, and friction coefficient of the roller and web. The friction will increase exponentially with the coefficient of friction and the contact angle [21].Finally, Equation (2-7) can be rearranged to calculate the minimum wrap angle to avoid slip.

$$\frac{T_2}{T_1} < e^{\beta\mu} \tag{2-8}$$

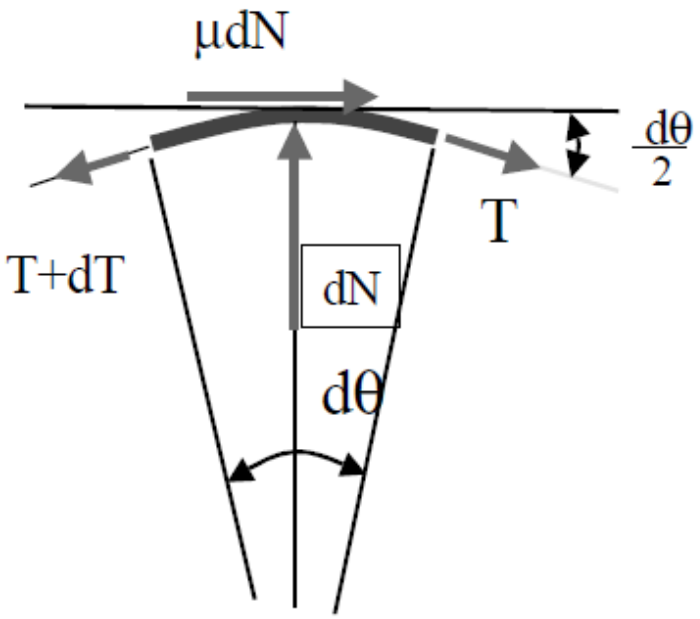

Figure 2-12: Amontons' friction law for a flexible belt. [21]

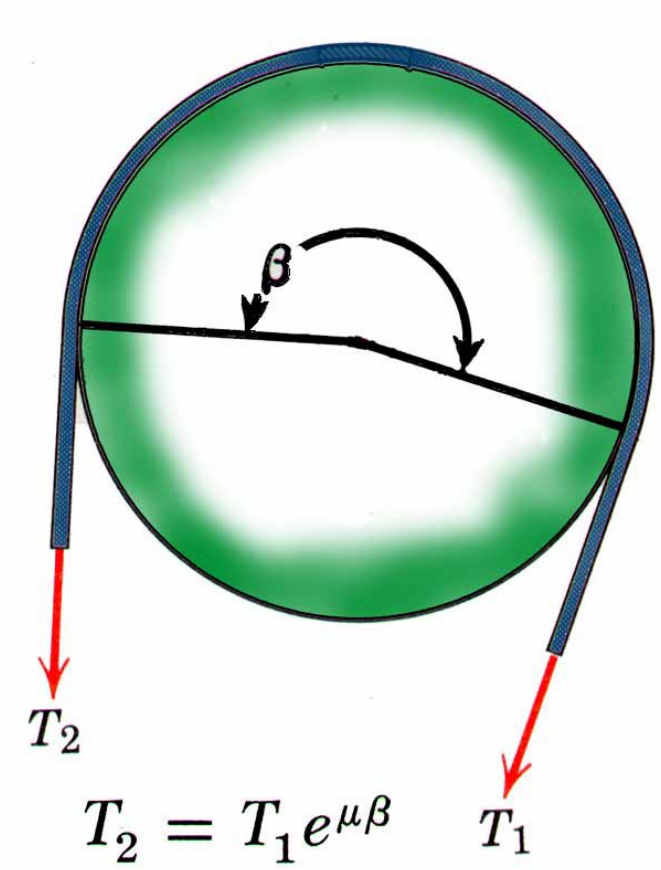

Figure 2-13: The Capstan equation for web friction [21]

2.2. Web Lateral motion control

It is often required to control the lateral motion of a moving web in Roll-to-Roll processing; lateral motion of the web can affect the quality of the printed product. In order to control the lateral motion, dynamics of a travelling web is required to be investigated. In addition, the dynamics of a Servo DC motor is also considered, as the actuator also have effect on the overall result of the system. In this section, Shelton's first order mathematical model that describes the web movement is introduced [22]-[23]. Shelton's first order model shows the dynamics of a moving web that take account of the relationship between lateral velocity to the longitudinal velocity and the input error [24]. The dynamics details of the web guide is illustrated Chapter 5. The general review is only covered in this section.

2.2.1. Shelton's first order dynamics model

In this dynamics model, assumption is made that the web has no shear strength and that it stretch in a straight line between rollers [22]. This model is built under the perpendicular entry rule or fundamental law of static steering. It is defined as "Webs tend to align themselves perpendicular to the approaching roller's axis of rotation." This can be illustrated in Figure 2-14, where the web is tending towards entry parallel to the surface vector of the downstream. Therefore, when the web leaves a series of non-parallel rollers, sharp angular break would be formed. By considering the transient relationship between the web and the downstream roller, the basis for the theory of lateral web dynamics is established. Due to the assumption of zero shear strength, the web in the entire free span is straight [22]. Every point in, and immediately preceding the contact area are steered straight relative to the roller as shown in Figure 2-15. Hence, the rate of lateral movement of the web edge is

proportional to θ, the angle of deviation from perpendicularity between the web and roller, and the velocity of the web.

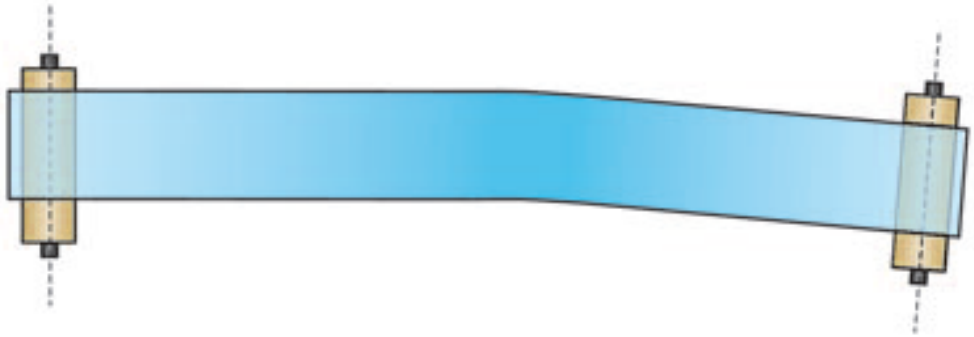

Figure 2-14: Shelton's first order model on perpendicular entry rule [13]

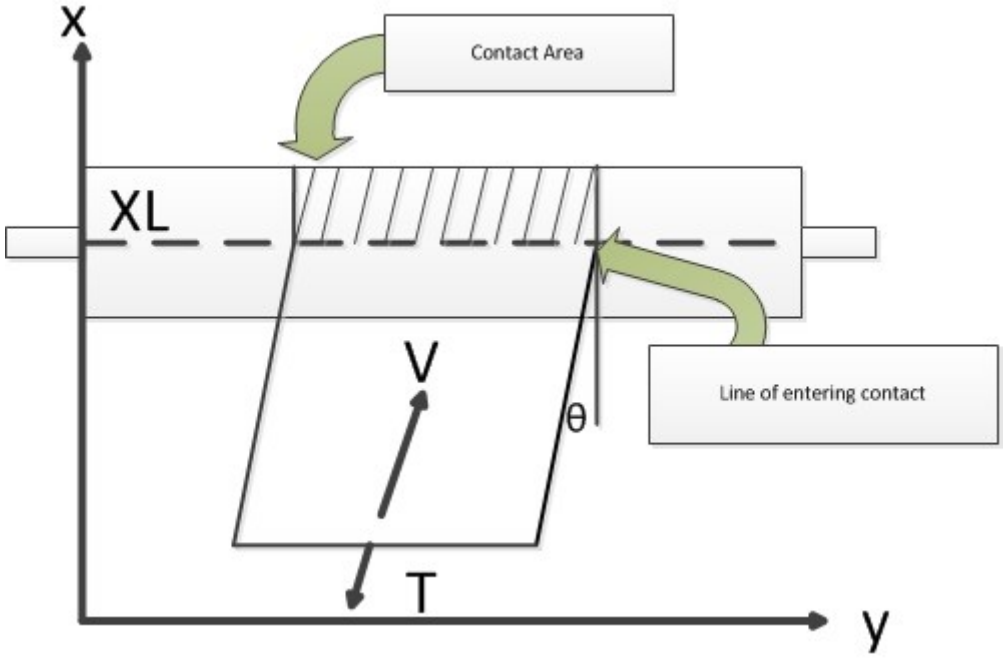

Figure 2-15: Steering action of idealized web

According to Shelton [22], if the roller is moving laterally, the total velocity of the web edge relative to the ground is equal to the sum of the velocity of steering of the web and the velocity of lateral transport of the web. Therefore, the velocity of the web edge relative to the ground is equal to the sum of the velocity of the web

edge relative to the roller and the velocity of the roller relative to the ground. The two component of web velocity at the downstream roller is:

$$\frac{dy_L}{dt} = -V\vartheta + \frac{dz}{dt} \qquad (2\text{-}9)$$

where z is the position of the downstream roller relative to the ground. The negative sign accounts for the fact that a positive angle as shown results in a negative velocity.

2.2.2. DC Motor Model

Figure 2-16 illustrates a dc servo motor with a closed loop to deliver controlled speed or controlled position. In order to control a DC Servo motor precisely, it is important to know the transfer function of the motor.

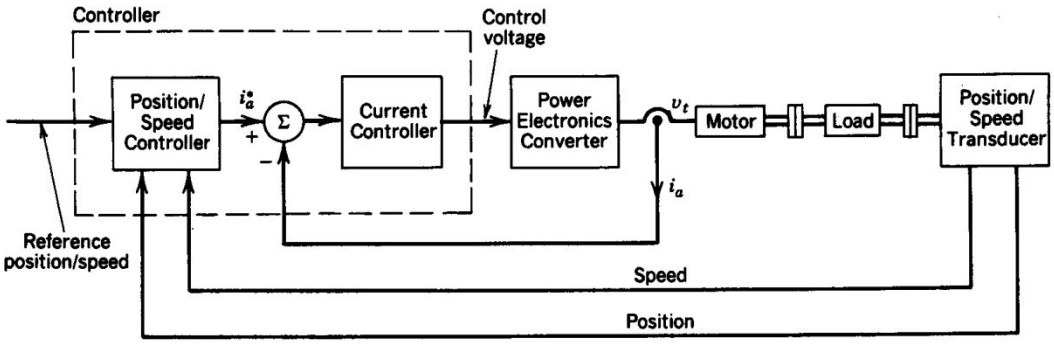

Figure 2-16: Closed loop DC servo motor block diagram

The speed of the DC motor is controlled through armature control method [25].The flux is kept constant corresponding to maximum utilization of the core material. The electromagnetic torque is produced by the interaction of the filed flux$\emptyset$ and the armature current i_a [26]:

$$T_{em} = k_a \emptyset i_a = k_t I_a \ ; \qquad (2\text{-}10)$$

where $\emptyset$ kept constant, k_a is the torque constant of the motor, k_t is a constant which is known as armature constant. The back emf is produced by rotation of armature conductors at a speed ω in the presence of field flux $\emptyset$:

$$\boldsymbol{e = K_a \emptyset \omega = k_e \omega} \quad ; \qquad (2\text{-}11)$$

where the k_e is a constant and is known as motor constant. Usually k_e and k_t is equal [25]. The proof details can be seen in Mohan [26].

Chapter 3. System design and Development

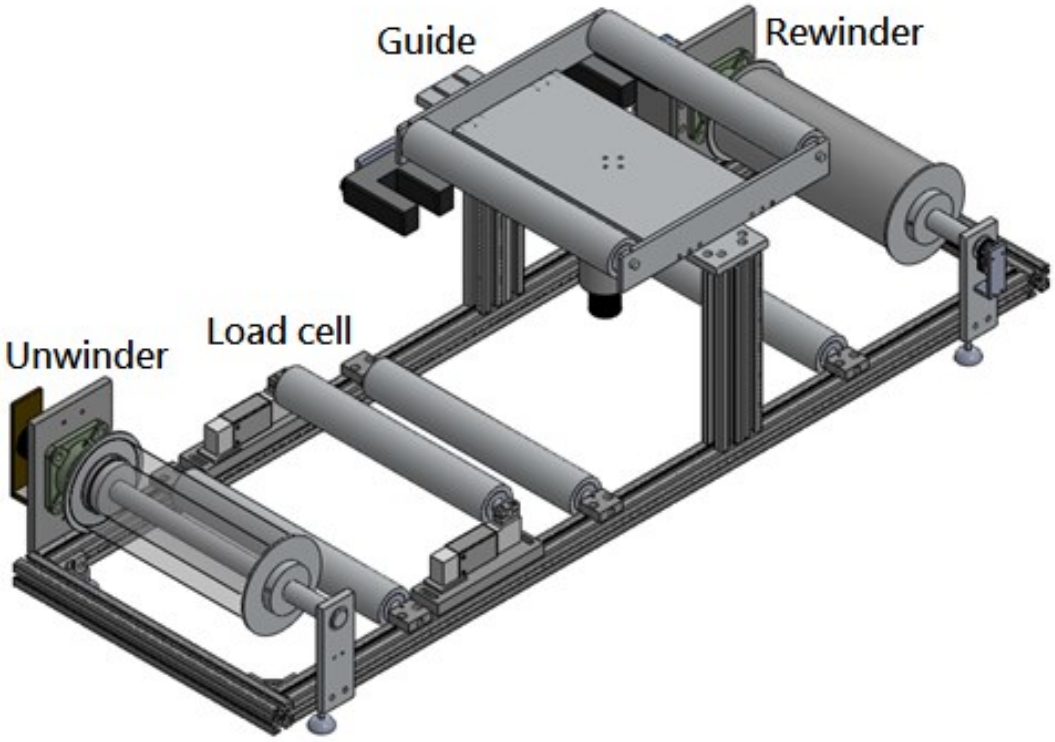

Figure 3-1: Overall System Design

In this chapter, the system design and development is discussed in the mechatronics system point of view with supporting theory. The overall system design is shown in Figure 3-1. The design methodology is discussed with the initial approach on how to design a mechatronics system. The basic specification of the of each sub unit, which includes the unwinder unit, load cell unit, guide unit, rewinder unit, aluminum framing and PCB design. Each of the sub units is discussed with the use of components, as well as how to integrate the components together. The manufacturing methods are addressed with tolerances method on the sub systems. Finally, integration of the complete Roll-to-Roll mechatronics systems is discussed.

3.1. Design Methodology

The system design in this project is especially critical as the research is conducted in National Tsing Hua University, where the working environment is different from Massey University, Palmerston North. New parts and components supplier is required to be researched into. The part standards may also be different to the standards in New Zealand. In addition, parts of the manufacturing methods are also different. In order to provide a robust design and maximize the quality of the system, the following key points are addressed with the purpose of achieving successful outcome of the project:

- Design by standard components
  - Design the machine dimension and components followed by the international standards.
  - Reduce time saving in design and development.
  - Support is available from engineers at the supplier company.
  - Reduce the price on components purchase.
- Modularity
  - Testing and improvement flexibility.
  - Easier to adjust and add additional module to the system.
  - Each subassembly can be tested outside the top-level system.
  - Capability to adjust parameters easily.
- Manufacturability consideration
  - Design should be able to manufacture.
  - Save the machining lead time and cost.
  - Design provides correct mechanical tolerances.

3.2. Web Coil Specifications

As seen in Figure 3-2, the Web material used in this project is a transparent PET web material. The web coil was given as a test sample from Symbio Inc [27], which supplies the substrate material for printed electronics industry. In the industrial scale, the width of the coil can range from 100mm to 2000mm wide. The weight of the coil normally ranges from 1 ton to 10 ton. However, only proof of concept is required in this project, web material used in this project has the following specification as shown in Table 3-1. The web coil used in this project weight 4kg only. This will help the project flow as it is not required to develop a large machine for research purpose. The Width of the coil is 345mm, with a thickness of 0.125mm. The coil has the inner diameter of 85mm and outer diameter of 131mm. The tensile strength of PET is 80Mpa and young's modulus is 2-2.7 N.m^2.

Figure 3-2: Web coil in this project.

Table 3-1: Web material specification

Parameter	Value	unit
Material	PET	
Coil Width	345	mm
Outer Diameter	131	mm
Inner Diameter	85	mm
Thickness	0.125	mm
Tensile Strength	80	Mpa
Young's Modulus of Elasticity	2-2.7	10^9N.m^2
Weight	4	kg

3.3. Roll-to-Roll System

The roll-to-roll testing system in this project is divided into 4 different sub systems/units which are integrated together; that are unwinder unit, load cell unit, guide unit, and rewinder unit. The enlarged figures of each unit are shown in Appendix 1.1. The unwinder unit unwinds the web material and provides pulling tension from the rewinder unit. The load cell unit provides the tension feedback to the system for providing constant tension. The guide unit guides the web material in order to counteract the lateral motion. Finally, the rewinder unit rewinds the web material back into the coil form in order to repeat the same process. In this section, each sub systems/units are discussed with the components used as well as the characteristics of each component how to integrate into a system. The details of each component datasheets are illustrated in Appendix 1.2

3.3.1. Unwinder unit

As mentioned in the introduction section, the unwinder unit unwinds the web material and provides the pulling tension required in the system. The exploded view

of the unwinder unit is shown in Figure 3-3. The unwinder is designed to have two ends supported (No. 4 and 10), which can reduce the bending as compared to the cantilever type. A ball bearing is press fitted inside the supporter (No.10) which can hold the shaft (No. 9) while rotating. The two coil guides (No.1) is used as a passive web guides in order to prevent excess web lateral motion which may cause by unbalanced assembly. However, the actual lateral guiding is achieved in the guiding unit. It is designed with the tolerance which can slide smoothly on the shaft. Both of the guides have set screws on the outer sides, which can be used to fix the position on the shaft. The inner side of the two coil guide is designed to fit through the coil (No.2) which can fix and unwind the coil material. A building with housing is bolted onto the unwinder back plate (No.4) which can provide the rotation of the unwinder.

A shaft coupling (No. 5) is used to connect between the shaft and the brake (No. 7). The housing of the brake (No. 6 and 8) is also designed to support the shaft on the brake.

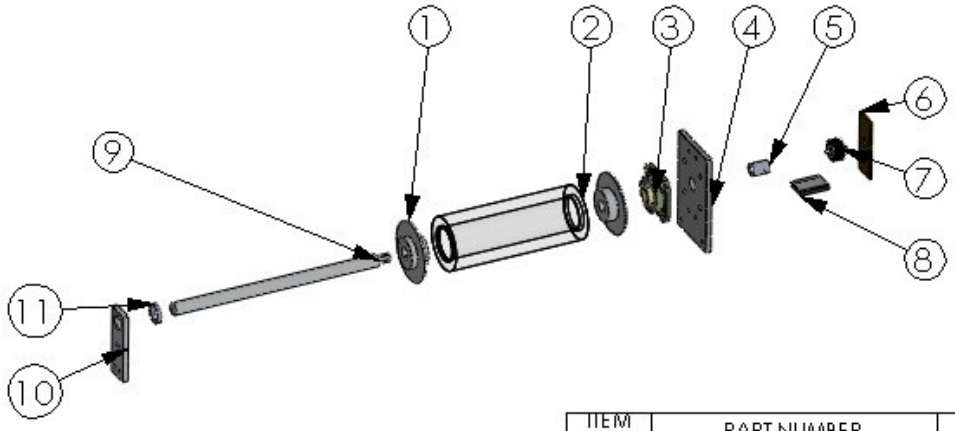

ITEM NO.	PART NUMBER	QTY.
1	coil guide	2
2	coil	1
3	housing1	1
4	unwinder_back plate	1
5	brake bushing	1
6	brake back plate_1	1
7	Brake2	1
8	brake back plate_2	1
9	shaft	1
10	supporter	1
11	bearing_support	1

Figure 3-3: Exploded view of unwinder unit with list of parts

3.3.1.1. Unwinder components

Bearing and Hysteresis clutch/brake are used in the unwinder unit. The bearings used in this project are ball bearings which is able to support radial and axial loads. The bearing fitted on the supporter is a double sealed ball bearing. On the other hand, the bearing unit (No.3) is a self-aligned bearing unit.

The Hysteresis clutch/brake used in this project is a permanent magnet clutch/brake. This component is shown in Figure 3-4. In this clutch/brake, multi-pole magnets are used to establish lines of magnetic force which provide an accurate and smooth torque. This hysteresis clutch/brake has a rated torque of 0.14Nm with maximum supply voltage of 24VDC. This device runs open loop, which can increase the rated torque to maximum of 0.14Nm depending on the input voltage ranging from 0V to 24V.

Figure 3-4: Hysteresis clutch and brake [28]

3.3.2. Load cell unit

In web roll-to-roll application, load cells are often used for measuring the tension, as the output can be convert straight into engineering units by calibration. Figure 3-5 illustrates an exploded view of the load cell unit and the list of parts that is

used for this unit. In the load cell unit, two low capacity single-point aluminum load cells (No. 3) are used to measure the tension of the web. The load cell is placed on top of the load cell platform (No. 5 and 6).An idler roller placed on top of the load cells with couplings (No.2 and 7) which can fixed the roller onto the load cell sensor.

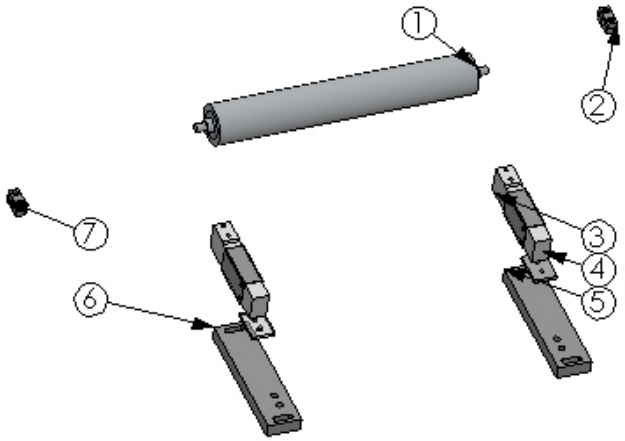

ITEM NO.	PART NUMBER	QTY.
1	Assem12	1
2	load cell coupling_1	2
3	loadcelll	2
4	loadcell plate	2
5	loadcell platform_right	1
6	loadcell platform_LEFT	1
7	load cell coupling_2	2

Figure 3-5: Exploded view of load cell unit with list of parts

3.3.2.1. Load cell components

The load cell sensor which used in this project is a Model 1041 low capacity single point aluminum load cells as shown in Figure 3-6. It is designed for direct mounting of low cost weighing platform. The rated capacity of these load cells are 10kg max.

Figure 3-6: Low Capacity Single-Point Aluminum Load Cells [29]

The output of the load cell can be calibrated with the following methods to read out the normal force exerted by the web:

- Place the roller on the load cell and measure the no load situation which can zero the output by offset the weight of the idler roller.
- Apply a string or web through the path and hang a known weight and adjust the output value to correct to this value.

The normal force is able to be determined by the orientation of the load cell and the wrap angle of the web [14] as shown on Figure 3-7. The net force can be calculated using the following formula [30]

$$F_T = \frac{4T\sin\left(\frac{B}{2}\right) - W\cos(A)}{2} \tag{3-1}$$

Where:

T=Tension,

F_T=Net Force,

B=Web wrap angle,

A=angle of normal force from vertical

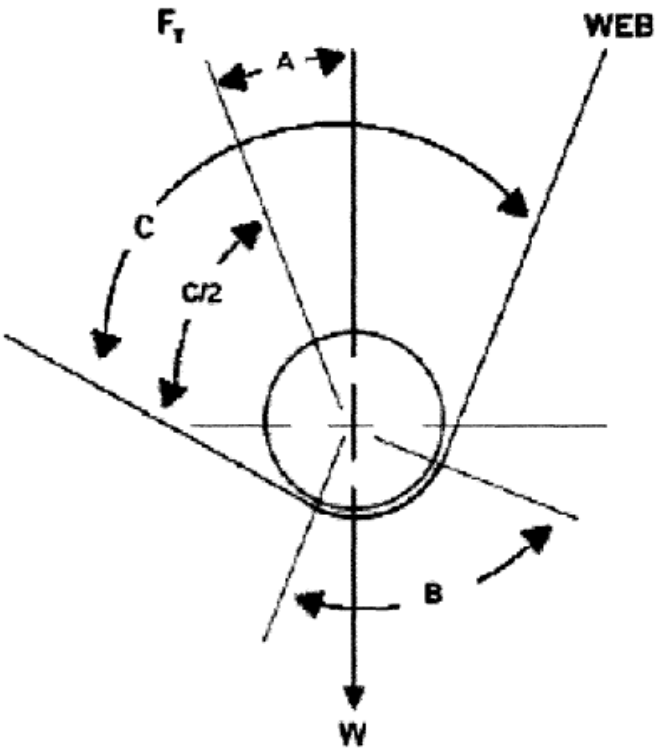

Figure 3-7: Calculation for determining resulting net force [30].

3.3.3. Guide unit

The guide unit is used to control the lateral motion of the web which can re-align the web to the center position of the roller. The exploded view is illustrated in Figure 3-8. The guide is designed to be center pivoted displacement guide. It has two rollers (No. 12) which changes the position of the web. The guide is rotated through a thrust bearing which provide the smooth operation in the radial direction. The guide is actuated using a DC servo motor (with encoder) which can sense the rotation and degree of turning. Ultrasonic edge sensor (No.8) is also used to sense the lateral movement of the web. The guide is placed on two 80x40 aluminum framing which can securely fix the guide unit.

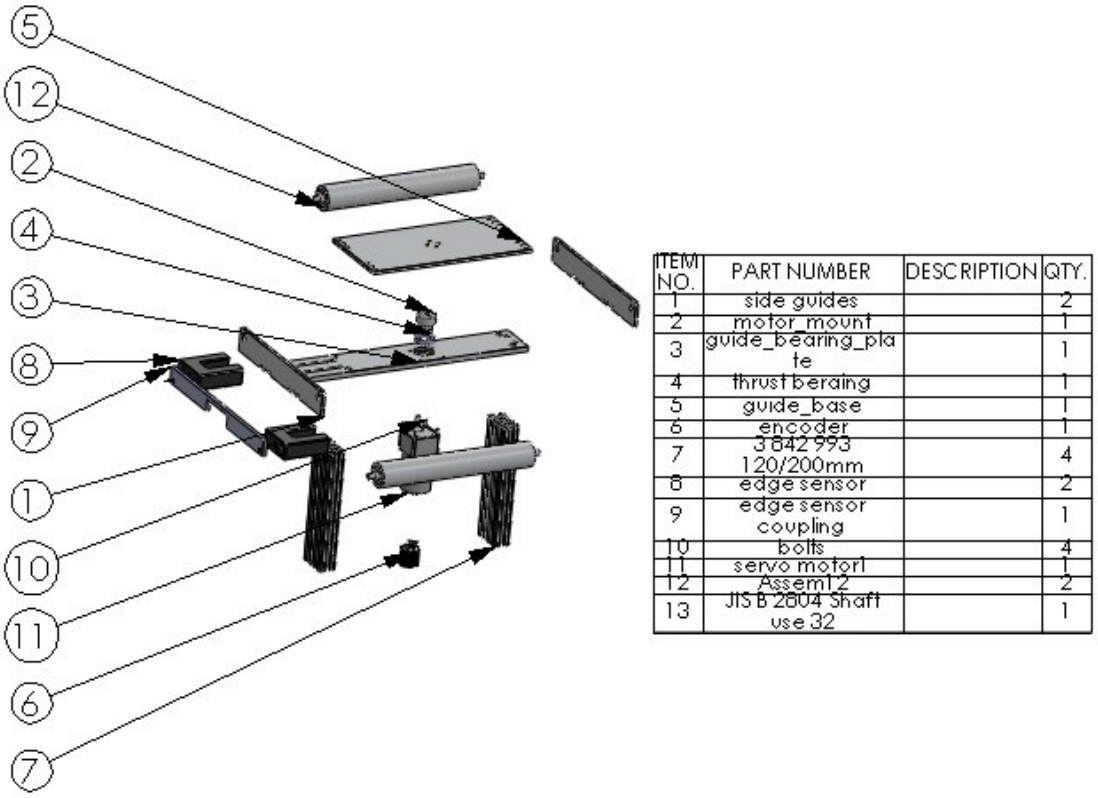

ITEM NO.	PART NUMBER	DESCRIPTION	QTY.
1	side guides		2
2	motor_mount		1
3	guide_bearing_plate		1
4	thrust beraing		1
5	guide_base		1
6	encoder		1
7	3842993 120/200mm		4
8	edge sensor		2
9	edge sensor coupling		1
10	bolts		4
11	servo motor1		1
12	Assem12		2
13	JIS B 2804 Shaft use 32		1

Figure 3-8: Exploded view of guide unit with list of parts

3.3.3.1. Guide Components

The DC servo motor consists of a DC gear motor and an encoder. The Maxway DC motor (without gearbox) output 15W which can be operated by 24VDC with a revolution of 2000RPM. The gear motor has a gear ratio of 36:1 with ball bearing in the gearbox. The maximum output speed of the DC geared motor is 55RPM.

The DC motor is driven by a 24VDC Full H bridge Maxway DC motor driver as shown in Figure 3-10. The motor is connected to the motor driver for stop, forward and reverse operation. The motor driver accepts external voltage (0-5V) for speed controls such that, 0V is the slowest speed and 5V is the fastest speed. When making the motor operation, such as forward, stop or reverse, the operation pins in (JP2) is required to be connected to the COM. For, example, when motor forward operation is desired, the Forward pin in JP2 is required to connected to the COM. Hence

additional circuit will be required to be built for making this process automatic. The details are shown in the PCB section.

Figure 3-9: DC Motor & DC Gear Motor [31]

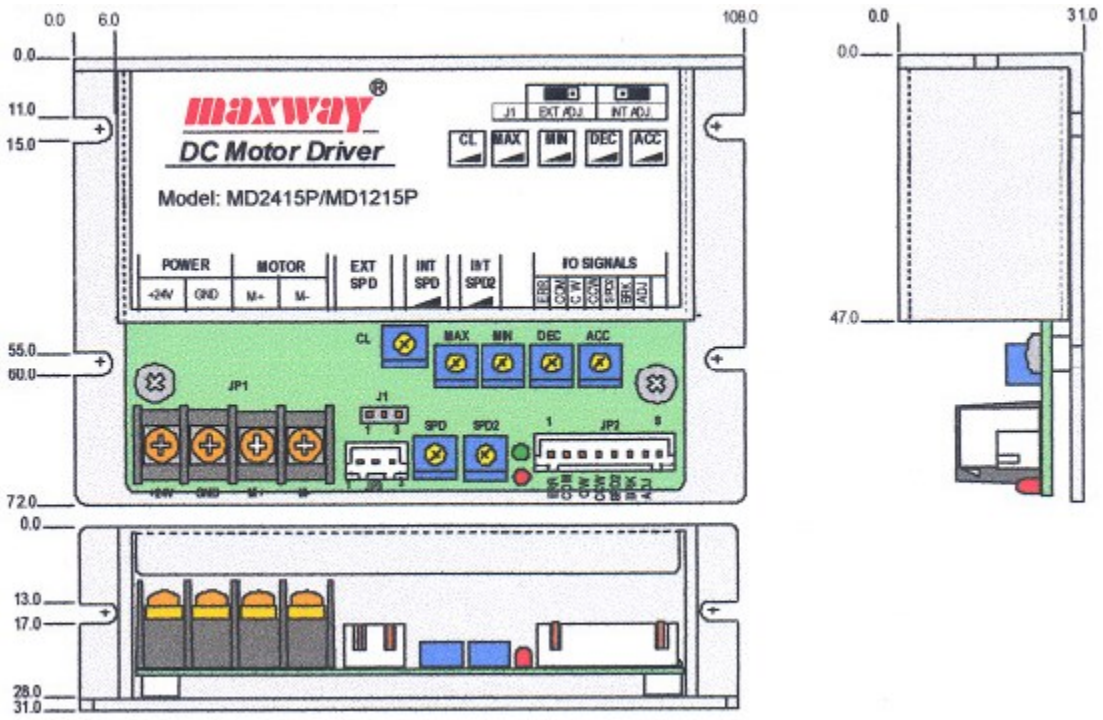

Figure 3-10: Maxway DC motor driver [31]

The encoder used in this unit is an incremental encoder for controlling the position of the motor. The encoder is operated with 5VDC and outputs 1000 pulses per revolution with ABZ phase. Channel A and B is positioned 90 degrees out of phase and Z is used to indicate the start of the encoder or the zero position. Channel

A and B can be used to indicate angular position and direction as well as calculating the speed. The encoder is mounted at the back of the motor. In this project, the encoder is decoded using x4 decoding a method which basically means the encoder can have a resolution 4 times the number of pulses per revolution. The algorithm for x4 decoding is based on identifying the transition for channel A and B. The x4 decoding timing diagram is shown in Figure 3-12. By taking the forward direction as an example, the working principle is able to be realized.

- When transition in A occurs and A is not equal to B, then increment position.
- When transition in B occurs and A is equal to B, then increment position.

Therefore, it is able to realize the position and also enable to calculate the velocity of the rotating shaft.

Figure 3-11: Rotary encoder image [32]

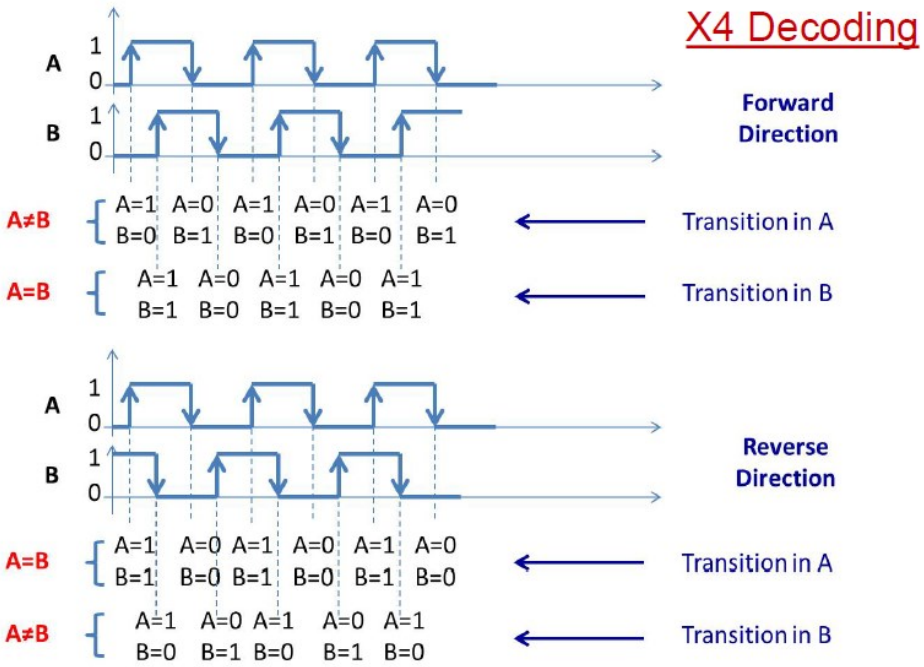

Figure 3-12: x4 decoding timing diagram [33]

Edge sensor is used in this project to identify any lateral error in the operation, which can realign the web into the right position and orientation as shown in Figure 3-13. The sensing range of this edge sensor is around 10mm (5mm each way from centerline). The edge sensor is connected to the controller for the sensor feedback.

Figure 3-13: Edge sensor [34]

The controller used in this unit is an Arduino 2560 which is based on ATmega2560 microcontroller as shown in Figure 3-14. The microcontroller has 14 PWM outputs (total of 54 digital IOs) and 16 analog inputs. In addition, the controller has a 16MHz crystal oscillator. This controller is used to controls solely the guide unit. Therefore, it will only require controlling the servomotor, edge sensor and the encoder.

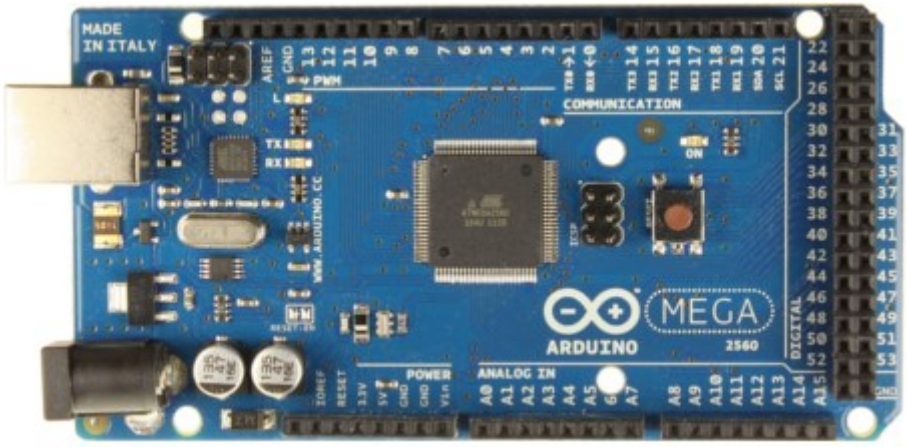

Figure 3-14: Arduino 2560 microcontroller [35]

3.3.4. Rewinder unit

The purpose of the rewinder unit is used to rewind the material back into the initial coil form. The exploded view of the rewinder unit is shown in Figure 3-15 with list of parts that is used. The Design of the rewinder is similar to the design of unwinder. Both of the designs have supporter, coil guide, and back plate. The unwinder is designed to have a supporter which supports one end of the rewinder. The rewinder also uses coil guides to prevent the excess lateral motion. The rewinder is actuated by a torque motor which can provide a constant tension during the rewind of the web. A motor coupling is used to connect between the torque motor and the shaft.

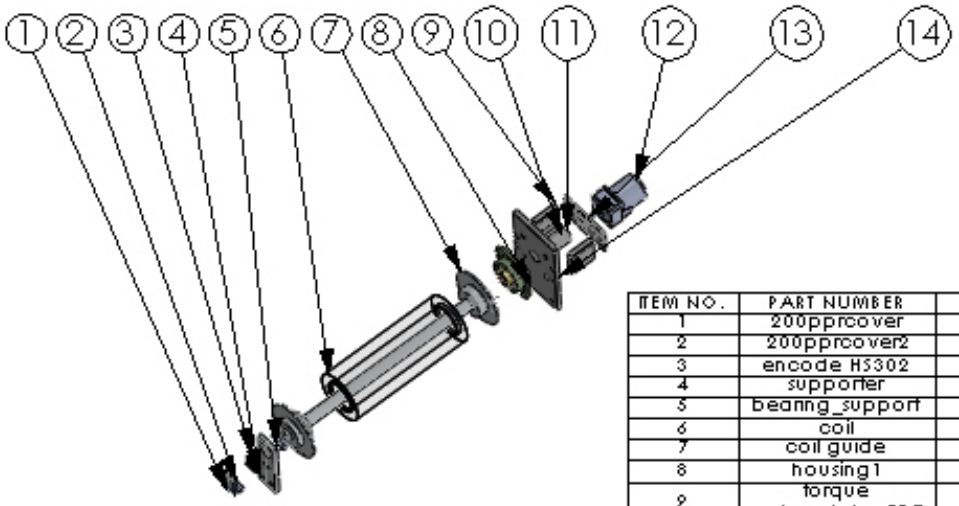

ITEM NO.	PART NUMBER	QTY.
1	200pprcover	1
2	200pprcover2	1
3	encode HS302	1
4	supporter	1
5	beanng_support	1
6	coil	1
7	coil guide	2
8	housing1	1
9	torque motor_plate_ EDIT	2
10	key	1
11	motor_coupling	1
12	TM306A+3GN3S	1
13	motorplate	1
14	rewinder_backplate	1
15	shaft_rewinder	1

Figure 3-15: Exploded view of rewinder unit with list of parts

3.3.4.1. Rewinder Components

Arduino uno microcontroller is used in this unit. A photo of this microcontroller is shown in Figure 3-16. The controller used in this unit is to control and integrate the peripheral components for the testing Roll-to-Roll system; that is unwinder, load cell, and rewinder. This microcontroller is based on the Atmega328, which has 14 digital input/output (6 can be used as PWM) pins and 6 analog input.

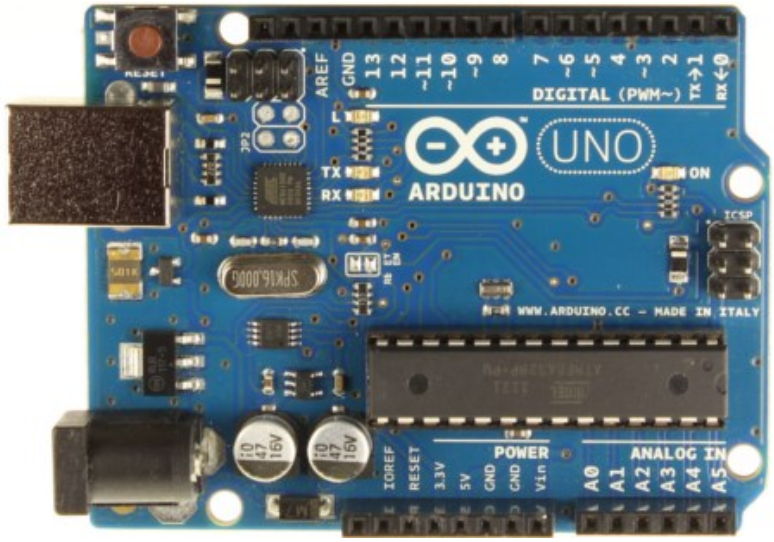

Figure 3-16: Arduino Uno microcontroller [36]

Oriental TM series torque motor (shown in Figure 3-17) is used in this unit for rewinding purposes. This motor is suitable for winding application, as the tension is kept constant while the torque is increasing and the speed is decreasing. As shown in Figure 3-18, the speed of this motor can vary widely depending on the sloping characteristics. The torque motors have high starting torque and sloping characteristics [37]. The speed control can be done by changing the voltage supplied to the motor.

Figure 3-17: Oriental TM Torque motor [37]

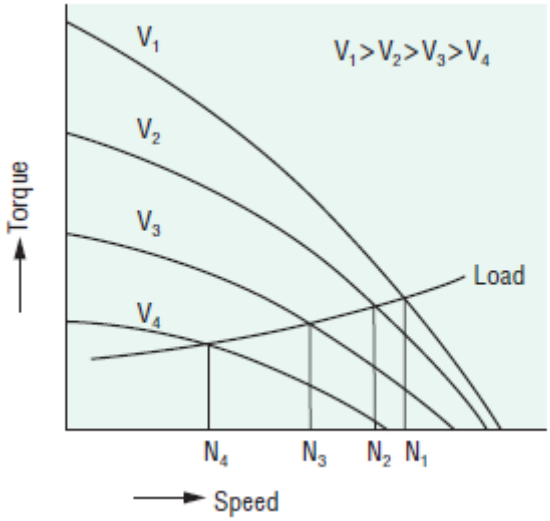

Figure 3-18: Torque vs. Speed characteristic curve [37]

A 200 pulse per revolution encoder is used in this unit for sensing the line-speed as shown in Figure 3-19. Therefore, the line-speed can be accurately monitored.

Figure 3-19: Line-Speed Encoder [38]

3.3.5. Aluminum structure

The aluminum framing design can be seen in the Figure 3-20. It is mainly developed using 40x40 frames as a platform for the Roll-to-Roll testing system. The platform is designed to be 1500 mm long and 500 mm wide. On the other hand, the guide system is supported using a 40x80 frame (ENG 4080) as shown. The aluminum framing is designed to have vibration pad on the four corners to reduce unwanted vibration.

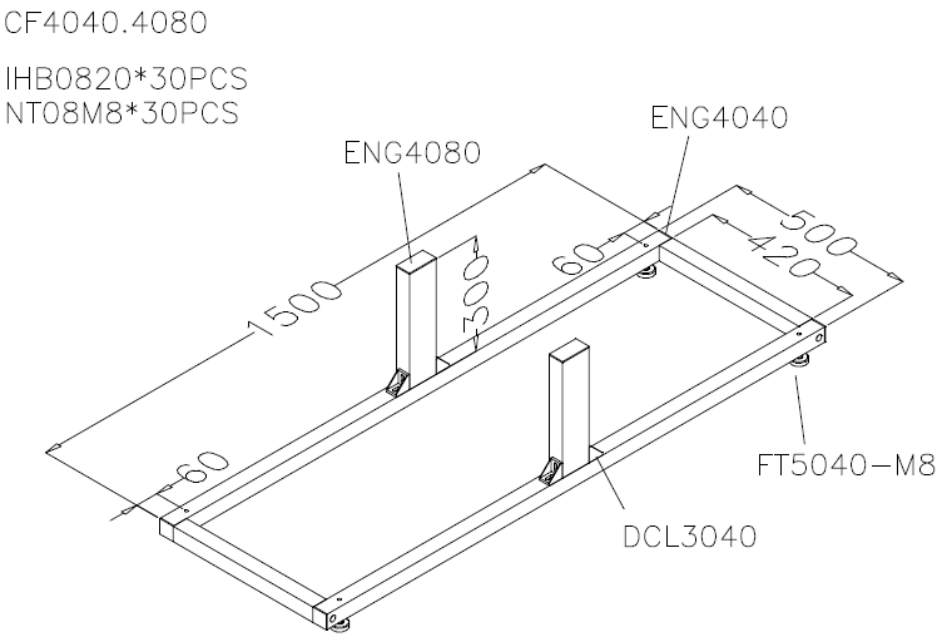

Figure 3-20: Aluminum framing structure layout

3.3.6. Control box design

The control box functional block diagram can be seen in Figure 3-21. There are two signal conditioning circuit used in this project. They are used to interface between sensor/actuators to the controller as well as instrumentation purposes. Signal conditioning 1 is used purely on guide unit. Conversely, signal conditioning 2 is used for unwinder, load cell and rewinder unit. There are two $\pm 12V$ power supplies which are used in this project. One of the power supplies is to be used to supply power to signal condition circuit1 and the guide servo motor in the project. On the other hand, the power supply 2 is used to supply the signal conditioning circuit 2 for peripheral sensor/actuators in unwinder unit, loadcell unit and rewinder unit. As a result, the control box is also used to hold all the communication and interfacing between each component. The details of signal conditioning circuits are illustrated in Appendix 2.1.

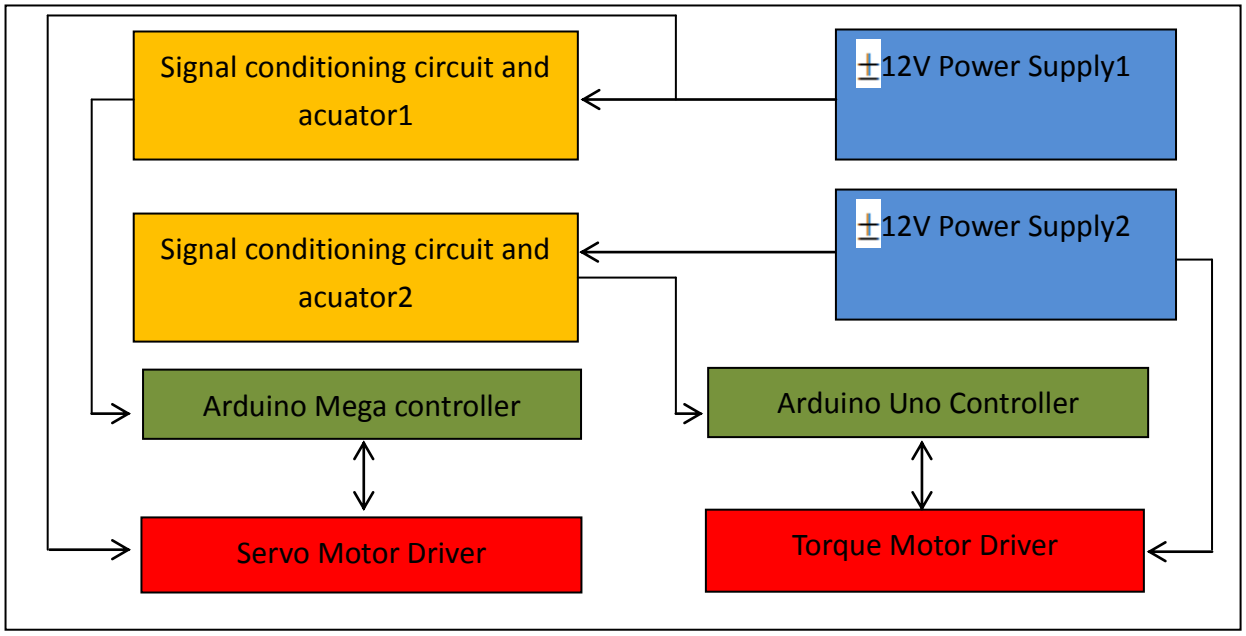

Figure 3-21: Control box block diagram

3.4. Manufacturing

The majority of the mechanical components are machined using CNC milling machine or lathes. The tolerances and fits of each component are based on ISO 286 standard. Depending on the types of fits; whether it is clearance fits, transition fits or interference fits, different tolerances and limits are used. In general terms, it is preferably to have tolerance zones at H7, H8, and H11 for hole tolerances. On the other hand, it is preferably to have tolerance zones at h6, h7, h9 or h11 for shaft tolerance zones. The selection of fits is also depending on whether the design is a hole basis system or in a shaft basis system.

3.5. System Integration

The overall control system block diagram is depicted in Figure 3-22. The overall system can be divided into 4 sections, namely unwinder unit, load cell unit, displacement guide unit and rewinder unit. There are two microcontrollers used in this system. One of the controllers is used to control the overall peripheral parts of the system; that is unwinder unit, load cell unit and rewinder unit. Whereas, the other controller is specifically used for Center pivot displacement web guides as shown in Figure 3-22.

The complete system is controlled by the User's command, such as, setting the production line-speed and tension, as well as the speed of web guide system. The Unwinder (1) in this system does not provide actuating source. Tension is generated by a hysteresis brake (CHB series) which provides the pulling resistance of the web. This allows the controller to control tension by the microcontroller through PWM modulation signal (0-24V). The Load Cell unit (2) provides a feedback signal (0-20 mV) to the controller in order to provide tension reading. The tension of the system can

also be maintained with the feedback from the system dynamics. It can also be changed through User's command.

The control system in the Guiding system unit (3) is realized by a dedicated microcontroller, which solely used for controlling the web lateral guiding. The controller receives the lateral position signal (-11 to 11V) from the edge sensors as well as the speed reading from the HTR-QB quadrature encoder. The displacement guide is actuated by a servo system which includes a Maxway DC Geared Motor and a quadrature encoder. This is controlled by a PID control system and tested through Simulink simulation in the later section.

Finally, the Rewinder unit (4) is used to rewind all the material back to a coil form as before. This is achieved through a torque motor which is able to keep the torque constant throughout the entire working cycle.

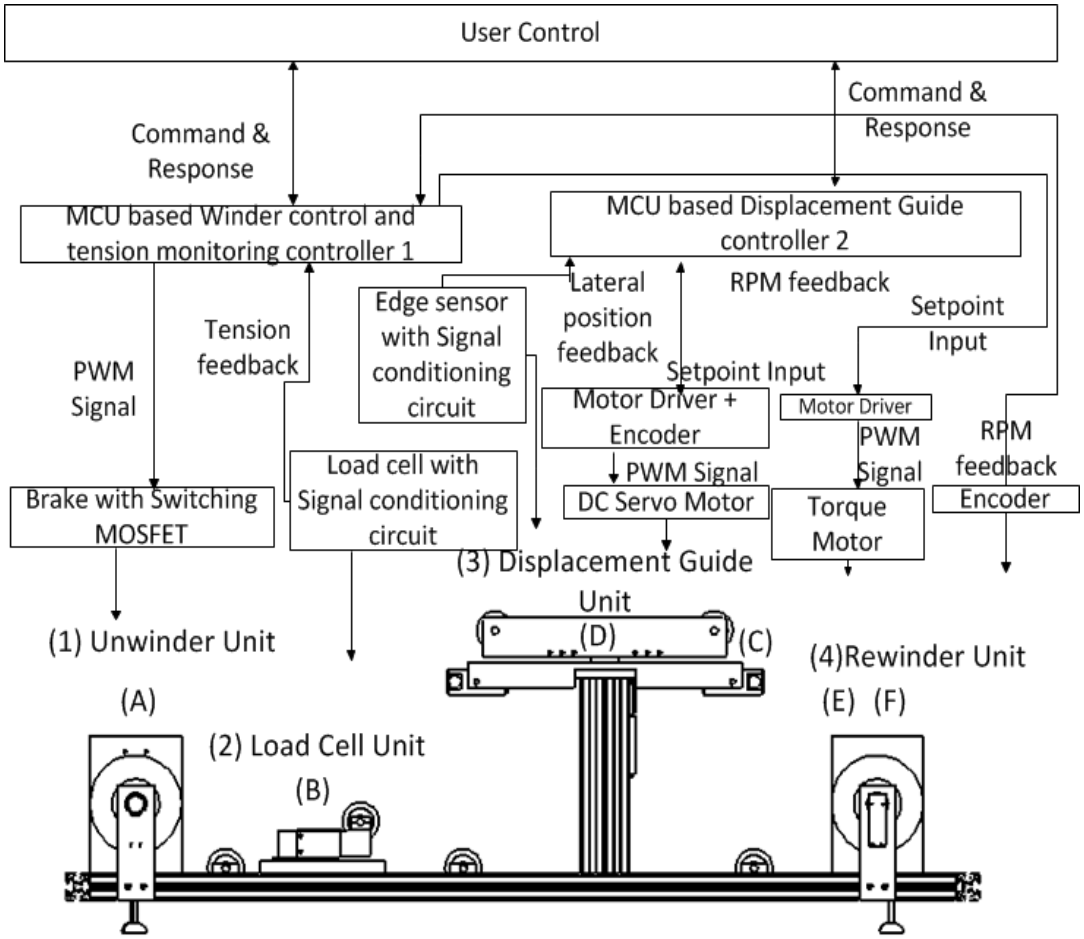

Figure 3-22: Complete system block diagram

3.6. Complete system images

Figures of the Roll-to-Roll testing system are shown in this section. The complete system images are shown in Figure 3-23, where unwinder, load cell, web guide and rewinder is shown respectively from the right. Figure 3-24 illustrated the web threading through from the unwinder to the load cell. The guide unit is also presented in Figure 3-24. Finally, the web is winded back into the rewinder as illustrated in Figure 3-26 and the control box is shown in Figure 3-27. Additional blue strings are added for restricting the guide system from excess rotation.

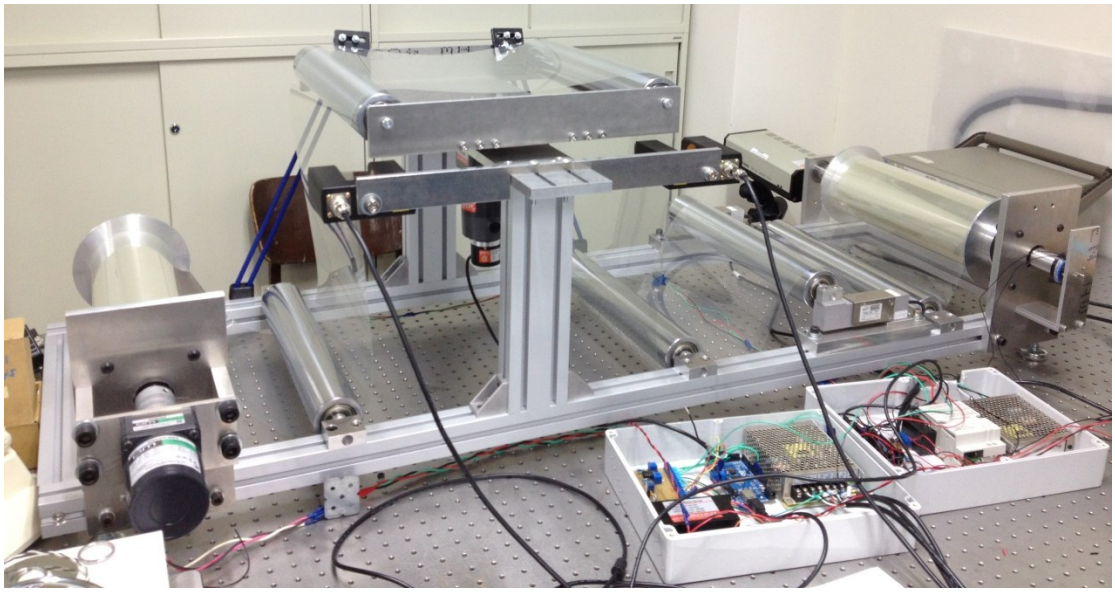

Figure 3-23: Complete System side view

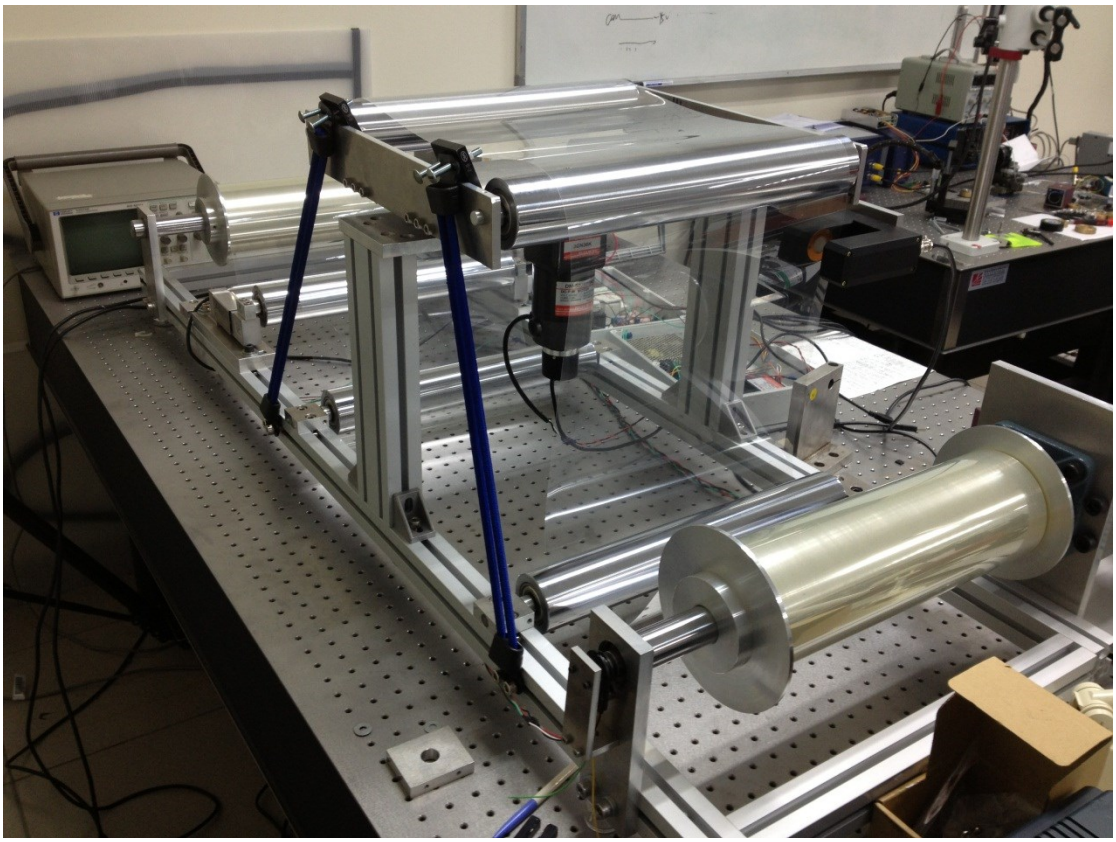

Figure 3-24: System view from angle 1

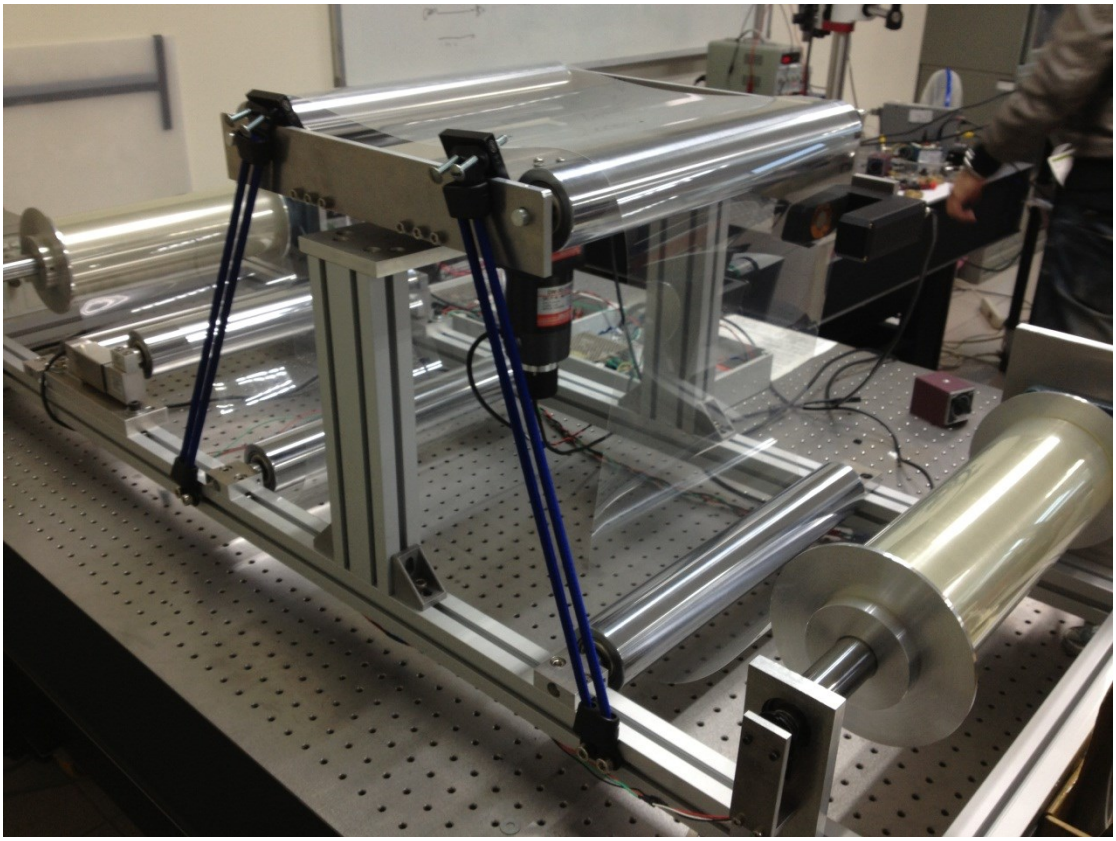

Figure 3-25: Guide system view from angle

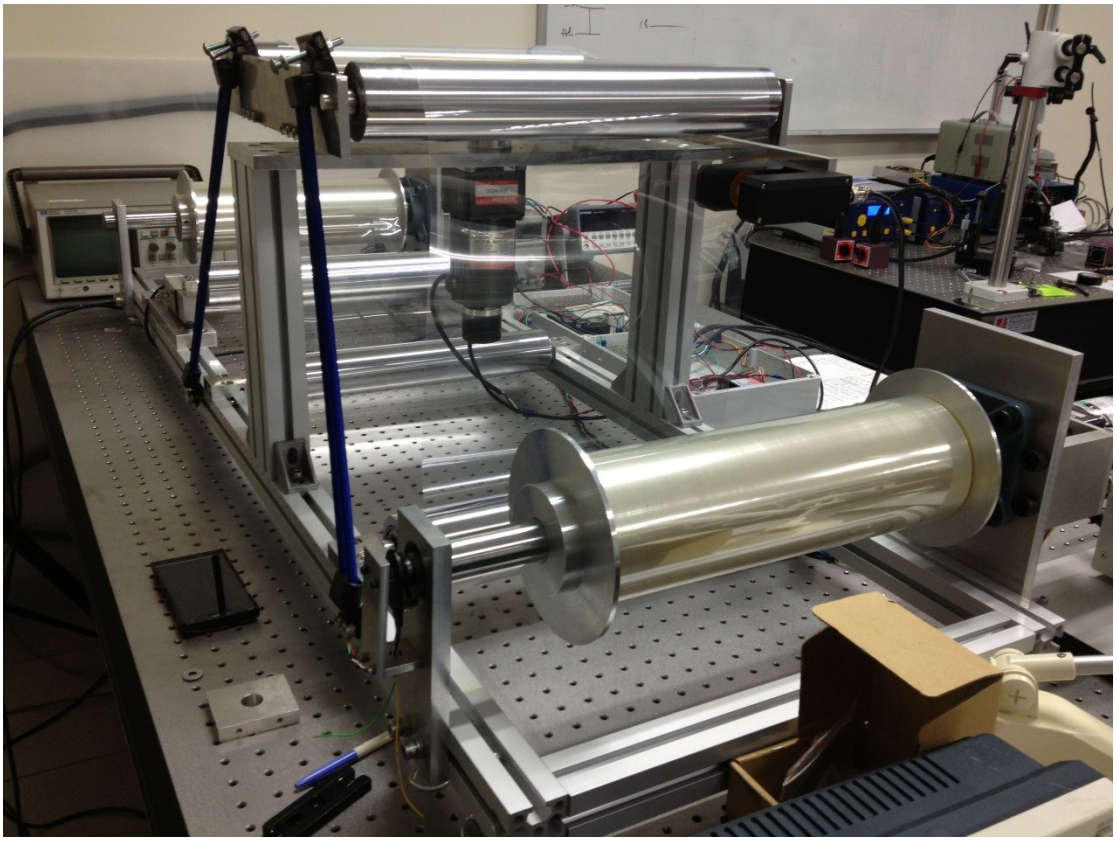

Figure 3-26: System view from angle 2

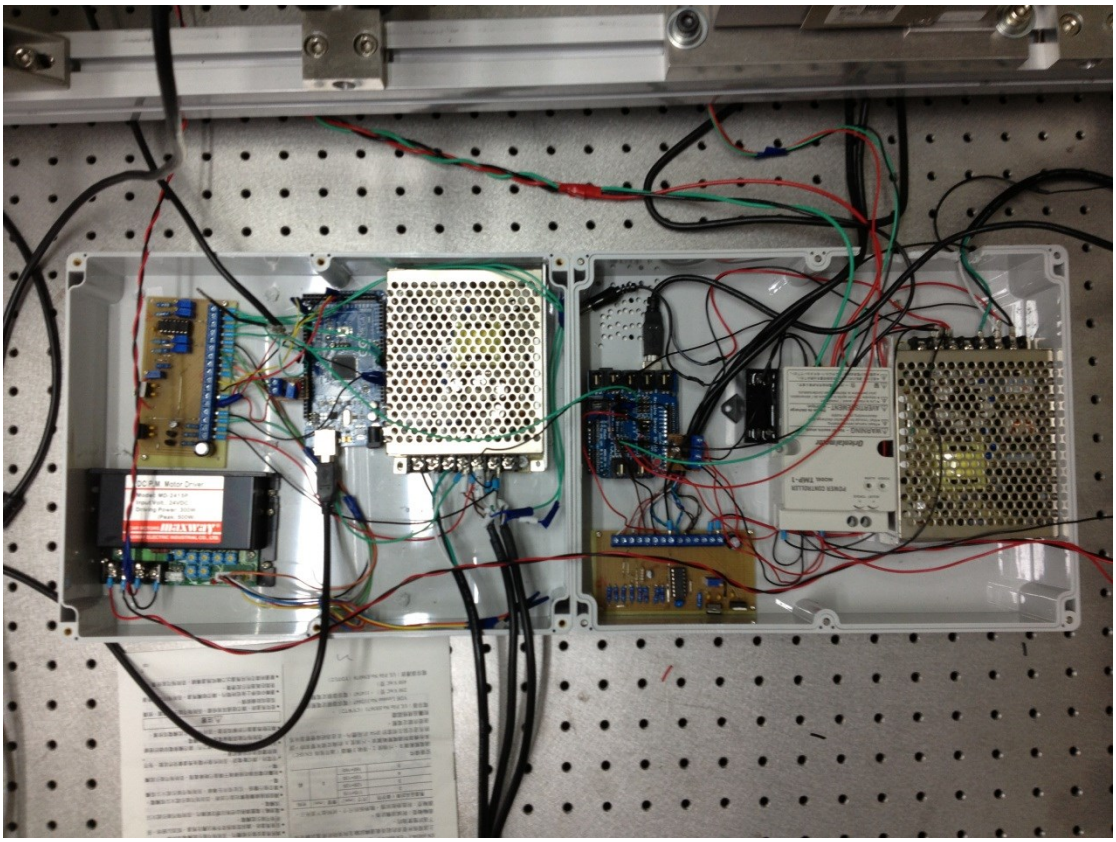

Figure 3-27: Electronics control box

Chapter 4. Sensors and actuators instrumentation

In this project, each of the sensors and actuators (edge sensor, hysteresis brake/clutch and load cell) has a different characteristic behavior and output voltage range. However, the Microcontroller (Arduino, Atmega328P) used in this project only accepts input voltages range between 0 to 5V. Therefore, additional calibration and instrumentation are required for such application. This section will focus on the sensors instrumentation and calibration on the Roll-to-Roll application. Theory and equations are introduced for interfacing and linearization of edge sensors operating in nonlinear region. In addition, experimental setup is applied for measuring the input and output of the sensor. The electronics hardware for microcontroller interfacing is also demonstrated. Finally, the corresponding experimental results are plotted and linearized for non-linearity on the output.

4.1. Instrumentation

In order to interface with the controller, signal conditioning circuit is often required to amplify the required signal. In the case of microcontroller, the input range is between 0 to 5V. Additional circuitry is required if the input signal from the sensor is only in the mV range. In this project, the interfacing circuit is based on a differential amplifier [39] which has equation of:

$$V_{out} = \frac{R_2}{R_1}(V_+ - V_-) \quad (4\text{-}1)$$

The negative terminals can be supplied with a constant voltage which has amplitude equal to the minimum sensor output voltage. The gain of the circuit can be the ratio between the maximum output voltage of the sensor and the maximum microcontroller sensing voltage. Hence the result is changed to:

$$V_{out} = \frac{R_2}{R_1}(V_+ - V_{Sense,Min}), \quad (4\text{-}2)$$

Where R1 and R2 are two resistors for the amplifier gain

4.2. Linearization

There are two parts of the edge sensor which produce non-linear output. The linearization technique using Taylor series expansion suggested by Nise [40] is summarized in this section.

Assume a nonlinear system operating at point A, [x0, y0]. Any small changes in the input can have a corresponding output affected by the slope of the curve at that point. Hence, if the slope of the curve at point A is m, then any small excursion of the input about point A, δx, will have small changes in the output related to the slope. That is

$$[f(x) - f(x0)] \approx m(x - x0) \quad (4\text{-}3)$$

and

$$f(x) \approx f(x0) + m(x - x0) \approx f(x0) + m\delta x \quad (4\text{-}4)$$

This allows using the Taylor series expansion [40] to expresses the value of a function in terms of the value of that function at a particular point as

$$f(x) = f(x_0) + \left.\frac{df}{dx}\right|_{x=x_0} \frac{(x-x_0)}{1!} + \left.\frac{d^2f}{dx^2}\right|_{x=x_0} \frac{(x-x_0)^2}{2!} + \cdots \quad (4\text{-}5)$$

Higher-order terms can be neglected for small excursion from x to x_0. Thus, the expansion can be changed to

$$f(x) - f(x_0) \approx \left.\frac{df}{dx}\right|_{x=x_0} (x - x_0) \quad (4\text{-}6)$$

4.3. Measurement and setup

Experimental setups for load cell and edge sensor were conducted. The output characteristics curve of the brake is already provided by the manufacture. The load cell is tested by applying different weights on sensor for different output voltage. The edge sensor is tested by a displacement Micrometer for different output voltage.

4.3.1. Load cell

Two 10 kg load cells from Tedea-Huntleigh [41] are used for measuring the web tension in the system. The setup of the experiment is illustrated in Figure 4-1. A power supply provides 10V between the two inputs (+ve and –ve) of the load cell. The load cell consists of a Whitestone bridge which outputs 2mV/V. Accurate weight measurement were conducted by placing different weights on the scale which can provide a resolution of 1g. The weights are then placed on the single point of the load cell and output readings are recorded from digital multimeter. Different data points have been taken in order to verify the accuracy of the reading from digital multimeter. Different data points have been taken in order to verify the accuracy of the reading.

The schematics of the load cell can be seen in Figure 4-2. The output of the sensor can be measured between the two output terminals. However, the –ve output of the load cell does not have the same potential as the –ve input. Therefore, a non-inverting amplifier cannot be used in this application for amplifying the output signal of the load cell.

Due to the difference in potential, the output reading is taken from the difference between the two terminals. The signal is then amplified with the correct gain to interface with the controller as shown in Figure 4-3 using (4-1). A high speed JFET amplifier (LF147) [42] is used to provide a high slew rate (13V/µs) and 2µs settling time for fast performance readings from the load cell.

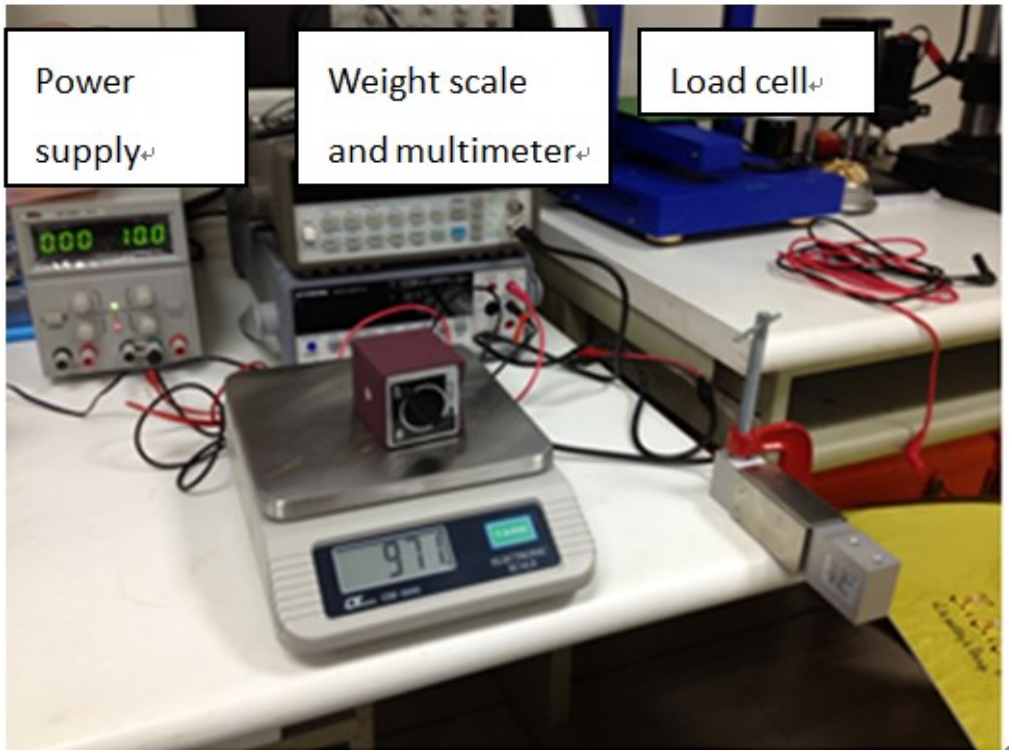

Figure 4-1: Experimental setup for load cell

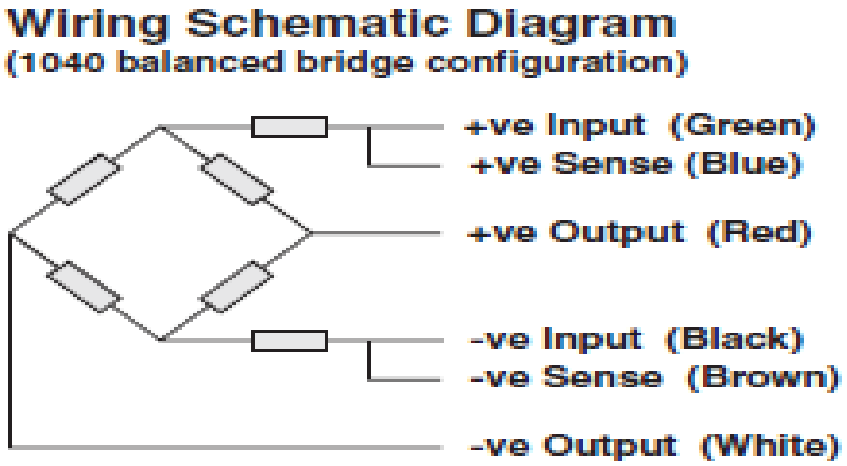

Figure 4-2: Schematics of load cell circuit [29, 43]

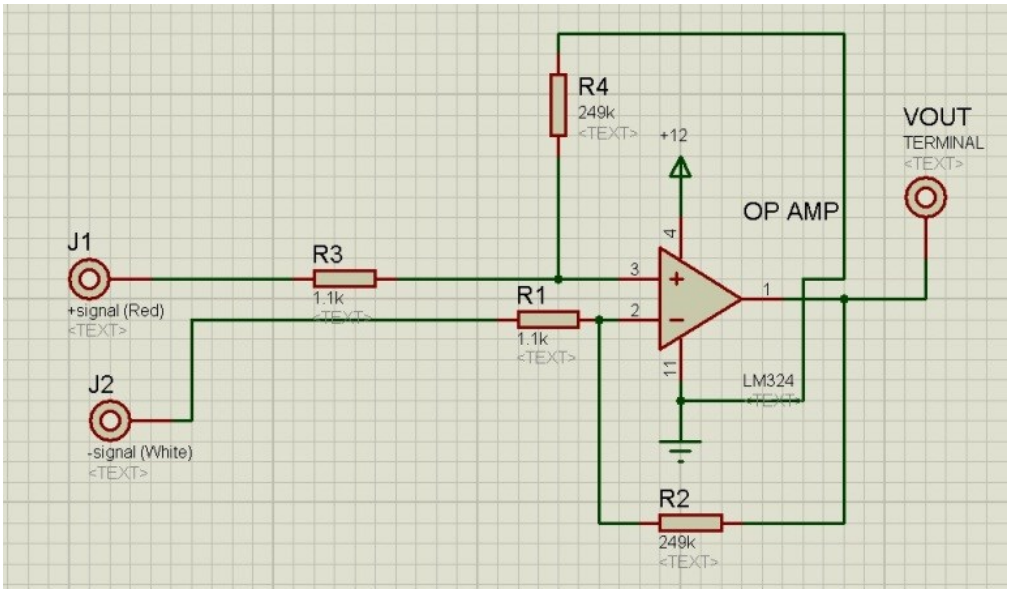

Figure 4-3: Signal conditioning circuit for load cell

4.3.2. Edge sensor

As seen from Figure 4-4, experimental setups for edge sensor measurement consist of an ultrasonic edge sensor (SNEC-USS02), a translation stage and leveled optical table. The ultrasonic edge sensor accepts ±12V power supply and output ±11V signal to indicate the coverage of the ultrasonic sensor. In this experiment, translation stage and sensor are both fixed on the optical table. The translation stage is moved to the center reference point of the edge sensor where the sensor outputs

0V. After that, the translation stage is moved in the scale of micrometer increment/decrement steps until the sensor produces output voltage values of positive 11V and negative 11V, respectively.

Due to the different outputs and operating conditions for the three components, additional hardware signal conditioning circuit is required for the controller. As seen from Table 4-1, the output of the load cell produces 0mV to 20mV. The edge sensor produces output of ±11V and the brake/clutch has a maximum operating voltage of 24V. However, the input/output range for the microcontroller is between 0V to 5V. Designs signal conditioning circuit between the three sensors/actuators are required and will be illustrated in the following sections.

The signal conditioning circuit can be seen in Figure 4-5. The Edge sensor outputs ±11V signal to indicate the coverage of the ultrasonic edge sensor. It is required to convert the output voltages between 0V to 5V. The signal conditioning circuit design for the edge sensor is also based on the difference amplifier. The voltage difference in this application is between a reference voltage of -11V and the output of edge sensor. However, the gain of this signal conditioning circuit is halved, as the reference voltage is a negative value which can cause the formula (4-1) to $V_{out} = \frac{R_2}{R1}(V_+ + V_-)$. Finally, precision adjustable resistors [43] are used on each input to provide the exact gain required for the output.

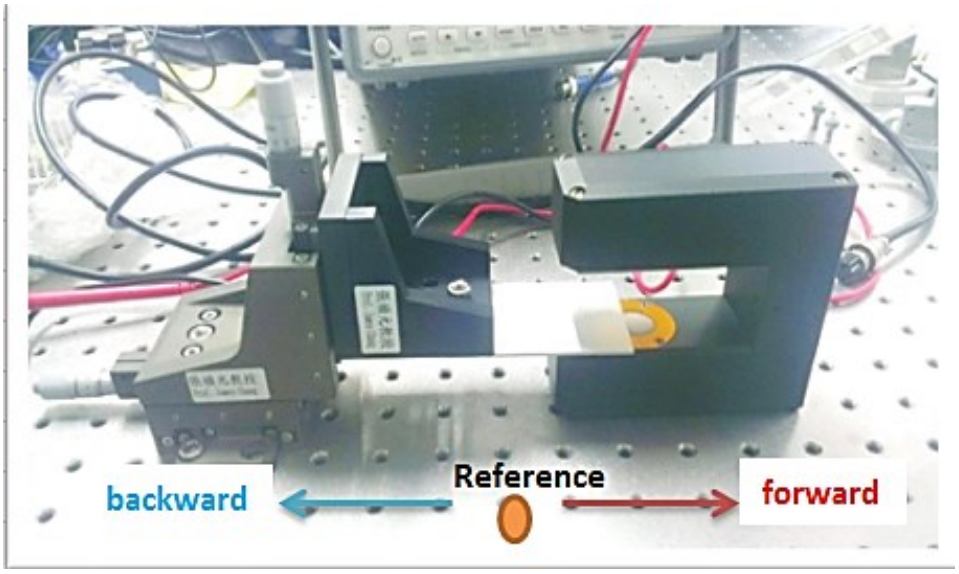

Figure 4-4: Experimental setup for edge sensor

Table 4-1: Comparison of Voltage Ranges

Type	Voltage range Output (input)	Required voltage range
Load cell	0-20mV (2mV/V)	0-5V input
Brake/clutch	24V (input)	0-5V output
Edge Sensor	±11V	0-5V input

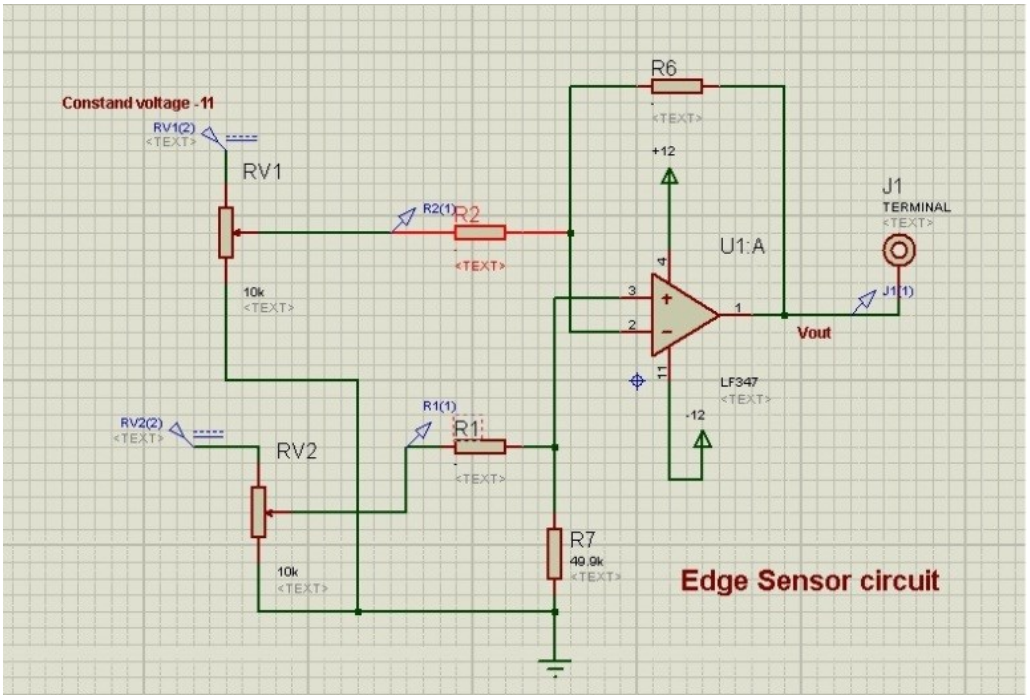

Figure 4-5: Signal conditioning circuit for edge sensor

4.3.3. Hysteresis Brake

The hysteresis brake used in this project can produce torque through a magnetic air gap without magnetic particles or friction components [28]. The brake of the system can be operated at 24V to provide maximum tension to the system. In order to provide the different tension for different kinds of web materials, the torque produced by the brake is needed to be altered. The tension of the web is controlled by the microcontroller through the pulse width modulation. The brake is connected to the transistor as shown in Figure 4-6 which acts as a switch to turn the brake ON and OFF using different duty ratio for each required torque.

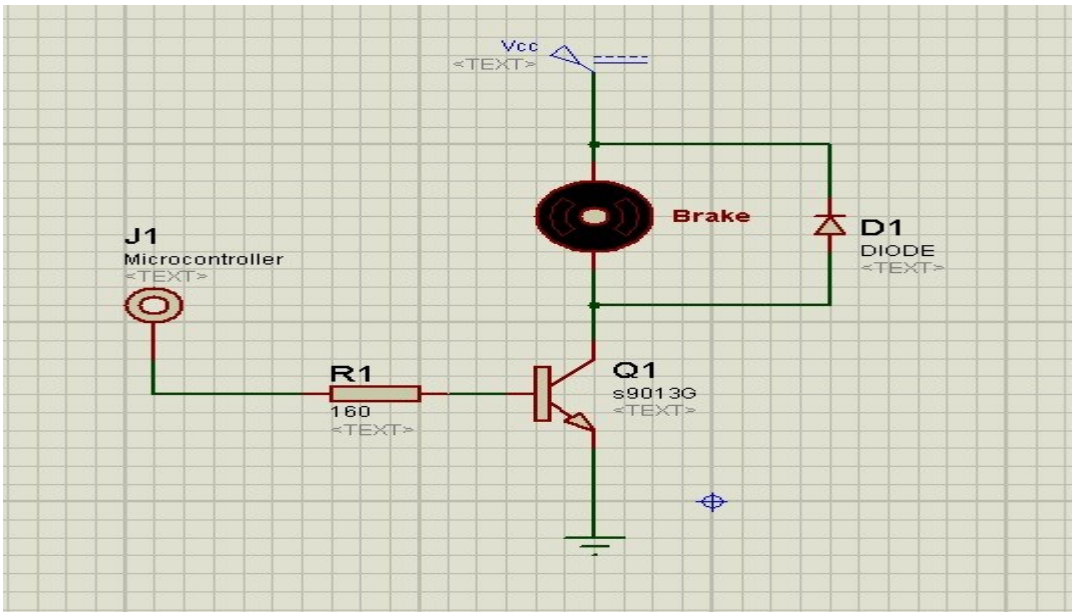

Figure 4-6: Brake actuating circuit

4.4. Experimental Results

4.4.1. Load Cell

The output of the load cell is measured and plotted in Figure 4-7. The relationship between the voltage and weight is shown to be linear. The output range of the load cell is between 0 to 20mV. The output of the signal that is conditioned by the designed circuit is shown to provide a reading between 0 to 5V. This linear relationship is demonstrated in Figure 4-8. The equation of the sensor reading after signal conditioning is

$$Y = 0.44XL + 0.27 \ , \qquad (4\text{-}7)$$

where YL is the load cell's output voltage in mV and XL represents the applied load in kilogram

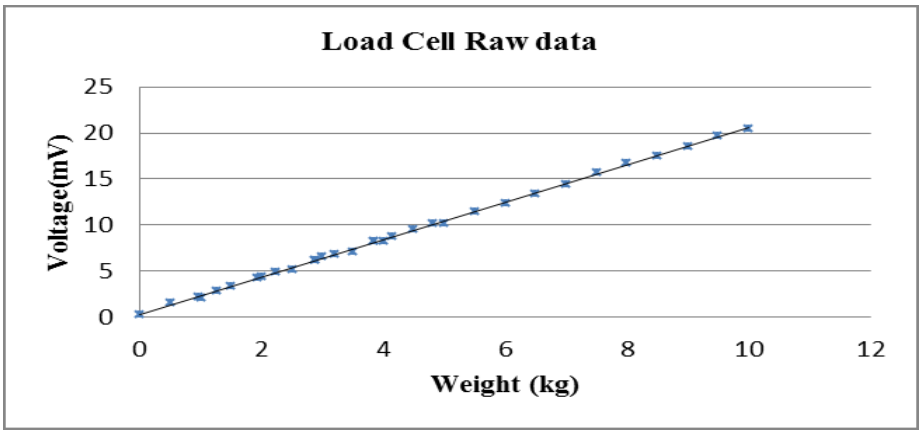

Figure 4-7: Load cell sensor output

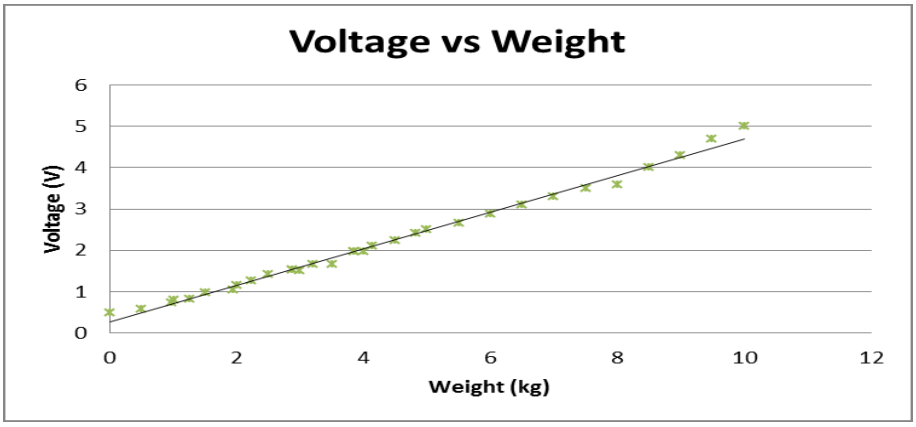

Figure 4-8: Load cell sensor output after Signal conditioning

4.4.2. Edge sensor

Figure 4-9 illustrates the sensor output for both before and after signal conditioning circuit. It can be seen that the output of the sensor have a linear region between -2mm and 2 mm. A straight line is fitted using Best-Fit Straight Line method [44] in the linear region to map the linearity of the sensor output. Equation describing such linear relationship is

$$YE = -0.94XD + 2.5 \tag{4-8}$$

where YE is the edge sensor's output voltage in mV and XD represents the displacement in mm.

On the other hand, the sensor is shown to have two non-linear regions for displacement over 2mm and -2mm. The non-linear region of the sensor is linearized using Taylor series. This is done by having derivatives equations in two non-linear, regions, -6 mm to 0 mm and 0 mm to 6 mm.

$$f(x) = \begin{cases} y = -0.5057x^2 - 4.4905x + 0.1483, & -6 < x < -2 \\ y = 0.6411x^2 - 5.5467x + 0.408, & 2 < x < 6 \end{cases} \tag{4-9}$$

In (4-9), *x* is displacement in mm and f(x) is the output voltage in V. Gradient *m* from (4-4) is then obtained at each of the input point. The voltage evaluation *f(x0)* is then obtained at the corresponding point. Thus, applying (4-4) or (4-5) with high order terms neglected. The linearized lines are shown on the Figure 4-10 and Figure 4-11. It can be seen from the figures that the gradient of the linearized line is changing from positive to negative as the displacement is changing from -6 to -2mm. Similarly, the gradient is also shown to change from positive to negative as the displacement is approaching from 2mm to 6mm

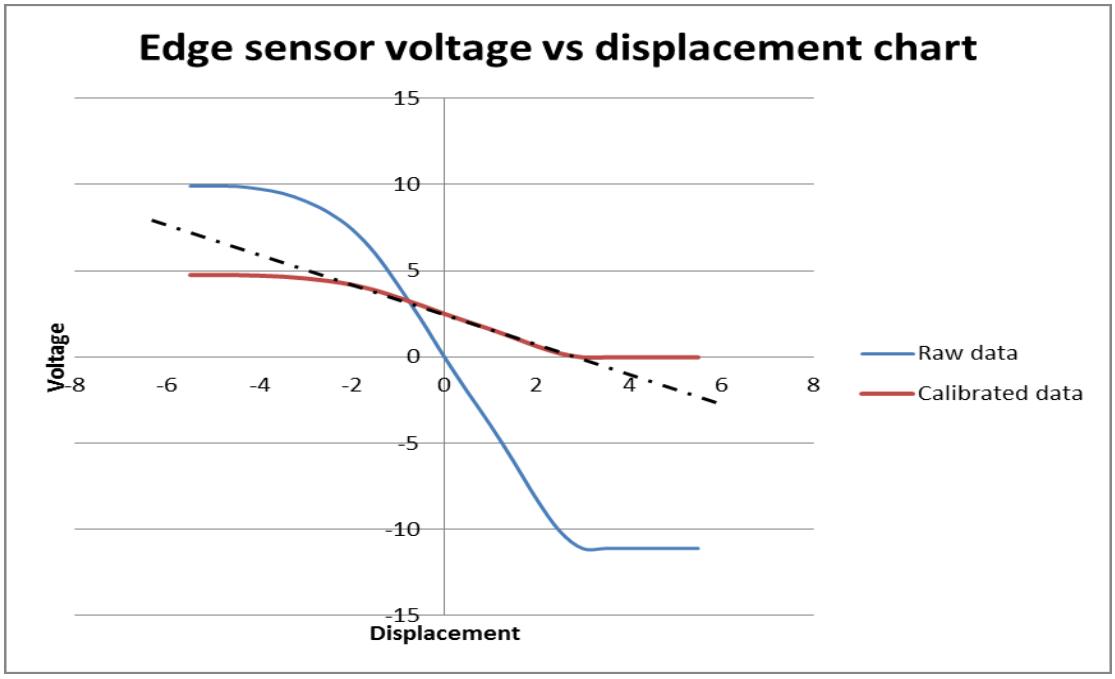

Figure 4-9: Edge sensor output with and without signal conditioning

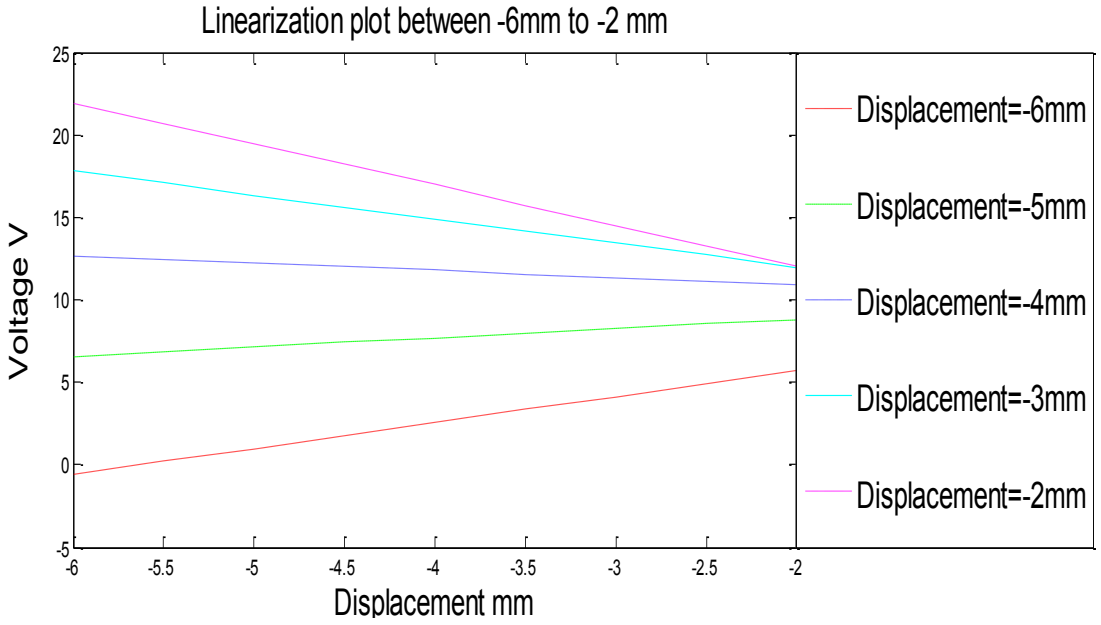

Figure 4-10: Edge sensor linearization for displacement from -6mm to -2mm

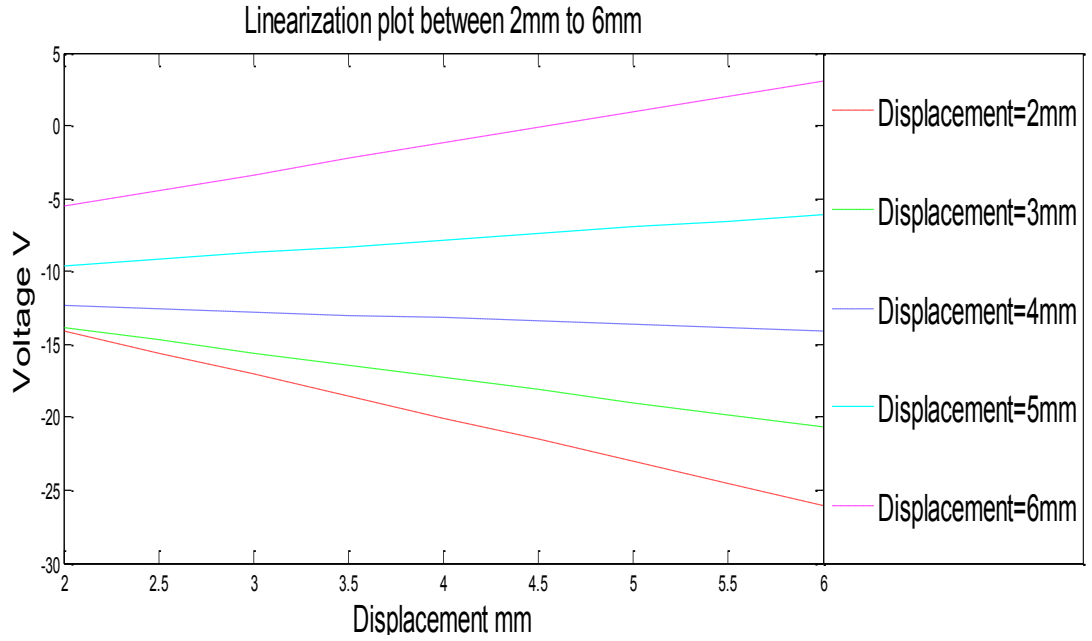

Figure 4-11: Edge sensor linearization for displacement from 2mm to 6mm

4.4.3. Brake

Torque characteristic curve for the brake was provided by the manufacturer. As seen from Figure 4-12, a linear behavior is shown to be above 15V. In order to have a

linear relationship between input and output, a straight line is plotted on the linear region of the curve. The equation of the straight line can be calculated to map the relationship between input and output. The equations of the straight is

$$\boldsymbol{YB = 0.013XB - 0.16,} \quad \text{(4-10)}$$

where YB is the brake's output torque Nm and XB represents the supplied voltage in V.

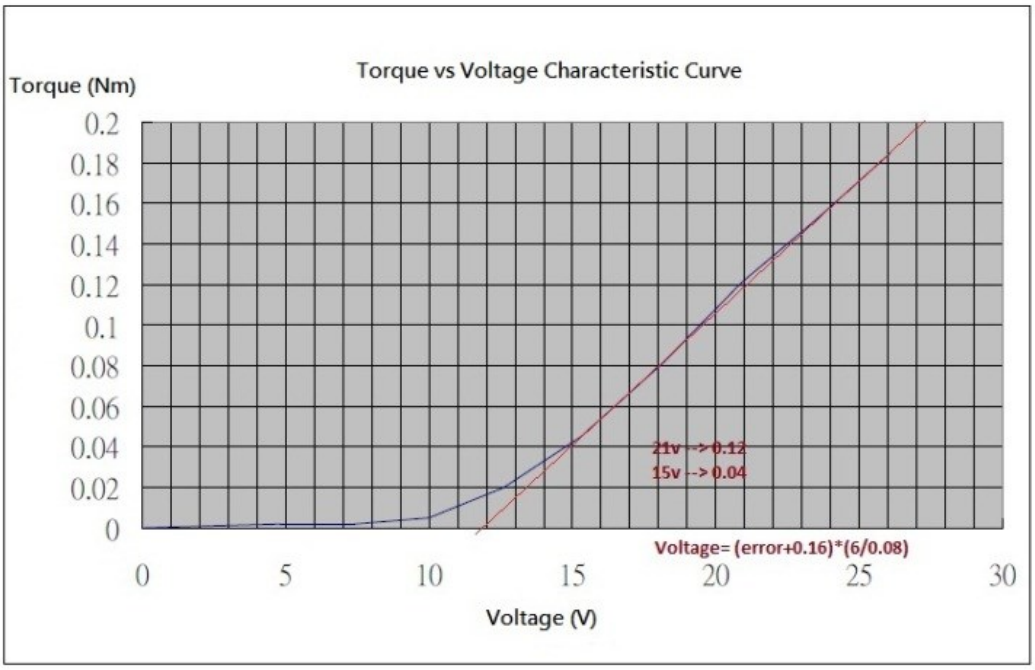

Figure 4-12: Brake Characteristic curve with Straight line fitted

4.4.4. Torque Motor with controller

There are three operations required for the torque motor, such as, clockwise (CW), counterclockwise (CCW) and stop. The stop operation does not have a dedicated input pin, but when both CW and CCW pins are turned ON simultaneously, the motor will stop. The input signal connection can be seen in Figure 4-13. The input signals are photo-coupler inputs and control circuit terminals are isolated from dangerous voltages based on reinforced insulation. The default setting is sink logic,

which means each of the input pins (CW and CCW) are required to be connected to the input COMMON in order to perform an operation. However, it is required to have a switch which can be controlled automatically between these terminals. Therefore, additional switching circuit is made as shown in Figure 4-14. Two transistors are used for the three machine operations (CW, CCW and stop). The base of each transistor is connected to the microcontroller switching control. The emitters of the transistors are both connected to COM. Each of the collectors is connected to CW and CCW. The freewheeling diodes are also used to protect the transistors from reverse current.

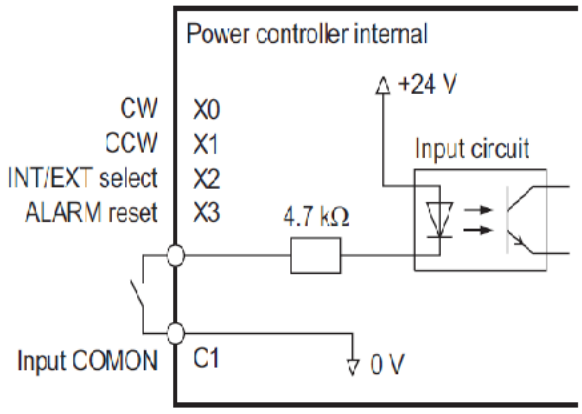

Figure 4-13: Sink logic torque motor controller/driver input signal connection [45]

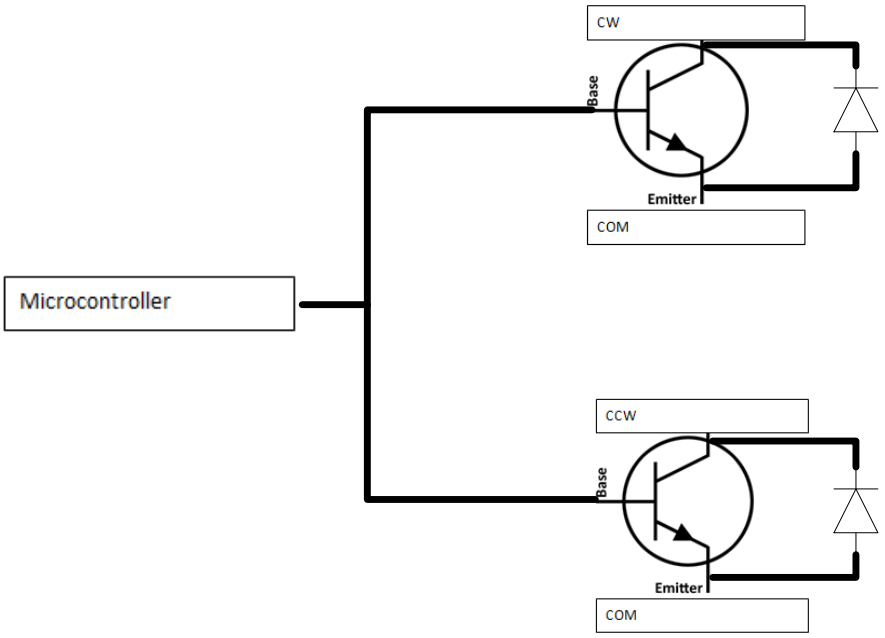

Figure 4-14: Additional switching circuit for control operation

4.4.5. Servo Motor driver with controller

The servo motor driver also is sink logic where the signal is connected to the common. Since the signal will have to connect to COM when it needs to be triggered, additional circuit will need to be applied. Therefore, the connection between servo motor driver and the controller is similar to the previous section where the torque motor driver is connected to the microcontroller. As shown in Figure 4-15, each of the signals (1 to 3) is connected to the microcontroller and the MOSFETs act as switches between the direction pin and COM. Depending on the operation on the servo motor, the action for switching between connections is chosen as shown in Table 4-2.

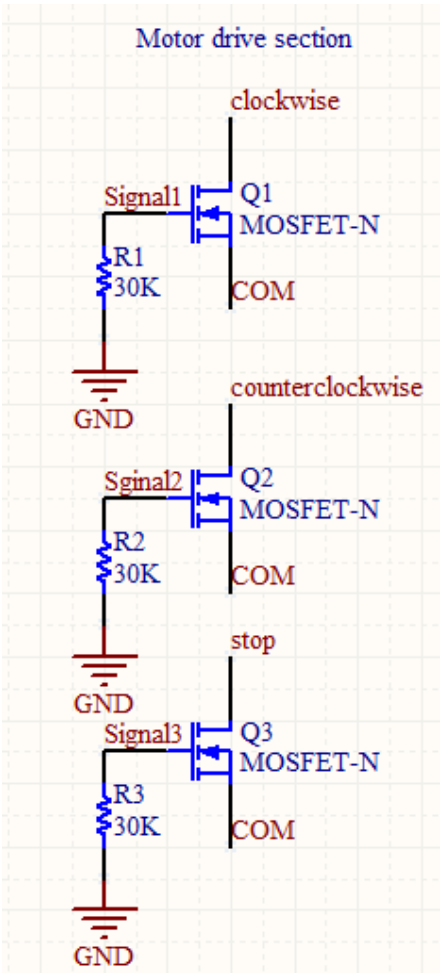

Figure 4-15: Switching schematics

Table 4-2: Servo motor operation table

Operation	**Action**
clockwise	Connect CW pin to COM
counterclockwise	Connect CCW pin to COM
stop	Connect Stop pint to COM

Chapter 5. Guide system simulation

In this chapter, lateral motion system model is discussed with supporting theory. Roll-to-roll control system integration is realized with a list of sensors and actuators.

Centre pivoted displacement web guides control system is designed with PID controller. Finally, the result is simulated and plotted to show performance of such guide system.

5.1. System Model

The block diagram of the conventional displacement guide is shown in Figure 5-1 [22]. Each of the blocks is filled with the dynamics of different parts of the system. The set point is input to the controller, where in our example is the PID controller. After that, it passes through to the actuator with DC Servo motor. It is then passes through to the actuator and summed with the lateral error. Finally, the result is sensed on the exit span and feed back to the original set point for adjustment.

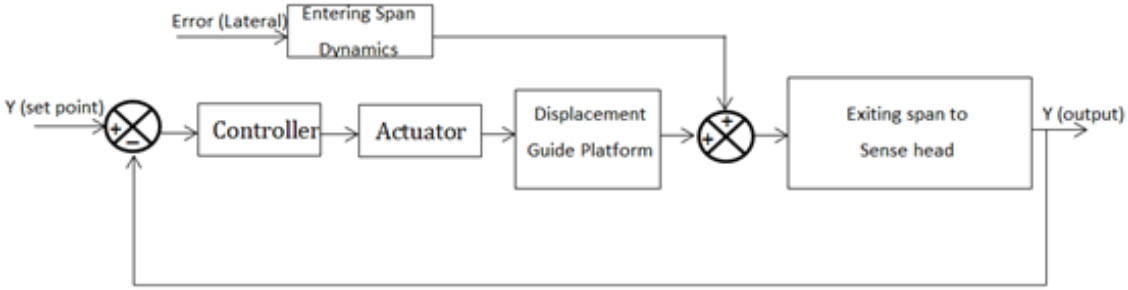

Figure 5-1: Block diagram of conventional displacement guide.

By using the previous derived differential equation, the response at Entering span dynamics can be considered. As shown in Figure 5-2, the two rollers are parallel and fixed, with the length of the free span L. The web input displacement at $x_0$isy_0. The output of the web displacement at $x_L$isy_L. The web's angle relative to the roller at $x_L$is $\frac{y_L - y_0}{L}$. the downstream roller is stationary. Therefore, from equation:

$$\frac{dy_L}{dt} = -V\vartheta + \frac{dz}{dt}, \quad (2\text{-}9)$$

$$\frac{dy_L}{dt} = -V\frac{y_L - y_0}{L}, \tag{5-1}$$

Or taking the Laplace transform and assuming zero initial conditions,

$$SY_L(s) = -\frac{V}{L}Y_L(s) + \frac{V}{L}Y_0(s). \tag{5-2}$$

Hence, the transfer function can be rearranged to:

$$\frac{Y_L(s)}{Y_0(s)} = \frac{1}{\tau_1 s + 1}, \tag{5-3}$$

Where $\tau_1 = \frac{L}{V}$ (5-4)

τ is the time required by a point on the web to traverse the free span.

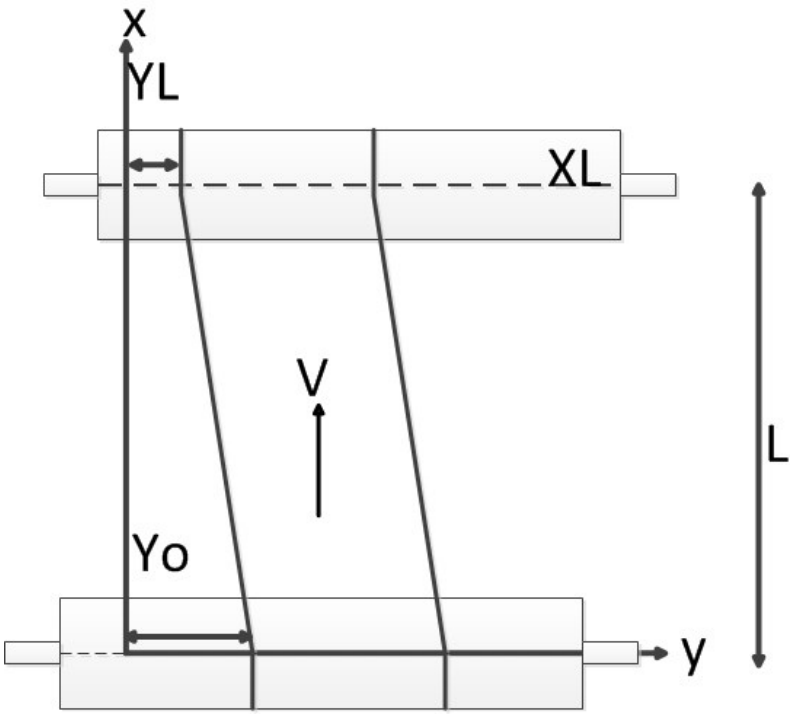

Figure 5-2: Schematic for Derivation of Response at Fixed Roller.

Shelton [22] has given an explained derivation of transfer function of a general Two-Roller Displacement Guide Dynamics. However it is be applied as a foundation to the function in this project. The rollers are assumed to be small in relation to the web spans, so the transport lags can be neglected. The derivation is based on Figure

5-3. The lateral motion of the first is $(1 - L/L_1)z$; therefore, its velocity is $\left(1 - \frac{L}{L_1}\right)\left(\frac{dz}{dt}\right)$. Substitute into The differential equation of motion of the entering span from (2-9):

$$\frac{dy_{L2}}{dt} = -V\left(\frac{y_L}{L}\right) + \left(1 - \frac{L}{L_1}\right)\left(\frac{dz}{dt}\right) \tag{5-5}$$

The above equation (5-5) can be converted to the transfer function:

$$\frac{dy_{L2}}{dt} = \frac{\left(1 - \frac{L}{L1}\right)\tau_2 s}{\tau_2 + 1} \tag{5-6}$$

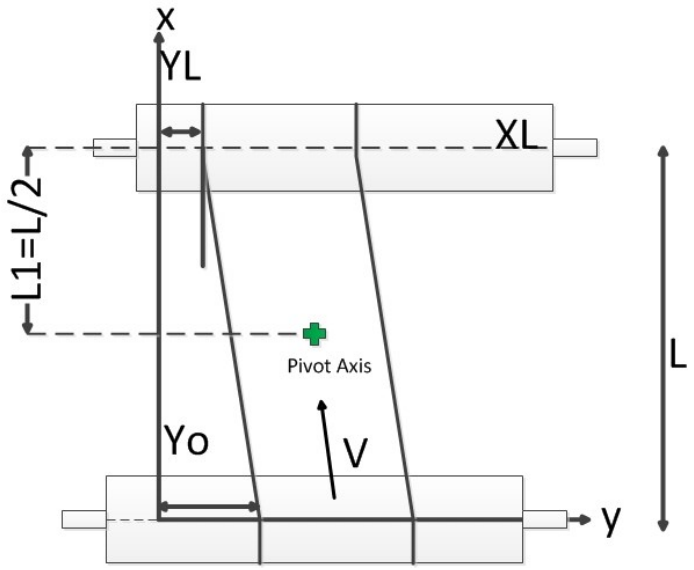

Figure 5-3: Schematic for Derivation of Response at displacement guide.

Finally, the exit span of displacement web guide [22] is derived as

$$\frac{Y_L(s)}{Y_0(s)} = \frac{\tau_3\left(1 - \frac{x_3}{L_3}\right)s + 1}{\tau_3 s + 1} \quad , \tag{5-7}$$

where: L_3 is the exit span length; x_3 is the distance from the sense head to the roll; τ_3 is $\frac{L_s}{V_s}$.

5.2. DC motor modeling

The modelling of dc motor is based on the equivalent circuit, which is demonstrated in Figure 5-4. In reality, a controllable voltage source *V* is applied to the armature terminals to establish i_a. Therefore, the current i_a in the armature circuit is determined by V, the armature-winding resistance R, and the armature-winding inductance L. The electric circuit equation is given by:

$$\boldsymbol{V = L\frac{di_a}{dt} + Ri_a + k_e\omega} \quad (5\text{-}8)$$

The dynamic equation of the motor under load condition is given by

$$\boldsymbol{T = J\frac{d\omega}{dt} + B\omega + T_{WL};\ \omega = \frac{d\theta}{dt}} \quad (5\text{-}9)$$

where J and B are the total equivalent inertia and damping, respectively. T_{WL} is the equivalent working torque of the load. By taking Laplace transform of equation (5-8) and (5-9):

$$\boldsymbol{V_{(s)} = RI_{a(s)} + k_e\omega_{(s)} + LSI_{a(s)}} \quad (5\text{-}10)$$

$$\boldsymbol{T = SJ\omega_{(s)} + B\omega_{(s)} + T_{WL(S)}} \quad (5\text{-}11)$$

By rearrangement of (5-10)

$$I_{a(s)} = \frac{V_{(s)} - k_e \omega_{(s)}}{R + SL_a} \tag{5-12}$$

By rearrangement of (5-11), Assume $k = k_e = k_t$

$$\omega_{(s)} = \frac{T_{(s)} - T_{WL(s)}}{B + SJ} = \frac{kI_{a(s)}}{B + SJ} = \frac{k[V_{(s)} - \omega_{(s)}]}{(JS + B)(LS + R)} \tag{5-13}$$

Rearrangement of equation (5-15)

$$\omega_{(s)} + \frac{k\omega_{(s)}}{(JS + B)(LS + R)} = \frac{kV_{(s)}}{(JS + B)(LS + R)}$$

So,

$$\rightarrow \omega_{(s)} \left[\frac{(Js + B)(Ls + R) + k^2}{(JS + B)(LS + R)} \right] = \frac{kV_{(s)}}{(JS + B)(LS + R)}$$

Finally, the equation of DC motor is

$$\frac{\omega_{(s)}}{V_{(s)}} = \frac{k}{JLS^2 + JRS + BLS + BR + k^2} = \frac{k}{JLS^2 + (JR + BL)S + BR + k^2} \tag{5-14}$$

The equation for the DC motor with load can be represented by the transfer function block diagram as shown in Figure 5-5.

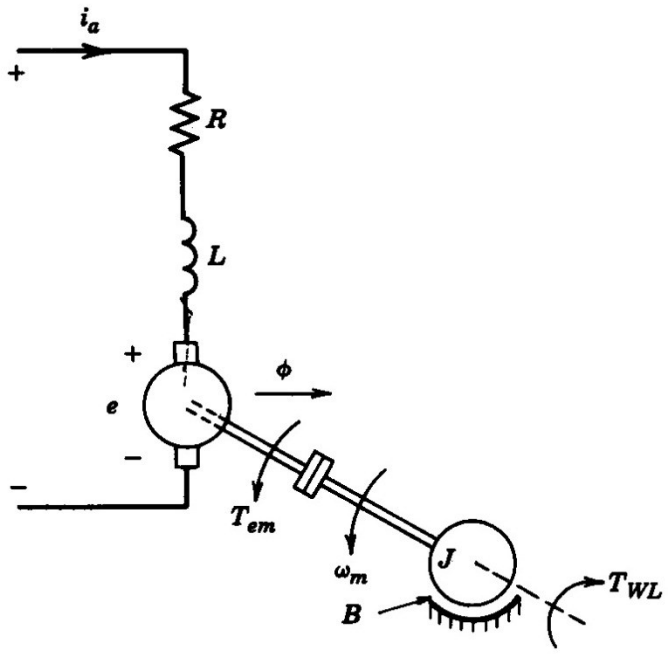

Figure 5-4: A dc motor equivalent circuit [26]

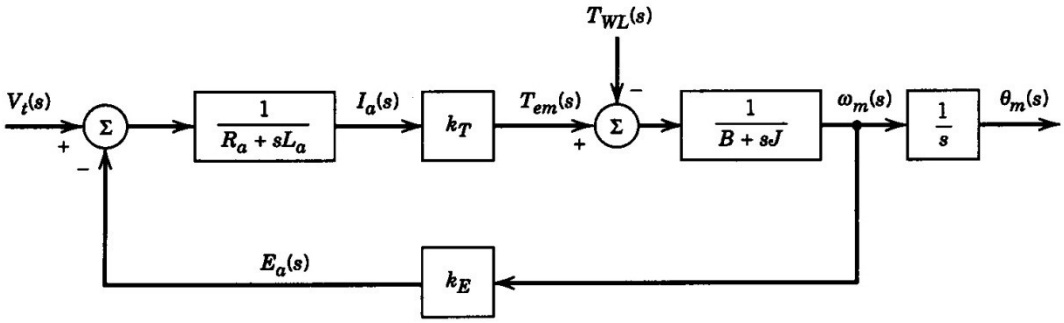

Figure 5-5: DC motor block diagram [26]

In order to model the DC motor, the parameters of the motor is required to be identified. These parameters include R, L, J B and K.

- **Find R**:

  This can be found by holding the rotating disk. Since we know (5-8), and w=0, and $L\frac{di_a}{dt}$**=0.**

Therefore, $\mathbf{R} = \frac{V}{I} = \frac{12}{3.3}$ =3.57 Ω

- **Find L**:

  This can be done by identify the rise time constant as shown in Figure 5-6:

Again this is found by holding the disk stationary and with a current to voltage converter; the motor starting curve is shown.

The electrical constant [26] is defined as

$$\tau_a = \frac{L_a}{R_a} \quad (5\text{-}15)$$

where τ_a is the electrical rise time constant.

Therefore, $\tau_a = \frac{L_a}{R_a}$ and La=τ × Ra =0.37x19.6ms x 3.57=0.0256H

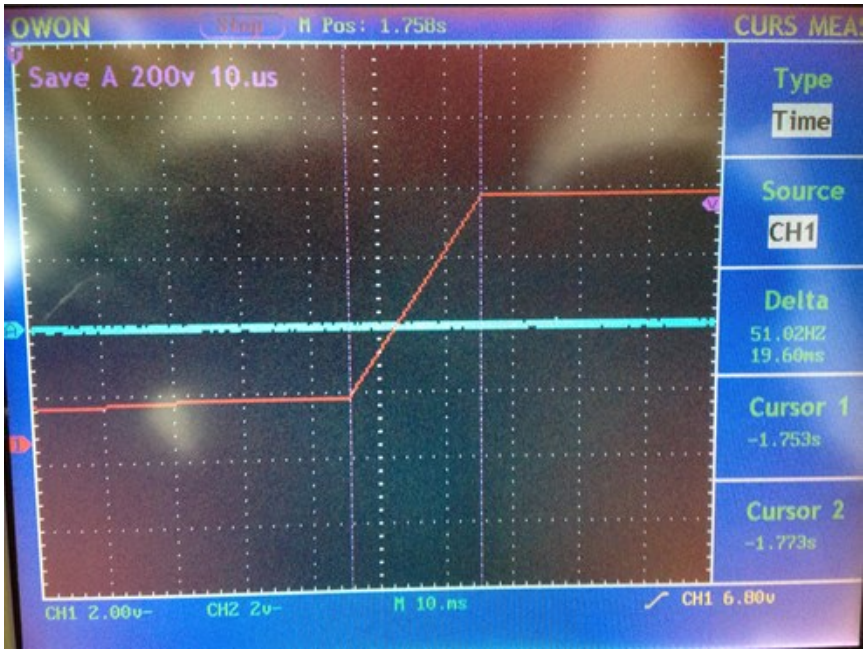

Figure 5-6: Electrical rise time with current to voltage converter

- **Find K**:

This is found by running the motor at steady state, where $L\frac{di_a}{dt}$**=0.**

$V = L\frac{di_a}{dt} + Ri_a + k_e\omega$ is then become $V = k_e\omega + Ri_a$

This is rearranged to $K = \frac{V-Ri}{\omega} = \frac{24-3.57\times0.3}{188} = 0.122$

- **Find B and J**:

This is found from the rise and fall time constant as shown in Figure 5-7 and Figure 5-8. The mechanical rising constant [26] is defined as:

$$\tau'_m = \frac{\tau_m RB}{RB + k^2} \quad (5\text{-}16)$$

and mechanical falling is defined as:

$$\tau_m = \frac{J}{B} \quad (5\text{-}17)$$

From Figure 5-7, τ'_m can be calculated as 0.37% of 720ms which is 266.4ms and τ_m can be calculated as 0.37% of 3.6s which is 1.332s

By rearrangement of equation (5-16), it is shown as:

$$\mathbf{B} = \frac{\tau'_m \times k^2}{\tau_m R - \tau'_m R} = 1.04 \times 10^{-3}$$

Then Rearrangement of (5-17)

$$J = B\tau_m = 1.39 \times 10^{-3} \mathrm{m}^4$$

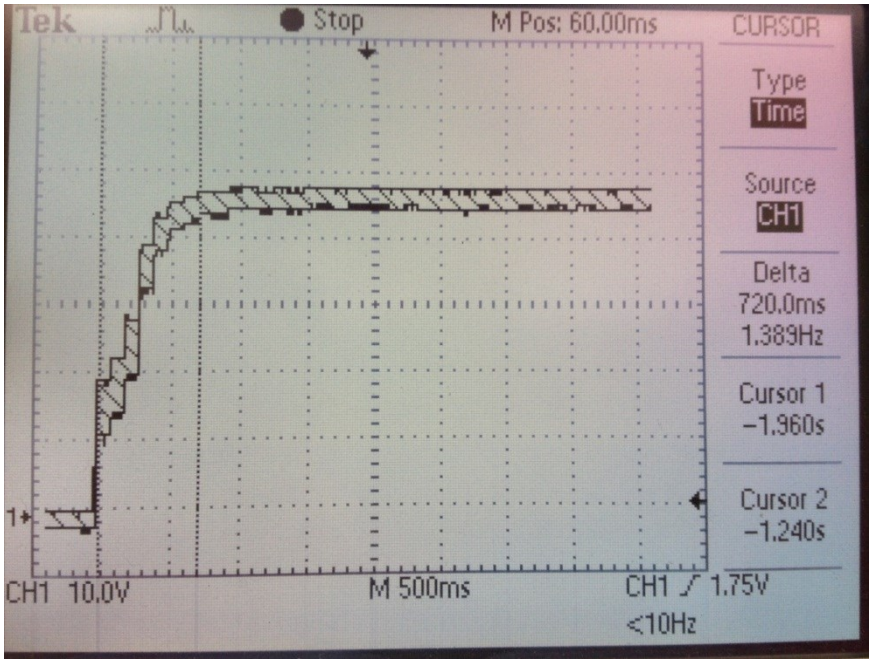

Figure 5-7: Motor start from stationary showing mechanical rise time

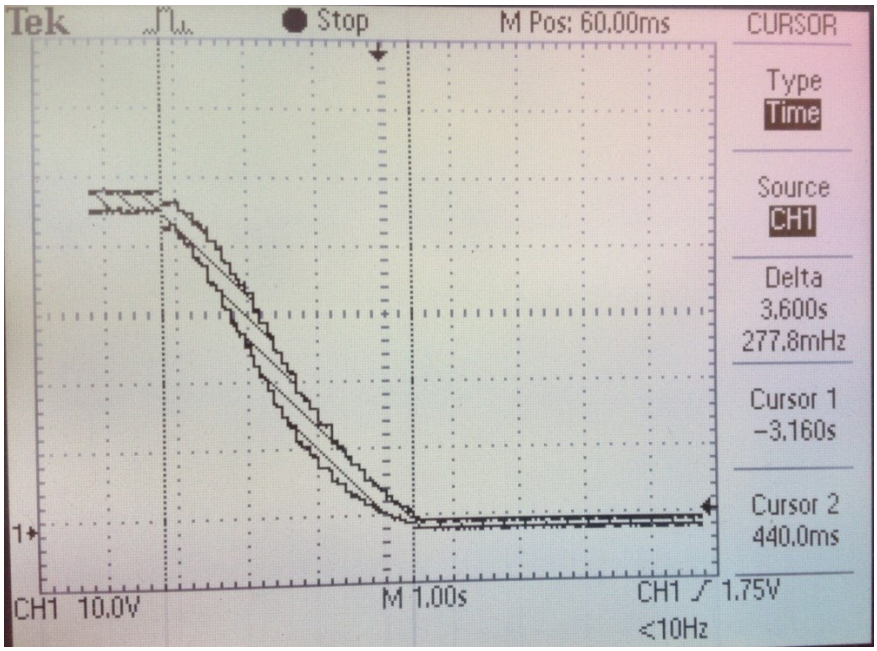

Figure 5-8: Motor stop from full speed

Therefore, the motor parameters can be seen as:

Table 5-1: DC motor parameter table

Symbol	Value
R armature resistance	3.57 Ω
L armature inductance	0.0256H
J inertia	$1.39\times 10^{-3}m^4$
B damping coefficient	1.04×10^{-3}
K constant	0.122

5.3. Design of Guide system

The design of the guide system is based on the displacement guide category, where the distance between the processes is relatively short. The pivoted axis is set in the middle position for equal amount of rotation angle between input and output of the web. The guide is actuated by a servo system which provides a feedback to the controller. The design of the guide system can be seen on the isometric view model as shown in Figure 5-9. It is supported by the aluminum frame and the motor is attached from the bottom.

There are three displacement spans in the guide as depicted in Figure 5-10. Each of the web spans is 360mm; L1 is the entry span and L2 is the guide span and L3 is the exit span. Two sensors are place on each end of the displacement guide. Sensor 1 is able to detect the input error before the web guide adjustment. Sensor 2 is placed after the web guide to detect the lateral movement changes after the web guide. The testing web materials used in this project is PET, which is 340mm width and 0.125mm thick as shown in Table 5-2. The maximum web processing velocity used in this project is 60m/min.

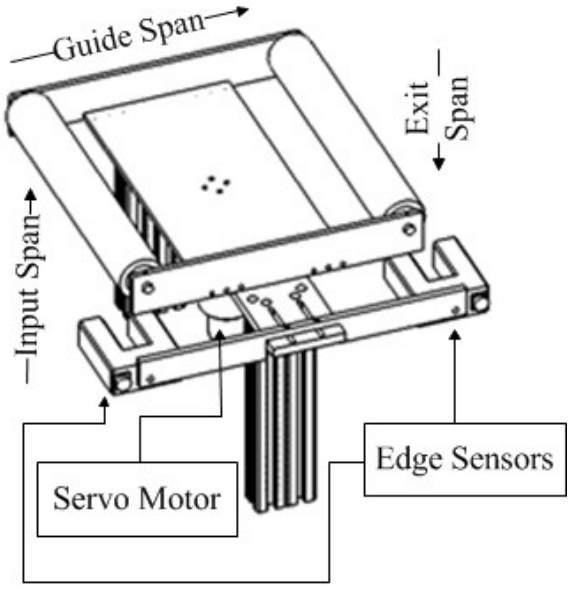

Figure 5-9: Displacement Guide Design

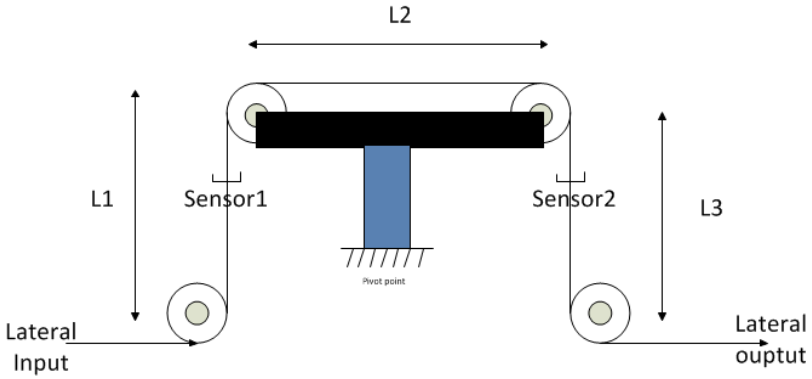

Figure 5-10: Simulated Web Model

Table 5-2: Simulation Parameter

Symbol	Parameter	Value	Unit
L1	Span length 1	360	mm
L2	Span length 2	360	mm
L3	Span length 3	360	mm
	Web Material	PET	
d	Sensing Distance	80	mm
w	Web width	340	mm
t	Web thickness	0.125	mm
V	Transport velocity	60	m/min
	Velocity to m/s	1	m/s

5.4. Controller modeling

By using the dynamic functions in section 5.1and 5.2, the dynamics of each part of the guiding system can be placed into the block diagram as shown in Figure 5-11. The actuator represents the DC motor dynamics which derived in section 5.2. The entering span dynamics, displacement guide dynamics and exit span are all included in the block diagram.

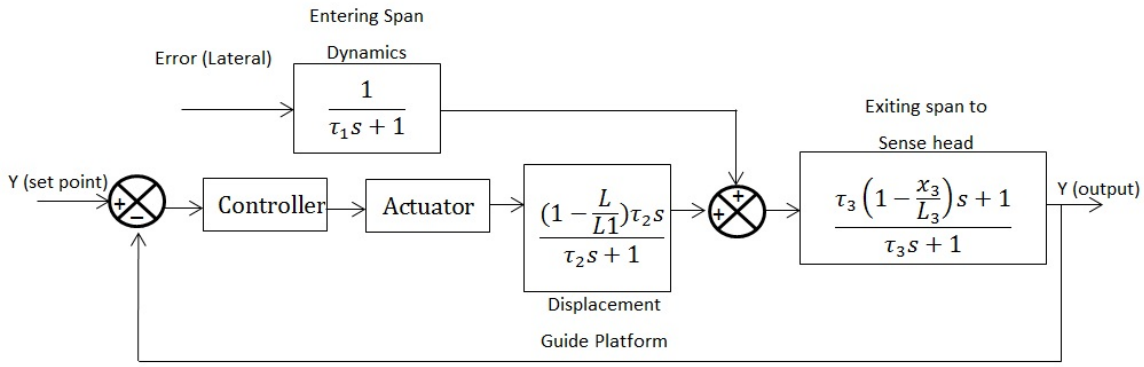

Figure 5-11: dynamics block diagram of guiding system

A PID control algorithm is also developed for the web guide lateral motion control. As seen from Figure 5-12, the desired state is input to k_p (proportional gain), k_i(integral gain) and k_d(derivative gain). The control signal is the proportional gain times the error plus the integral gain times the integral of the error plus the derivative gain times the derivative of the error. The simulation is executed using Matlab/Simulink as seen in Figure 5-13. The enlarged version of this figure is shown in Appendix 2.2. The signal is input to the PID controller and goes through the DC motor modeling and then each of the web spans. Finally, the error is feed back to the system for error correction.

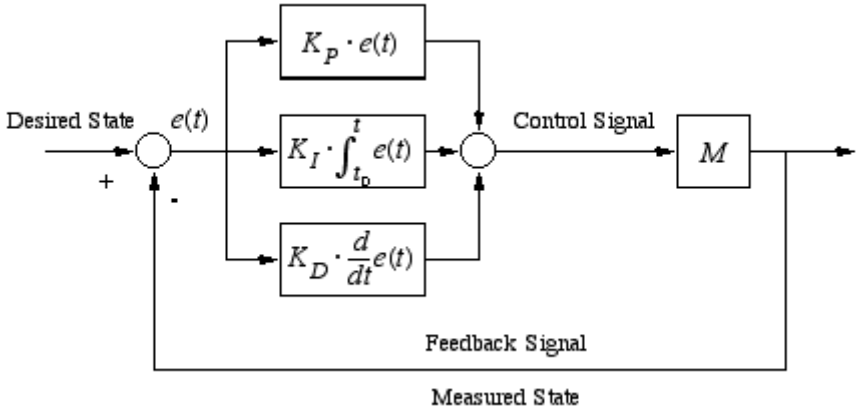

Figure 5-12: PID controller diagram [46]

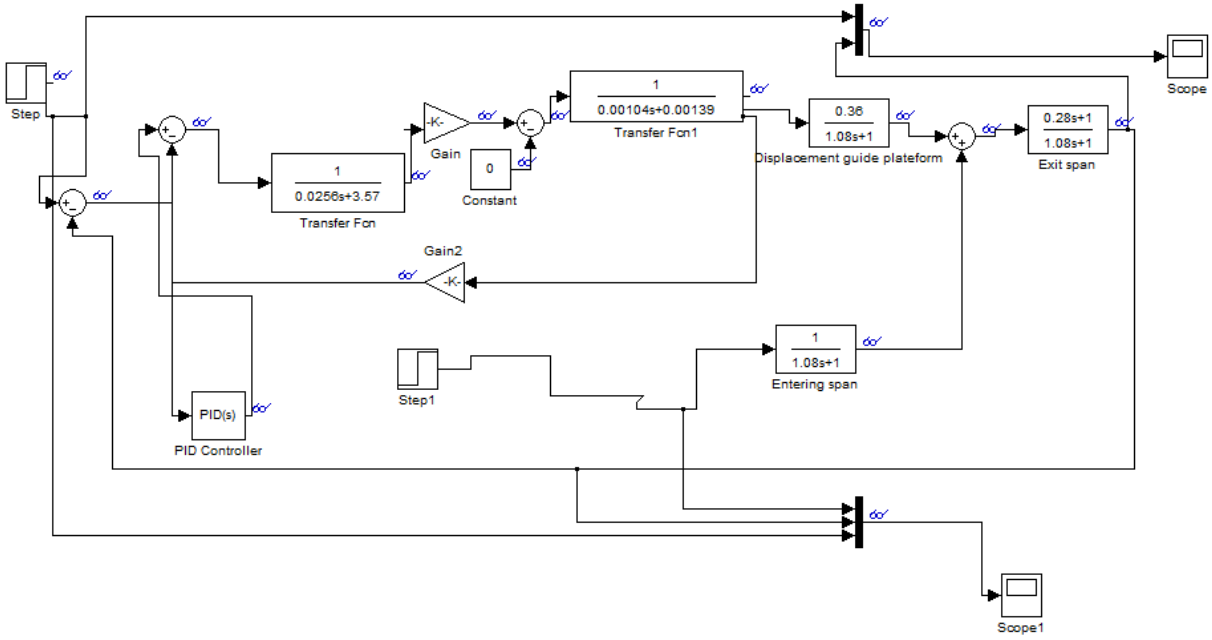

Figure 5-13: Simulink block diagram

In this project, the tuning of PID method is based on Ziegler and Nichols method [25] with following steps:

1. Reduce k_i and k_d to the minimum values.
2. k_p is set to low and gradually increased.
3. Observe the response when a small disturbance is applied to the system.

4. When continuous oscillations occur, the gain k_p and the period of the oscillations T_s are measured.

By continuously increase the proportional gain, the system starts to oscillate when k_p is equal to 20. The oscillations T_s is measured as illustrated in Figure 5-14, where T_s is equal to 27s. Therefore, the tuning table is illustrated in Table 5-3 where k_p is 12 k_i is 0.06 and k_d is 0.26.

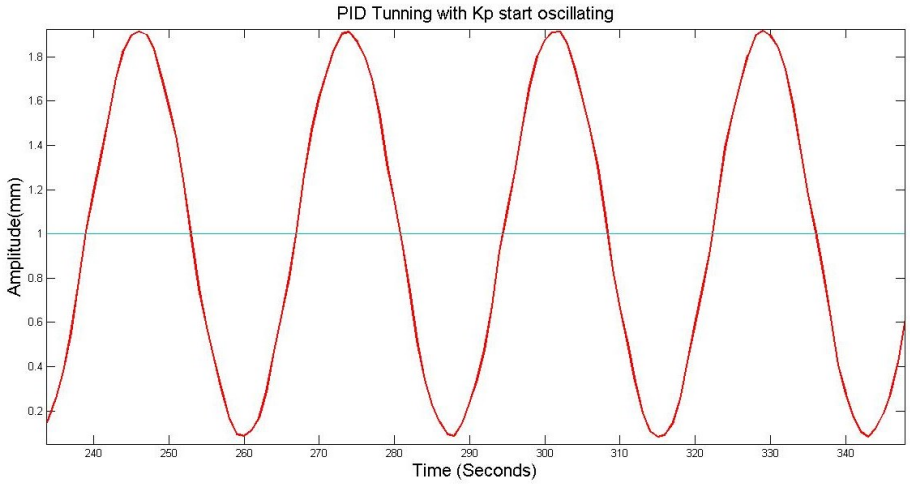

Figure 5-14: PID tuning with Ziegler and Nichols method when the system start to oscillate

Table 5-3: Ziegler and Nichol PID tuning table

Control Mode	Kp	Ki	Kd
P-alone	10.00		
PI	9.00	0.04	
PID	12.00	0.07	0.3

In order to identify the stability of the guide system, root locus is used. In control engineering [25] stable response system much have all the poles located at the negative half of the plane. The root locus of the complete system can be seen in Figure 5-15. The system has all the poles in the negative half of the plane as seen in Figure 5-16

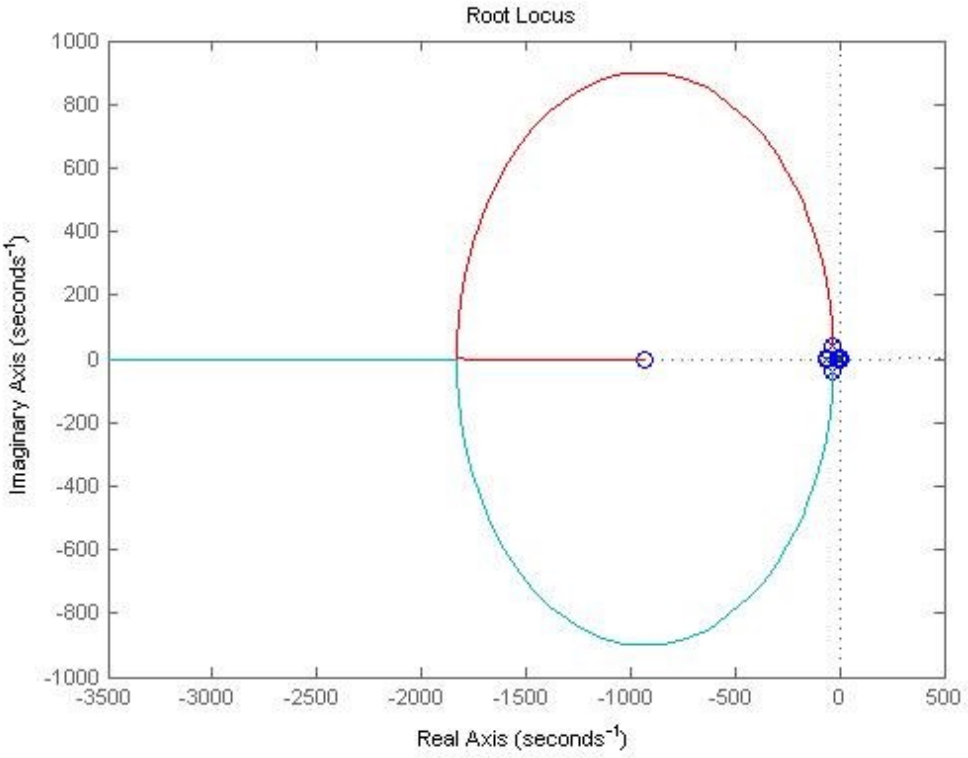

Figure 5-15: Root locus of the system

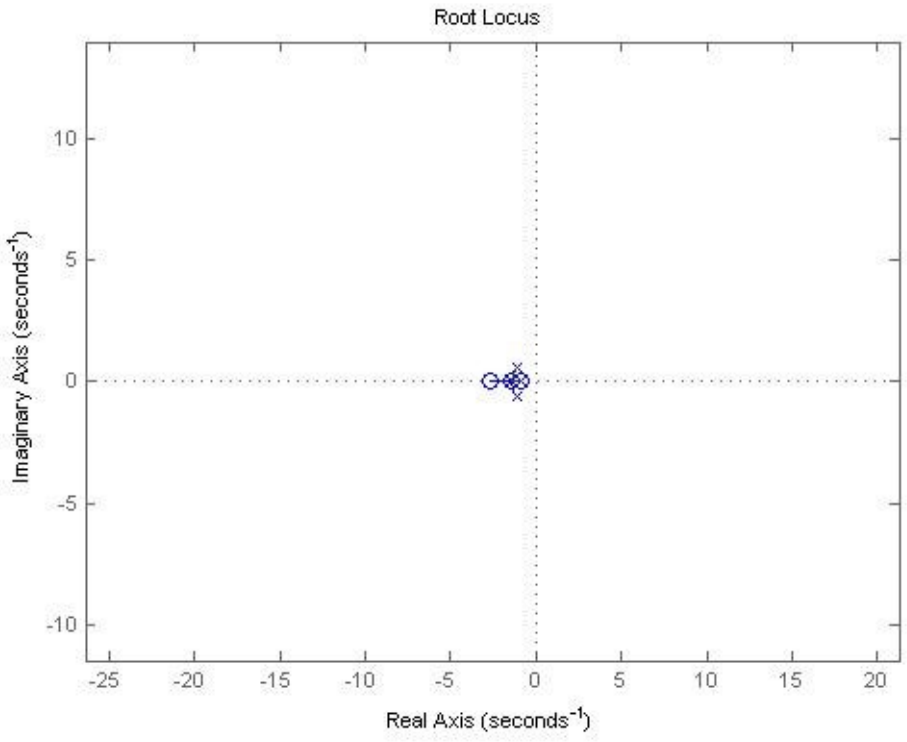

Figure 5-16: Root locus showing all the poles are on the negative side of the Real Axis

5.5. Simulation Results

The simulation is parametrically examined at the web's transport speeds of 20m/min, 30m/min and 60m/min as in the actual production line. The input set point of 1 mm is used for this simulation. The input error is applied using a sine wave with amplitude of 0.5 mm, since the lateral error of the actual production is often sinusoidal. The output of the each simulation is plotted in Figure 5-17, Figure 5-18 and Figure 5-19. In Figure 5-17, the output result is shown to have an overshoot at 10 seconds. After the output has reduced down to the position similar to the input, the output is shown to have a similar pattern to the lateral input error. However, the lateral motion is controlled within 22µm for 20m/min line speed as shown in Figure 5-17. When the line speed is increased to 40m/min it can be seen in Figure 5-18 that the outputs have higher amplitude of fluctuation. The lateral motion is able to be controlled within 39µm of lateral motion. Conversely, the output does not indicate to have an overshoot when the line speed is 40m/min. Finally, the output result of 60m/min line speed is shown in Figure 5-19 to have the most fluctuation in comparison to the other two. Hence, the results show that the lateral motion control is inversely proportional to the line speed. The lateral motion is controlled within 50µm, which is very close to the input error. Hence, the limit of lateral motion control in this system is when the line speed is approaching 60m/min. However, this does not indicate that the guide cannot be used with 60m/min. This is because the output is still able to reduce the lateral motion when the input error is changed to a step input.

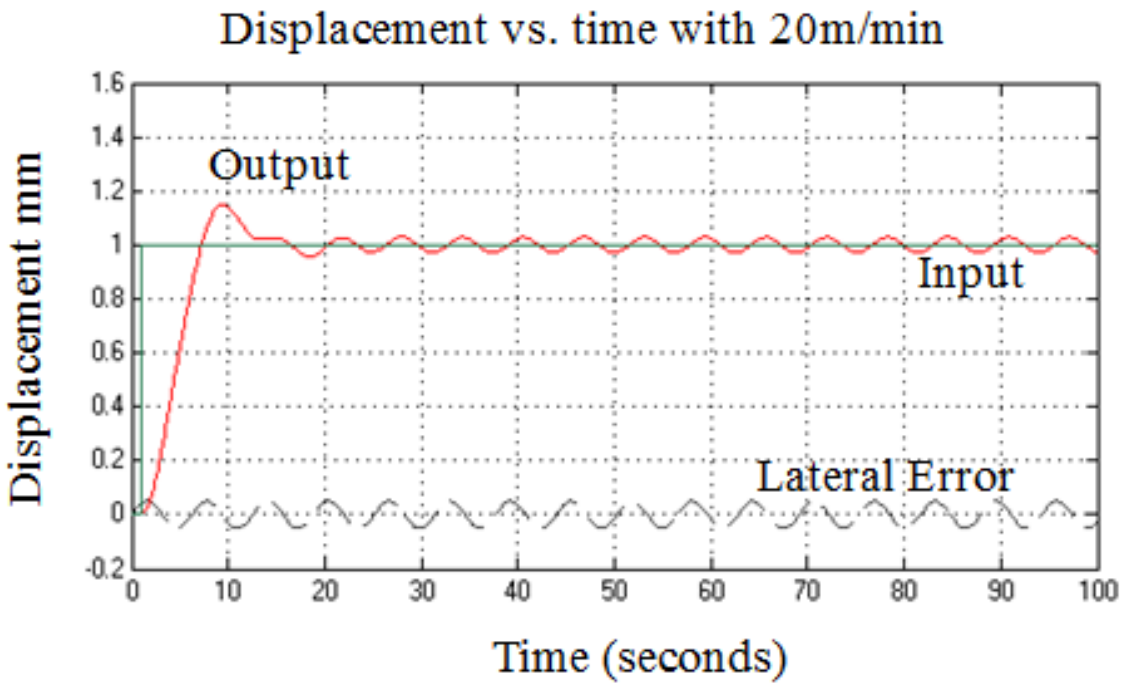

Figure 5-17: Simulated Output with 20m/min

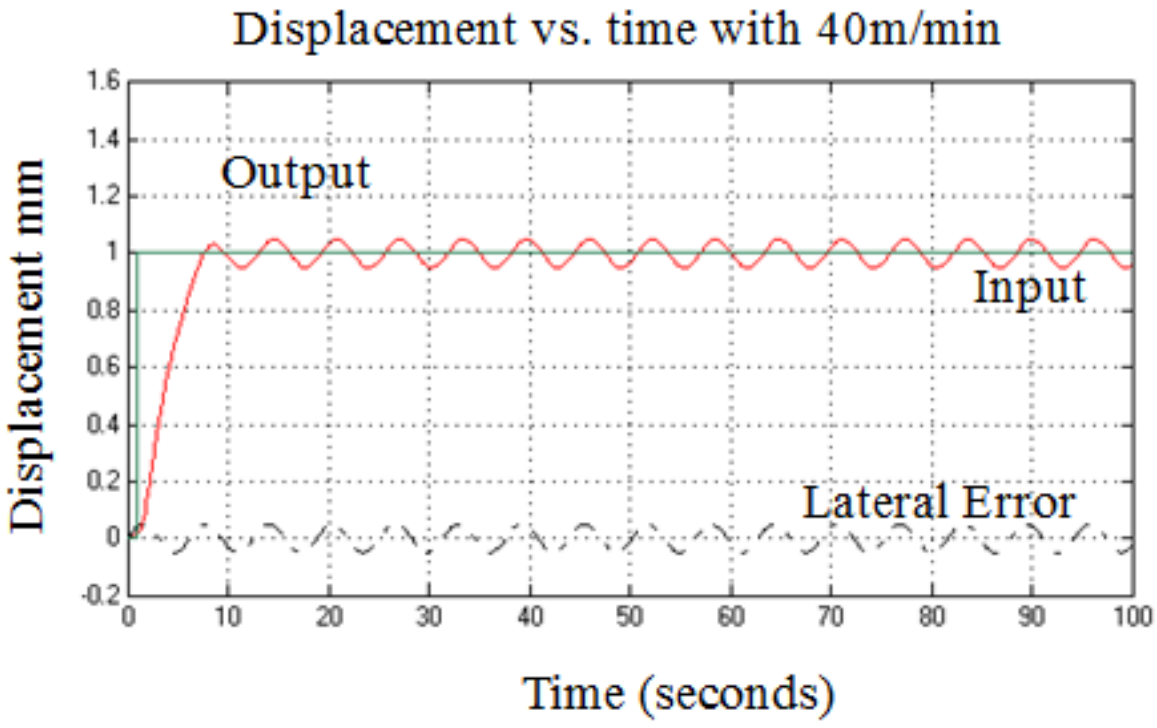

Figure 5-18: Simulated Output with 40m/min

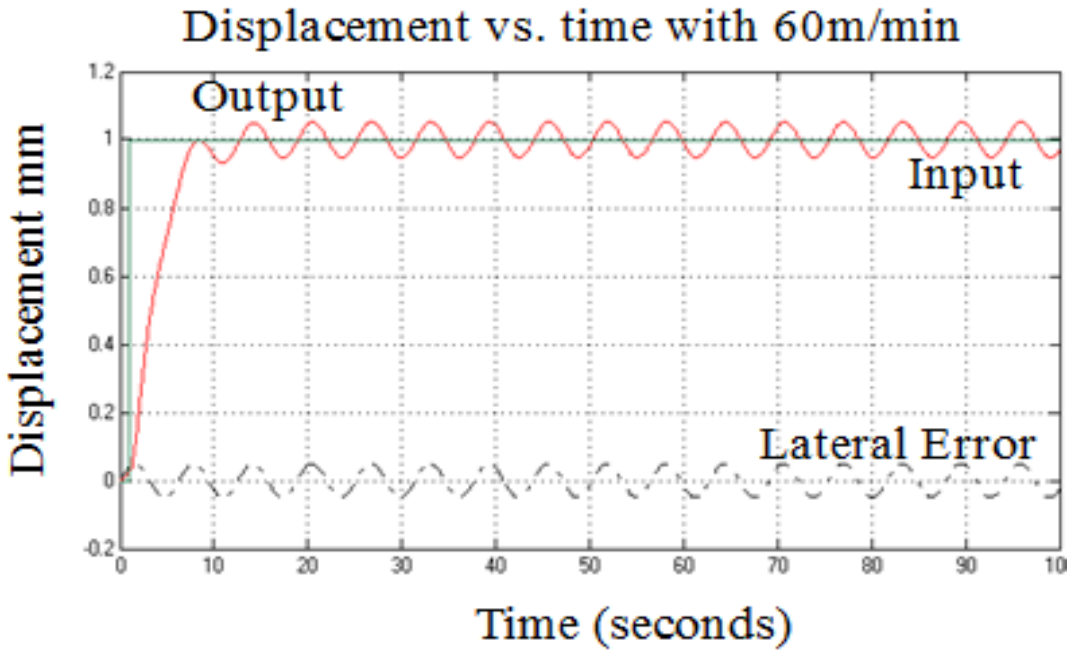

Figure 5-19: Simulated Output with 60m/min

5.6. Result and Implementation

In this section, the actual testing of the system is analyzed with running conditions, such as, 20m/min, 40m/min and 60m/min. The Edged sensor is used to record any lateral response. The system is firstly arranged to be running without the guide system in order to record any lateral response of the system. This will demonstrate any lateral response at the normal running condition (without web guide) of the system at the particular speed (20, 40, and 60m/min). It is then compared with the result which is running with the guide system. In addition, an Impulse lateral error is also generated in the beginning of each test in order to see any improvement of the lateral response. Each of the results is plotted in the following subsections. The Edge sensor ADC reading is plotted against the sampled data points. It is a 10 bits ADC reading with each increment equals to 0.011mm. The result is sampled at 10ms which can demonstrate lateral response without too much sensitivity.

5.6.1. Speed with 20m/min

The web is set to be running at 20m/min in this section. The output of the sensor reading can be illustrated in Figure 5-20. This is plotted against the centerline position (511 shown in red), which is the middle value of the ADC. In this figure, the system is running without the guide system. The measured reading output is shown to have a continuous sinusoidal response between 400 to 800 ADC values.

As shown in Figure 5-21, the system is running with the guide system. As seen in the figure, an impulse of disturbance is applied in the beginning of the plot at the direction of maximum ADC value. The output is shown have reduced the disturbance significantly and follow the centerline position. Moreover, two disturbances are applied in Figure 5-22. Disturbances are applied from two difference direction; from ADC 1023 and ADC 0 at data points 30 and 140 respectively. As a result, the output is also shown to have reduced the lateral error significantly. The after settling time outputs of each two figures are shown to have reduced the fluctuation significantly compared to Figure 5-20.

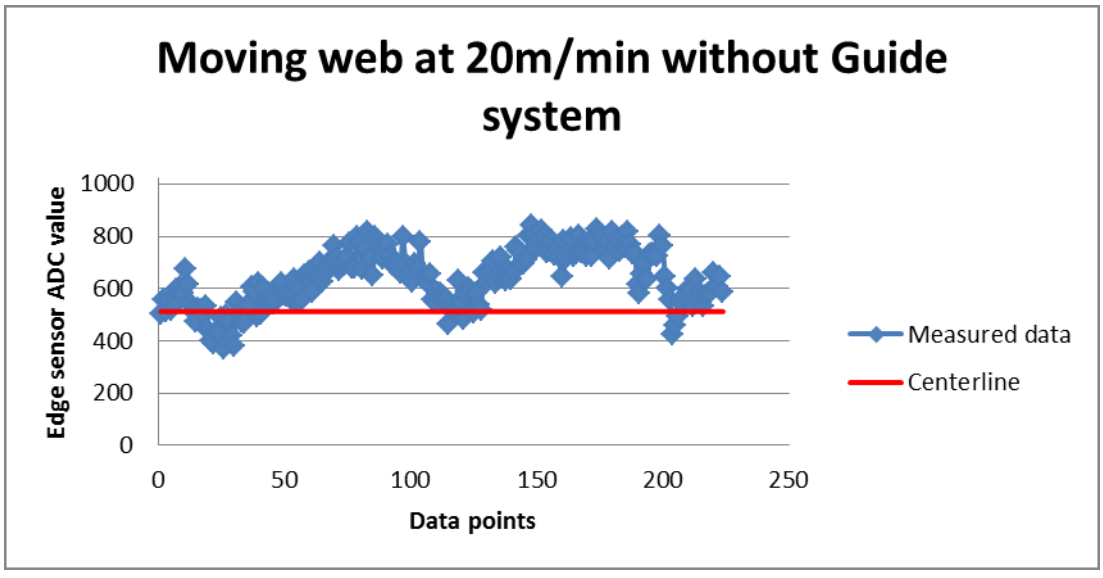

Figure 5-20: Sensor reading with web at 20m/min without guide system

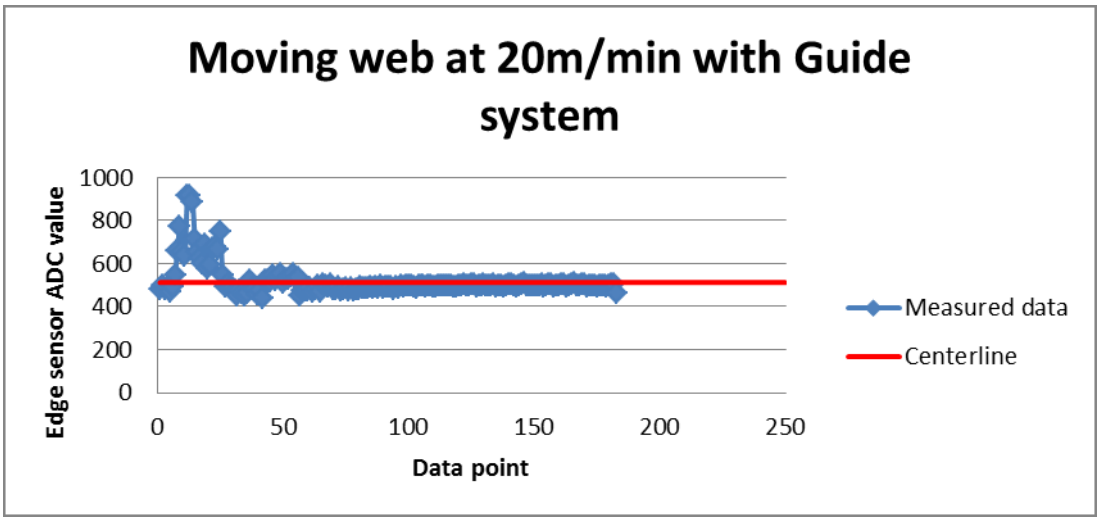

Figure 5-21: Sensor reading at 20m/min showing disturbance input at the start

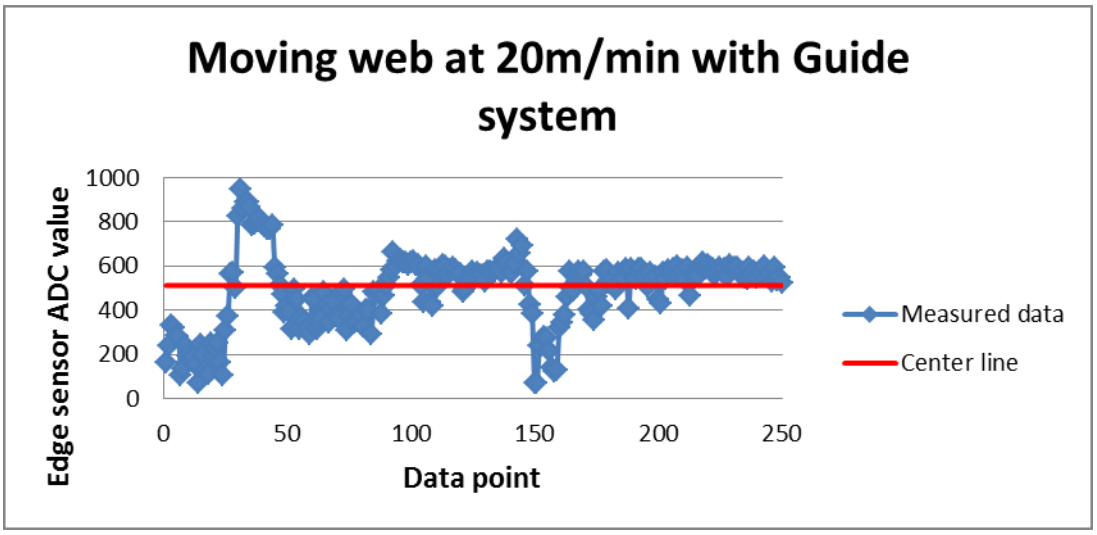

Figure 5-22: Sensor reading at 20m/min showing two disturbances

5.6.2. Speed with 40m/min

The sensor output of the running web without guide system is shown in Figure 5-23. Again, the measured data is plotted against the centerline position as shown. The output is also shown to have a continuous sinusoidal oscillation around the centerline position. However, the output is shown to have larger amplitude compared to the web running at 20m/min.

An impulse is input to the system at the beginning as shown in Figure 5-24. The impulse is input to have the direction at 1023 ADC value. The system is recovered

after 50 data points. After the impulse, the system is shown to have much smaller lateral fluctuation as compared to Figure 5-23. It is fluctuated between 400 and 600 ADC values. On the other hand, an impulse of opposite direction (0 ADC value) is applied to the system as shown in Figure 5-25. The response is shown to be similar to Figure 5-24. After the system is settled after the disturbance, the lateral error is also shown to have reduced as compared to Figure 5-23.

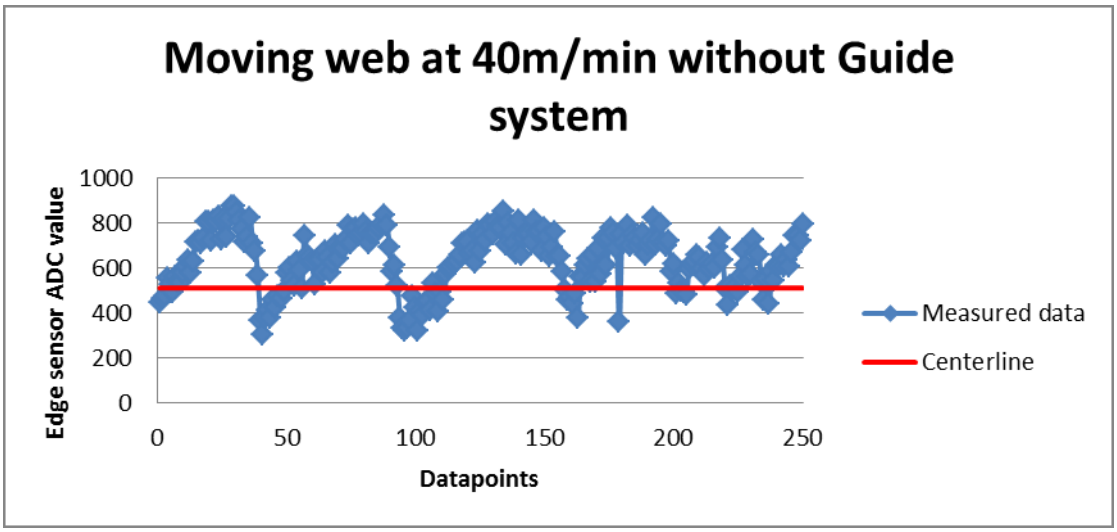

Figure 5-23: Sensor reading with web at 40m/min without guide system

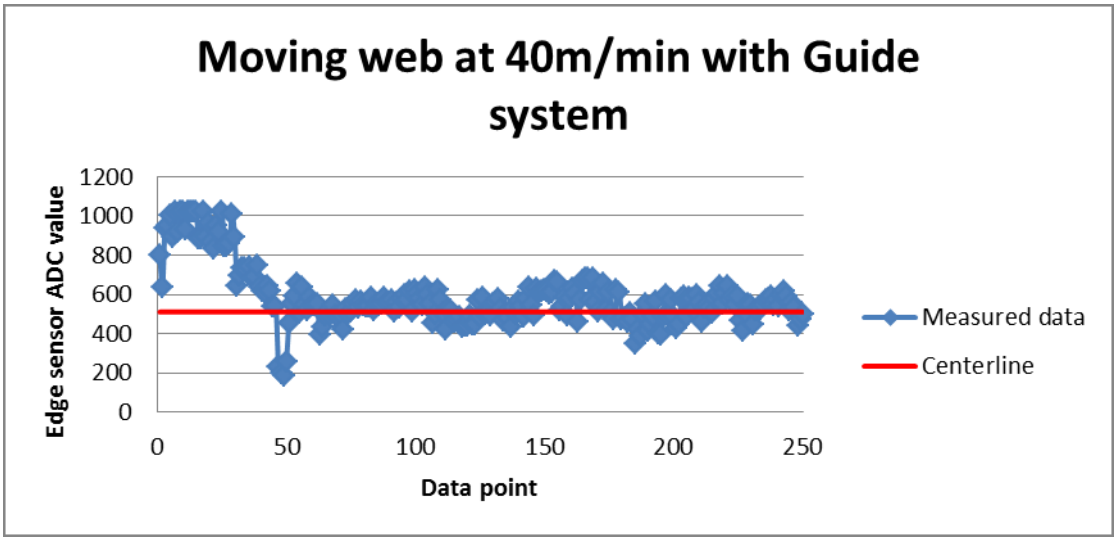

Figure 5-24: Sensor reading at 40m/min showing disturbance input at the start

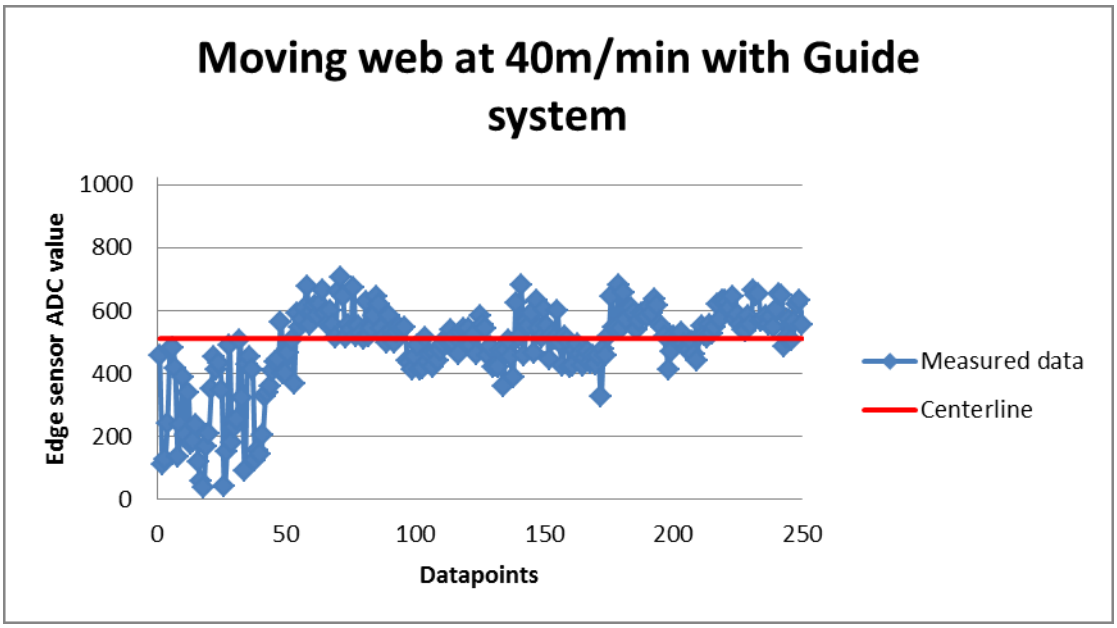

Figure 5-25: Sensor reading at 40m/min showing disturbance input at the start

5.6.3. Speed with 60m/min

The lateral position measurement without guide is shown in Figure 5-26. The response is shown to have the largest continuous sinusoidal oscillation as compared to the previous two speed (20 and 40m/min). As shown in Figure 5-27, the system is shown to have reduced the lateral error when an impulse is applied to the system. However, the system is shown to have a larger oscillation compared to 20 and 40m/min after the response for the impulse is settled. On the other hand, an impulse with the opposite direction is input to the system as shown in Figure 5-28. The response is shown to have a few oscillations after the impulse is input to the system.

The system is still shown to be able to recover from the impulses from the two different directions. Both systems are shown to have similar result after the impulse is input to the system. The result is shown to have recovered the impulse and also reduce the lateral error when the system is running without the guide system (Figure 5-26).

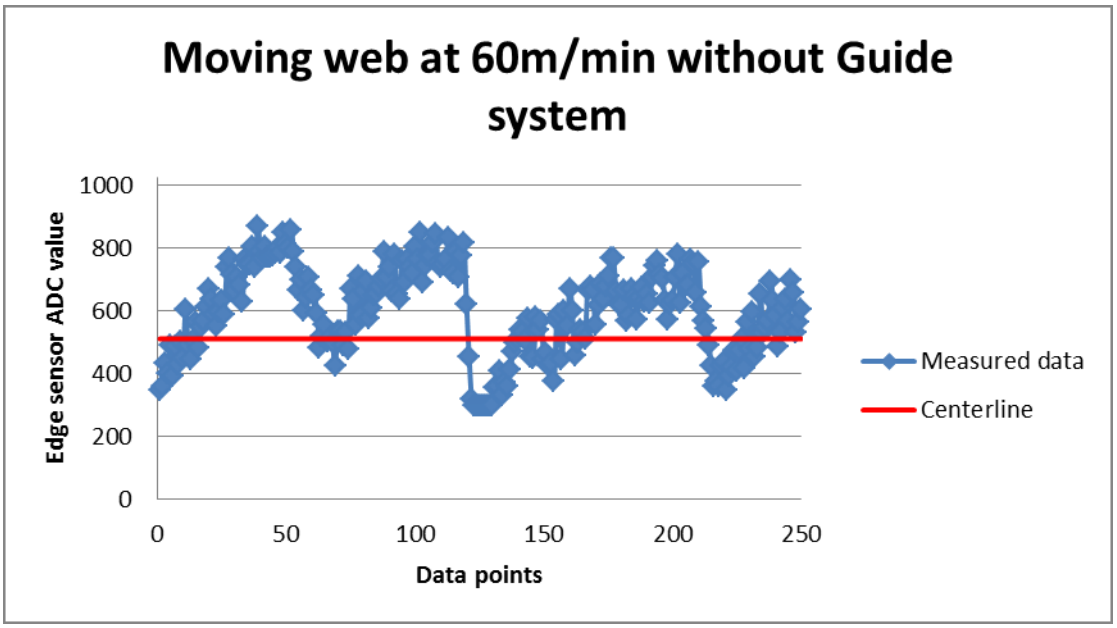

Figure 5-26: Sensor reading with web at 60m/min without guide system

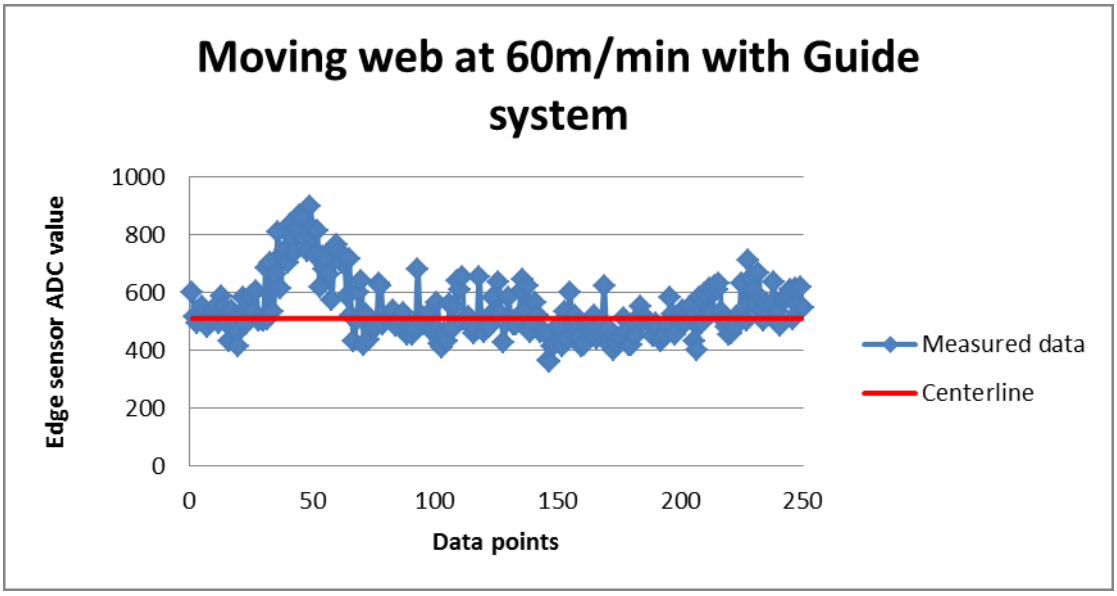

Figure 5-27: Sensor reading at 60m/min showing disturbance input at the start

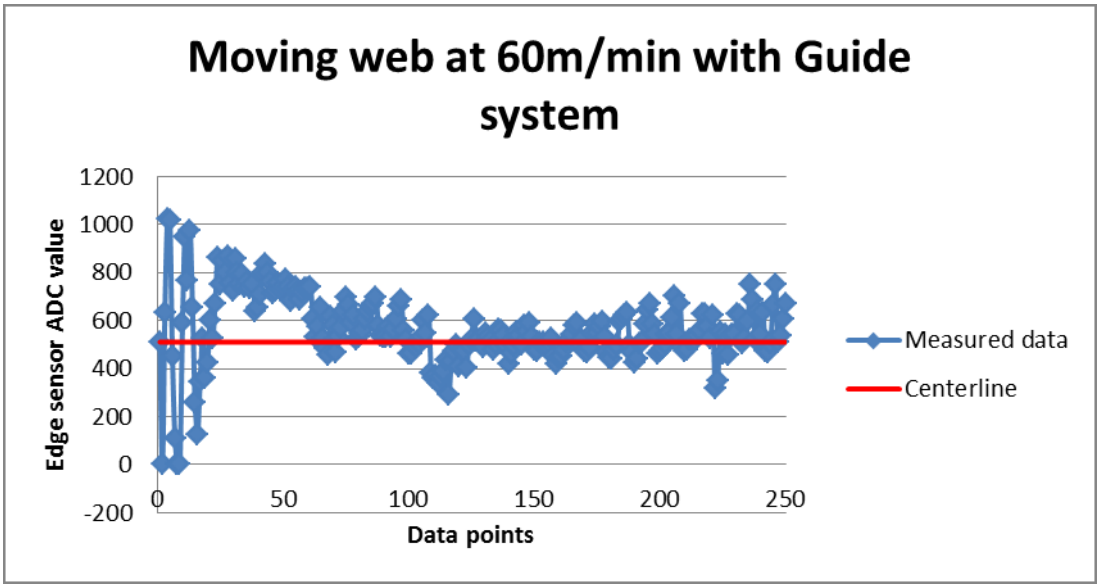

Figure 5-28: Sensor reading at 60m/min showing disturbance input at the start

5.6.4. Overall result

Finally, the overall performance of the guide system is tabulated in the Table 5-4 using Root mean squared deviation (RMSD). The results are taken from the figures above and shown in ADC values, but the actual position reading (mm) is shown in the bracket. The differences between the centerline and the sensor reading values are able to be measured using RMSD. In addition, the effect with and without the guide system is also able to be realised. When the system is running at 20m/min, the RMSD value is shown to be 166.57 (1.66mm). However, when the system is running with guide, the lateral error RMSD is reduced down to 19.3 (190um). When the system speed is set at 40m/min, the RMSD value is 177.26(1.77mm). The RMSD value is shown to reduce to 69.59(700um) when the guide system is applied. Similarly, the RMSD value is 194.33(1.94mm) when the system is running at 60m/min without guide system. This is able to reduce down to 126.33(1.26mm) with the guide system.

As a result, it can be clearly seen that when the speed is increased, the RMSD value is also increased whether it is with or without guide. Conversely, the RMSD

value is clearly reduced when a guide system is applied in the system. Hence the lateral response is reduced when the guide system is applied to the system.

Table 5-4: Root mean squared deviation (RMSD) of the result.

	Without Guide	With guide
20m/min	166.57(1.66mm)	19.30 (190 um)
40m/min	177.26(1.77mm)	69.59 (700um)
60m/min	194.33(1.94mm)	126.33(1.26mm)

Chapter 6. Overall conclusion

Lateral motion control for Roll-to-Roll systems is an important task, as it affects the performance of printed products. In this project, a Roll-to-Roll testing system is designed and manufactured. The testing system consists of 4 main units, such as, unwinder unit, load cell unit, guide system unit and rewinder unit. These system units are controlled by two microcontroller (Arduino Atmega 328P and 2560) with additional signal conditioning circuits which interface different sensors and actuators with the controller. The guide system is investigated analytically and experimentally with supporting theory. The limitation of the system is discussed and also potential future work which can be carried out for this project.

6.1. System design and development

The entire system is designed and developed from the beginning. A series of processes have been followed in order to achieve such mechatronics system. These processes include the design methodology, web coil specifications, Roll-to-Roll system design, Manufacturing and System Integration. The initial design consideration has been identified to initiate system design. In addition, the system is designed based on the ability to handle the web coil specification. Each of the unit design such as, unwinder unit, load cell unit, guide unit and rewind unit have carefully analysed. The 3D design is put into practice and manufactured into real system. Finally, the complete system integration was demonstrated. The result is demonstrated in the photos which taken in order to illustrate the complete system design and development.

6.2. Sensors/actuators

Instrumentation

Load cell, edge sensor and brake are one of the most commonly used sensors and actuators in a Roll-to-Roll system. The load cell is used to measure the tension of the web, edge sensor is used to measure the lateral movement of the web and brake is for tension generation in the system. Each of the sensors and actuator has different operating condition and output signal. However, common microcontroller has fixed input/output operating range from 0V to 5V. Sensor instrumentation for microcontroller based R2R system are presented, discussed and evaluated in this paper. From the circuit realization and experimental measurements, it was shown that output signal of load cell is conditioned from 20mV/V to 0 to 5V whereas output signal of edge sensor is successfully conditioned from -11 - 11V to 0 - 5V. The brake is able to be controlled using 0 to 5V for an operating voltage of 24V.

The load cell sensor is shown to have linear output behavior. The torque generated by the brake is shown to have a linear region. Straight line is fitted in the linear region to calibrate linear relationship of the inputs to outputs of the actuator. The edge sensor also has a linear displacement region between -2mm and 2mm. Linearization of the edge sensor non-linear outputs is through Taylor Series expansion from -6mm to -2mm and also from 2mm to 6mm. The output of the linearized result is shown to have different gradient relationship, depending on input displacement values

6.3. Guide system

The center pivoted displacement guide is examined in this section through simulations and experimental measurements. The guide system is controlled by a PID servo system to provide accurate control, and is parametrically examined at transport speed of 20m/min, 40m/min and 60m/min, respectively. In the experimental study, the RMSD value is able to be reduced down to 190um when the speed is 20m/min. When the speed is increased to 40m/min, the result is able to be controlled to have RMSD value of 700um. When the speed is increased to 60m/min, the RMSD value is shown to be 1.26mm.

Both of the simulated and experimental results are shown have reduced the lateral response significantly. The experimental is shown to have a larger value than the simulated value. There are many other factors, which the simulation was not taken into account. Hence there are some differences between the simulated value and the actual experimental result. As a result, with the proposed method, it is demonstrated the lateral motion can be reduced significantly.

6.4. Future work

This project has demonstrated a working Roll-to-Roll testing system with web guides system. However, there are many different components of the system and potential of the future projects which may be able to carry out. These are listed in the following:

- Change servo motor to increase accuracy

  The DC servo motor used in this project has demonstrated reasonable performance to the system. However, if the performance is required to be increased, it is recommended to change the motor to a commercial industrial

scaled servo motor where the actual servo drive is provided with preloaded precision software.

- Improve mechanical design to increase positioning accuracy of guide system

  The mechanical part of the system can be improved such as restricting the position of the guide rotation (such as the blue string added). Without this, the positioning can only be achieved through encoder control. This will require more tasks on the electrical control system.

- Investigate the relationship between tension affect and lateral motion

  In this project, the tension is set to be constant. However, further study on the relationship between tension effects with the lateral response can be a future topic. Therefore a parametric study with speed, tension can be both related to the lateral response of the system.

- Different control algorithm on the guide system.

  PID control algorithm is developed in this project. However, different control algorithms such as, Fuzzy logic control and neural network control can be applied to see the different responses of each algorithm. Comparison can be carried out to see the performances of the algorithm.

References

[1] T. Ho, H. Shin and S. Lee, "Development of a Lateral Control Simulation Software for Roll-to-Roll Systems," in The International Federation of Automatic Control, Seoul, 2008.

[2] M. Tree, “Web offset inks,” [Online]. Available: http://www.virajinkschem.com/web-offset-inks.asp. [Accessed 10 12 2012].

[3] H. Shin, T. Ho and S. Lee, "Steering guide-based lateral control for roll-to-roll printed electronics," *Journal of Mechanical Science and Technology,* vol. 24, no. 10.1007/s12206-009-1150-5, p. 319~322, 2010.

[4] S. Chin, "Report: Flex display market to grow 83.5% a year," 23 03 2006. [Online]. Available: http://www.eetimes.com/electronics-products/other/4082955/Report-Flex-display-market-to-grow-83-5-a-year. [Accessed 12 10 2012].

[5] C. Ober, "Schwartz R2R Processing," 11 05 2006. [Online]. Available: http://people.ccmr.cornell.edu/~cober/mse542/page2/files/Schwartz%20R2R%20Processing.pdf. [Accessed 12 10 2012].

[6] J. Marcus, "UCLA researchers demonstrate fully printed carbon nanotube transistor circuits for displays," UCLA, 30 11 2011. [Online]. Available: http://newsroom.ucla.edu/portal/ucla/fully-printed-carbon-nanotube-219814.aspx. [Accessed 11 12 2012].

[7] C. Lee, H. Kang, C. Kim and K. Shin, "A Novel Method to Guarantee the Specified," *JOURNAL OF MICROELECTROMECHANICAL SYSTEMS,* vol. 19, no. 5, p. 1243, 2010.

[8] H. Koc, D. Knittel, M. d. Mathelin and G. Abba, *IEEE TRANSACTIONS ON CONTROL SYSTEMS TECHNOLOGY,* vol. 10, no. 1063-6536, p. 197, 2002.

[9] P. Ganapati, "HP's Unbreakable Flexible Display," 21 1 2009. [Online]. Available: http://thefutureofthings.com/news/6245/hps-unbreakable-flexible-display.html. [Accessed 11 10 2012].

[10] V. Lau, "Technologies for licensing," 2008. [Online]. Available: http://www6.cityu.edu.hk/kto/AvailableTech.aspx?id=257. [Accessed 12 06 2012].

[11] M. Ponjanda-Madappa, "ROLL TO ROLL MANUFACTURING OF FLEXIBLE," 2006.

[Online]. Available: http://dc.library.okstate.edu/utils/getfile/collection/theses/id/4104/filename/4105.pdf. [Accessed 12 6 2012].

[12] "Flexographic Printing," Prism Pak, Inc., [Online]. Available: http://www.prismpak.com/Printing-Options-s/103.htm. [Accessed 12 12 2012].

[13] K. Hopcus and J. Plumb, "Guide selectrion," [Online]. Available: maxcessu.com/files/Fife_Guide_Selection.pdf. [Accessed 12 04 2012].

[14] A. Stagnaro, "Design and Development of a Roll-to-Roll Machine for Continuous High-Speed Microcontact Printing," Massachusetts Institue of technology, 2008.

[15] “DB2 Motor 3,” [Online]. Available: http://www.technology.heartland.edu/faculty/chrism/automation%20and%20control/VFD/DB2%20Motor%203.pdf. [Accessed 13 04 2012].

[16] S. S. Jape, B. Ganapathysubramanian and J. A. Wickert, "Exploring the Effect of Stick-Slip Friction Transition Across Tape-Roller," *IEEE TRANSACTIONS ON MAGNETICS,* vol. 48, no. 3, p. 1189, 2012.

[17] N. Rothwell, "Double R Controls' Concept Of Continuous Process Web Handling Principles," Double R Group, 09 08 2000. [Online]. Available: http://www.drc.co.uk/DRC/TECH-DOCS/Docs/WebHandling.pdf. [Accessed 12 6 2012].

[18] D. Roisum, "Web 101.00, Web Handling and Converting," [Online]. Available: www.seminarsforengineers.com. [Accessed 12 04 2012].

[19] D. Morozov, "Optimizing Tension Control in Center-Driven Winders," [Online]. Available: www.usa.siemens.com/converting. [Accessed 8 7 2012].

[20] D. Whiteside, "Basic of Web Tension Control Summary," in *PLACE Conference*, St Louis, 2007.

[21] S. W. Attaway, "The Mechanics of Friction in Rope Rescue," 1999. [Online]. Available: www.jrre.org/att_frict.pdf. [Accessed 12 05 2012].

[22] J. J. Shelton, "Lateral dynamics of a moving web," ph.D dissertation, Oklahoma State University, Stillwater, 1968.

[23] J. J. Shelton and K. N. Reid, "Lateral dynamics of an ideal moving web," *ASME Journal of Dynamics System Measurment Control,* vol. G, no. 3, pp. 187-192, 1971.

[24] H. Shin, T. Ho and S. Lee, "Steering guide-based lateral control for roll-to-roll printed electronics," *Journal of Mechanical Science and Technology,* vol. 24, no. 10.1007s12206-09-1150-5, p. 319~322, 2010.

[25] S. C. Mukhopadhyay, *Instrumentation, Electronics And Control Engineering,*

Palmerston North: College of Science, School of Engineering and Advanced Technology, 2010.

[26] N. Mohan, T. M. Undeland and W. P. Robbins, Power Electronics, New Jersey: John Wiley, 2003.

[27] "Symbio, Inc.," Symbio, Inc., [Online]. Available: http://www.symbioinc.com.tw/index.php. [Accessed 10 04 2012].

[28] "Hysteresis Clutch and Brake," Chain Tail Co., Ltd, 2012. [Online]. Available: http://www.chaintail.com/hysteresis-clutch-brake.htm. [Accessed 10 05 2012].

[29] "Low Capacity Single Point Aluminum Load Cells," 18 07 2012. [Online]. Available: http://www.vishaypg.com/docs/12009/1040-1041.pdf. [Accessed 10 08 2012].

[30] "Dover Flexo Electronics, Inc," [Online]. Available: http://www.dfe.com. [Accessed 10 4 2012].

[31] "Maxway," [Online]. Available: http://www.motor-net.com/self_pages/products.html. [Accessed 10 05 2012].

[32] "ROTARY ENCODER (Incremental) (hollow shaft) > HTR-HB," [Online]. Available: http://www.hontko.com.tw/sayaproduct.php?CateID=120&LineID=46. [Accessed 10 08 2012].

[33] A. d. Silva and K. Craig, "optical encoder and arduino 2012," 2012. [Online]. Available: http://multimechatronics.com/images/uploads/design/2012/Optical%20Encoder%20and%20the%20Arduino%202012.pdf. [Accessed 10 8 2012].

[34] "Singuno Technology," Singuno, [Online]. Available: http://www.singuno.com.tw/c_1.html. [Accessed 10 02 2012].

[35] "Arduino Mega 2560," [Online]. Available: http://arduino.cc/en/Main/ArduinoBoardMega2560. [Accessed 10 11 2012].

[36] "Arduino Uno," Arduino, [Online]. Available: http://arduino.cc/en/Main/ArduinoBoardUno. [Accessed 27 05 2012].

[37] "Torque motor," Oriental Motors, 2011. [Online]. Available: http://www.orientalmotor.com.tw/products/ac/torque_tm_f/. [Accessed 10 08 2012].

[38] H. SENSOR, "HS302 Encoder Module," 2009. [Online]. Available: http://global.honestsensor.com/pdf/HS302_en.pdf. [Accessed 10 01 2013].

[39] J. Nilsson, Electric Circuits Forth Edition, Addison-Wesley 54987, 1993.

[40] N. S. Nise, Control Systems Engineergin, New York: John Wiley & Sons, Inc, 2000.

[41] "Model 1040/1041- Low Capacity Single-Point Aluminum Load Cells," 18 07 2012. [Online]. Available: http://www.vishaypg.com/docs/12009/1040-1041.pdf. [Accessed 11 10 2012].

[42] "Wide Bandwith Quad JFET Input Operational Amplifiers," National Semiconductor Corporation, 1999.

[43] "Square Trimpot® Trimming Potentiometer," Boums, 2010.

[44] Gavnilovska, L.;, Application and Multidisciplinary Aspects of Wireless 13 Sensor Networks, Computer Communications and Networks, London: Springer, 2011.

[45] "Torque Motor and Power Controller Package TM Series," ORIENTAL MOTOR CO., LTD, Taipei, 2008.

[46] T. Dean, "Sensors and Sensing," 11 02 2002. [Online]. Available: http://cs.brown.edu/~tld/courses/cs148/02/sensors.html. [Accessed 05 01 2013].

Appendices

1.1. : Mechanical design

Unwinder Unit

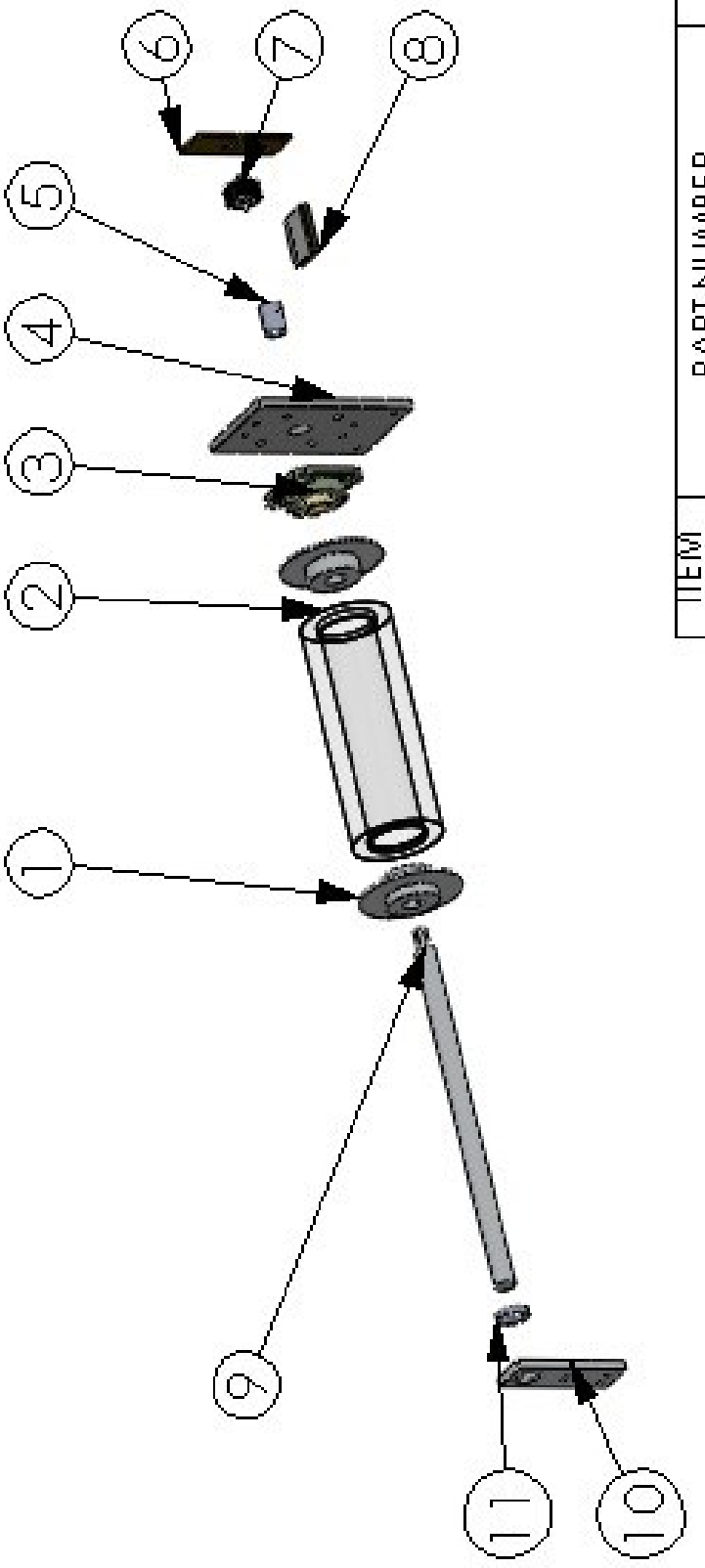

ITEM NO.	PART NUMBER	QTY.
1	coilguide	2
2	coil	1
3	housing1	1
4	unwinder_back plate	1
5	brake bushing	1
6	brake back plate_1	1
7	Brake2	1
8	brake back plate_2	1
9	shaft	1
10	supporter	1
11	bearing_support	1

Load cell Unit

ITEM NO.	PART NUMBER	QTY.
1	Assem12	1
2	load cell coupling_1	2
3	loadcell	2
4	loadcell plate	2
5	loadcell platform_right	1
6	loadcell platform_LEFT	1
7	load cell coupling_2	2

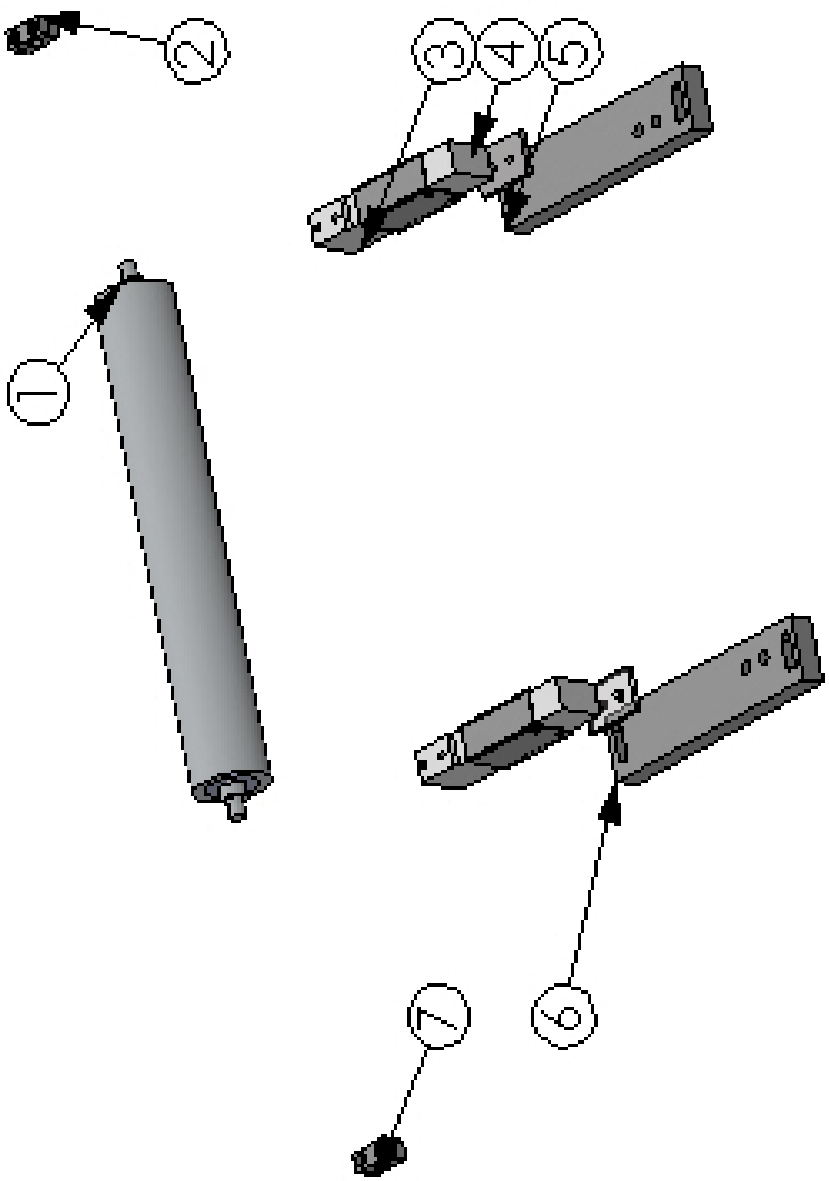

Guide Unit

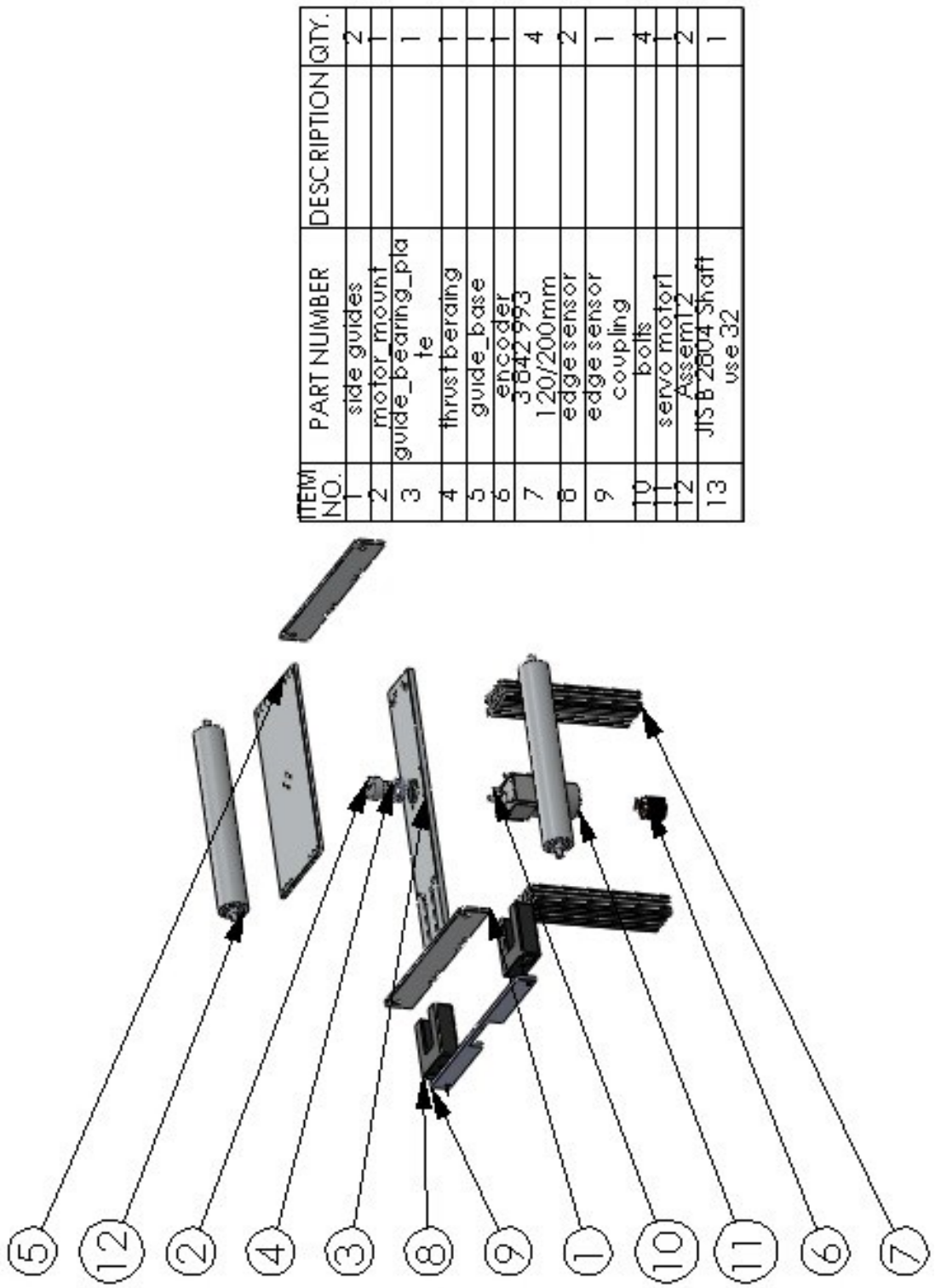
ITEM NO.
PART NUMBER
DESCRIPTION
QTY.
1 side guides 2
2 motor_mount 1
3 guide_bearing_plate 1
4 thrust beraing 1
5 guide_base 1
6 encoder 1
7 3842993 120/200mm 4
8 edgesensor 2
9 edgesensor coupling 1
10 bolts 4
11 servo motor1 1
12 Assem12 2
13 JIS B 2804 Shaft use 32
5
12
2
4
3
8
9
1
10
11
6
7

Rewinder Unit

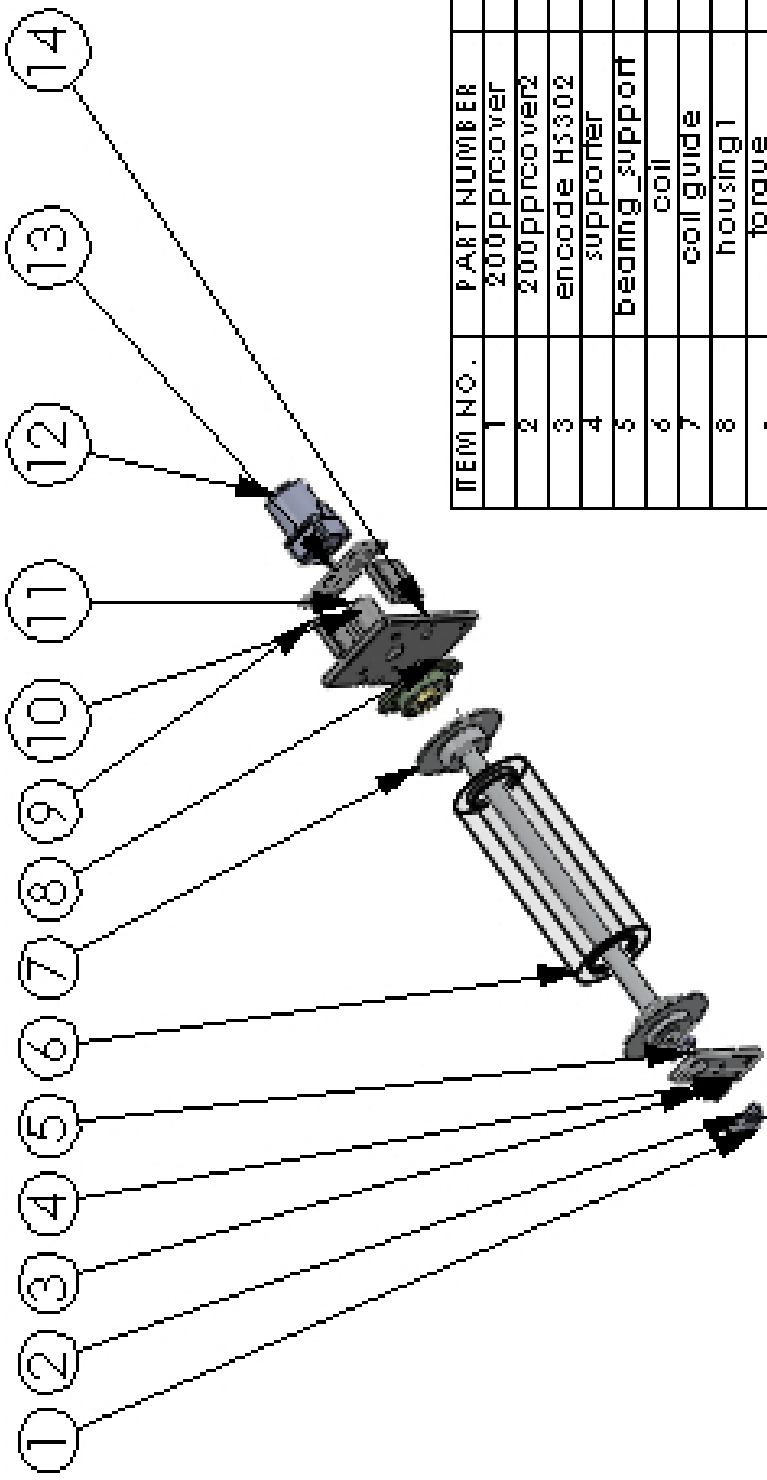

ITEM NO.	PART NUMBER	QTY.
1	200pprcover	1
2	200pprcover2	1
3	encode H3302	1
4	supporter	1
5	beamg_support	1
6	coil	1
7	coil guide	2
8	housing1	1
9	torque motor_plate_EDM	2
10	key	1
11	motor_coupling	1
12	TM3064A+3GN33	1
13	motorplate	1
14	rewinder_backplate	1
15	shaft_rewinder	1

1.2. : Components Data sheet

Unwinder unit:

- **Hysteresis Brake**

CHB Series

Hysteresis Brake

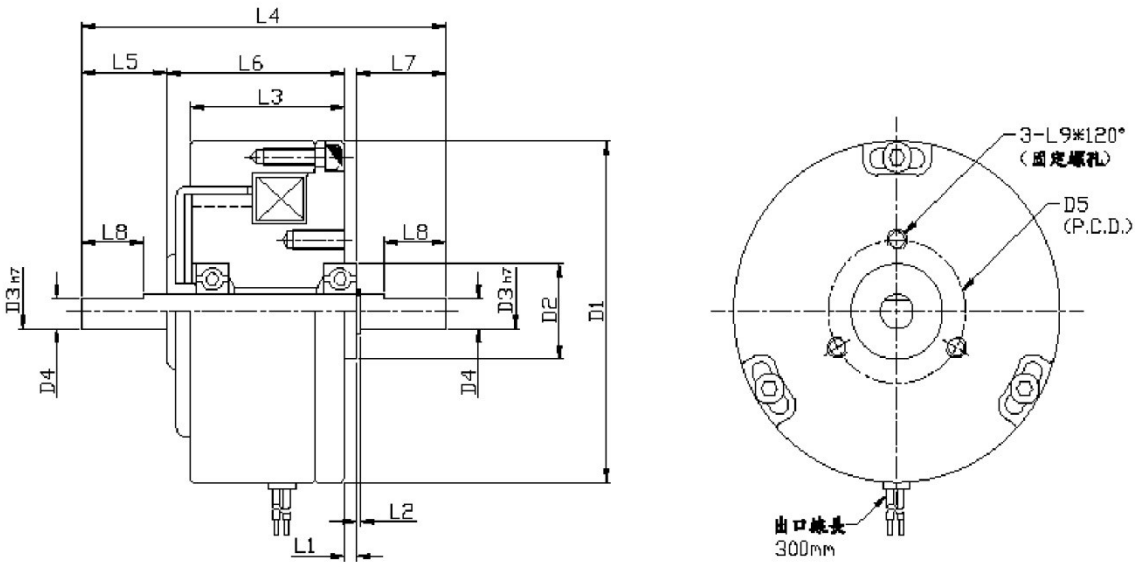

Model	Rated torque (Nm)	Capacity			Inertia J(kg*cm^2)	Permited speed (rpm)	Weight (kg)
		Voltage (VDC)	Power (W)	Current (A)			
CHB0S2AA	0.02	24	3.3	0.14	$4.3*10^{-3}$	3000	0.1
CHB0S7AA	0.07		3.2	0.13	$4.4*10^{-2}$		0.23
CHB1S4AA	0.14		4.8	0.2	$4.55*10^{-2}$		0.33
CHB3S5AA	0.35		6	0.25	$1.7*10^{-1}$		0.8
CHB010AA	1		6	0.25	1.1		1.85

Model	Dimension (mm)													
	D1	D2	D3	D4	D5	L1	L2	L3	L4	L5	L6	L7	L8	L9
CHB0S2AA	31.8	10	3	-	19	2	0.25	18.7	42.2	8	23.6	8.6	-	M2.5*4L
CHB0S7AA	45.7	14	5	4.3	19	2.4	0.6	20.7	52.6	12.3	25.5	12.4	9.5	M2.5*5L
CHB1S4AA	50	14	5	4.3	21	1.8	0.6	23.6	55.8	13	27.3	13.7	9.5	M3*6L
CHB3S5AA	60	17	7	6.3	25	2	0.9	39.7	76.6	15.3	43	16.3	10	M4*10L
CHB010AA	92	22	10	9	38	2.5	1	39.1	100	25	51.4	21.1	16	M4*10L

- **Encoder**

HS-302 SERIES

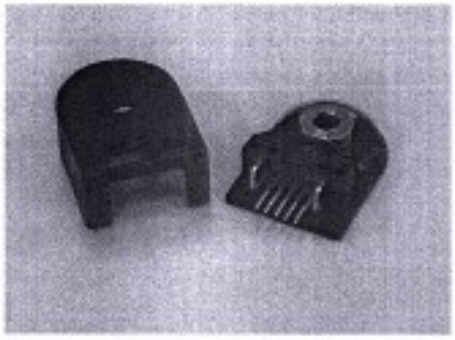

▶ Feature

- Two Channel Quadrature Output
- Easy Mounting
- Low Cost
- Campact Size
- Ttl Compatible
- Single 5v Dc Supply
- With Agilent Heds-97xxmodules

▶ Resolutions 解析度 P/R

100, 200, 256, 360, 400
500, 512

▶ Order Form 型號

HS-302- □□□ (P/R) - 6 (Hollow dia)

▶ Electrical Characteristics 電器特性

Power Source 使用電源	DC 5V± 10%
Current Consumption 消耗電流	40 mA or below
Response Frequency 響應頻率	100K Hz
Output Current 輸出電流	5 mA per Channel

▶ Environmental 環境條件

Environmental 保存溫度	-40℃ to 60℃
Operating Temperature 操作溫度	塑膠碼盤是-40℃ to 60℃ 金屬碼盤是-40℃ to 100℃
Vibration 振動	20g,5 to 1KHz

▶ Connection 接線方式

PIN1	PIN2	PIN3	PIN4	PIN5
GND	EMPTY	CHA	Vcc	CHB
Black	Yellow	White	Red	Green

▶ Outline

Unit:mm HS-302

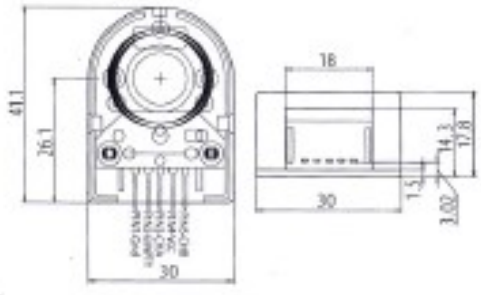

▶ Mounting Considerations

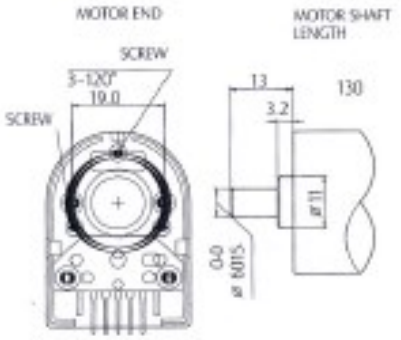

Load cell Unit:

- **Load cell**

Model 1040/1041

Tedea-Huntleigh

VISHAY PRECISION GROUP

Low Capacity Single Point Aluminum Load Cells

OIML NTEP ATEX FM

FEATURES

- Capacities 5-100kg
- Aluminum construction
- Single point 400 x 400mm platform
- OIML R60 and NTEP approved
- IP65 protection
- Available with metric and UNC threads

OPTIONAL FEATURES

- EEx ia IIC T4 - hazardous area approval
- FM approval available
- IP67available

DESCRIPTION

Models 1040 and 1041 are low profile single point load cells designed for direct mounting of low cost weighing platforms.

Their small physical size, combined with high accuracy and low cost, makes these load cells ideally suited for retail, bench and counting scales.

Available in anodized aluminum these high accuracy load cells are approved to NTEP and other stringent approval standards, including OIML R60. For hazardous environments this load cell has EEx ia IIC T4 level of approved option.An optional special humidity resistant protective coating assures long term stability over the entire compensated temperature range.

The two additional sense wires feed back the voltage reaching the load cell. Complete compensation of changes in lead resistance due to temperature change and/or cable extension, is achieved by feeding this voltage into the appropriate electronics.

APPLICATIONS

- Bench scales
- Counting scales
- Grocery scales

OUTLINE DIMENSIONS in millimeters

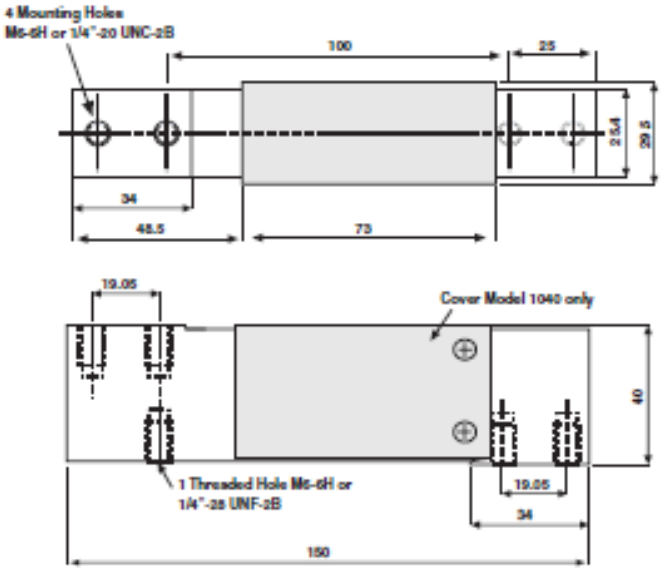

Guide Unit

- **Motor**

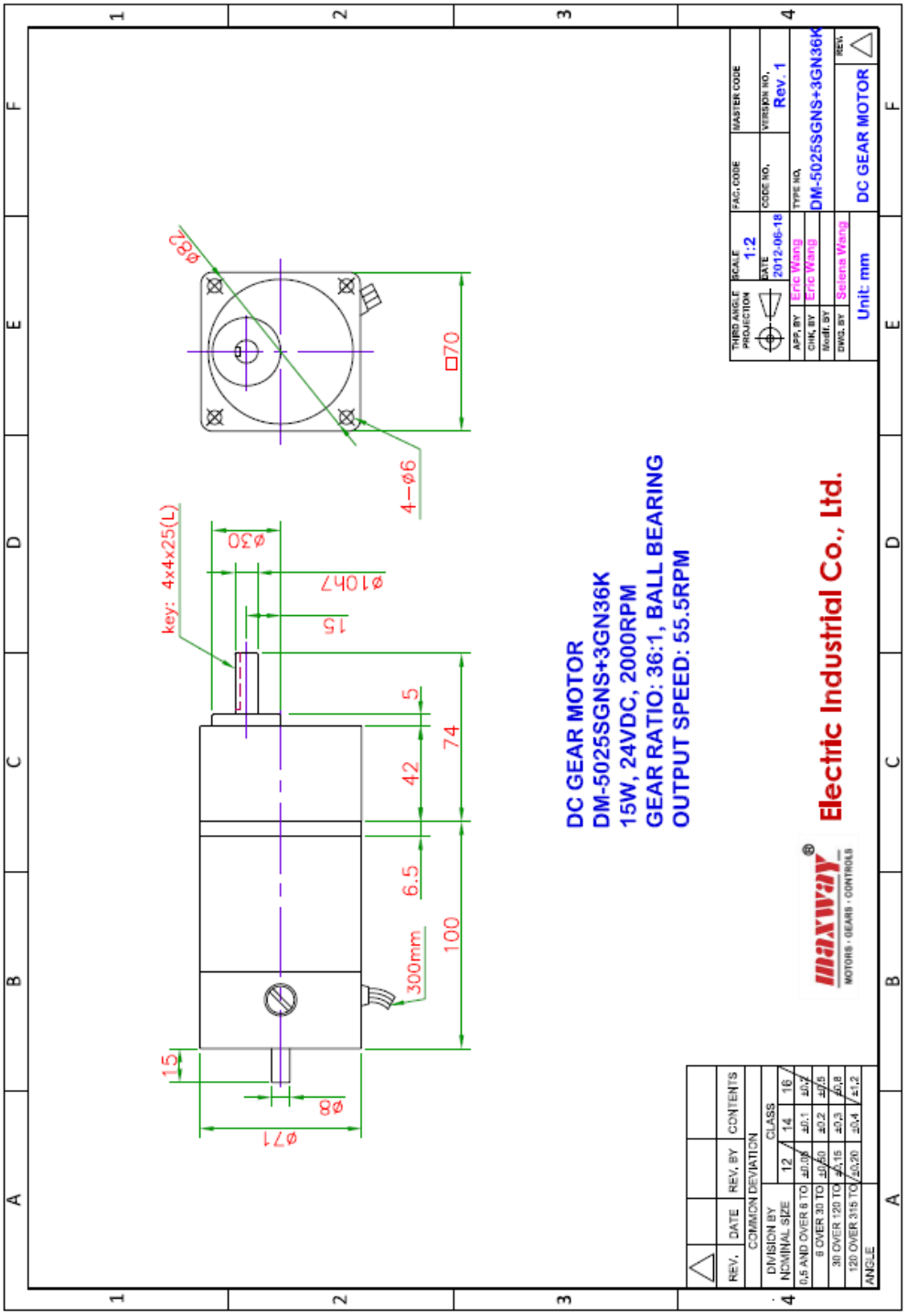

- Encoder

HONTKO

HTR-HB

HOLLOW TYPE ROTARY ENCODER

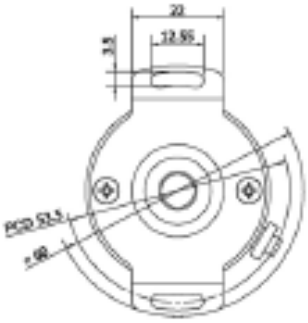

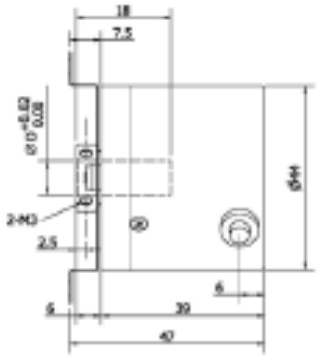

ELECTRICAL SPEC.

Detection System	Incremental 增量型
Output Wave 輸出波形	Square Wave 方波
Standard Number of Pulse Per Revolution 解析	2, 5, 12, 10, 20, 30, 40, 50, 60, 80, 100, 120, 150, 160, 180, 200, 250, 300, 360, 400, 500, 600, 720, 800, 900, 1000, 1024, 1200, 1250, 1500, 1800, 2000, 2048, 2500
Output Phase 輸出相	AB phase or ABZ phase
Electronics 電路特性	NPN Voltage, NPN Open Collector, Push Pull or Line Driver
Power Supply 供應電源	DC 8~26V, DC 5V fixed
Current Consumption 消耗電流	≤ 60 mA
Output Capacity 輸出容量	Sync. Current: 20 mA, Residual Voltage: 0.5V or less
Max. Response 最大應應頻率	10K Hz ~ 100K Hz
Phase Different 相位差	A, B phase different 90°±45° (T/4±T/8), Z phase T±T/2
Wave Form Rise / Fall 波形上下時間	2 µs or less
Polarity 極性保護	Against Reverse Protection (not with DC 5V)

MECHANICAL SPEC.

Hollow Shaft Diameter 孔徑	5, 6, 6.35, 8, 9.525, 10 mm
Shaft Loading 軸荷重	(10 ~ 400 PPR) Axial 軸向: 1 Kg, Radial 徑向: 2 Kg (over 400 PPR) Axial 軸向: 0.5 Kg, Radial 徑向: 1 Kg
Starting Torque (at 25°C) 起動轉矩	30 gf-cm or less
Max. Speed 最大機械容許速度	6,000 rpm
Vibration 震動	10g (10±1,500 Hz)
Shock 衝擊	20g per 11 ms
Cable 電線	Ø4.5, 50 cm long
Weight 重量	≤ 200g

ENVIRONMENTAL SPEC.

Operating Temp. / Humidity 操作溫度/濕度	0°C ~ 60°C, RH 35% ~ 90% (No Condensation)
Storage Temp. 儲存溫度	-20°C ~ 80°C
Protection 保護等級	IP50: Dust Proof

ORDERING INFORMATION

HTR-HB -

Hole Size 中空軸徑	Pulse per Revolution 解析	Output Phase 輸出相	Electronics 電路特性	Supply Voltage 供應電源
5: 5 mm 6: 6 mm 6.35: 6.35 mm 8: 8 mm 9.525: 9.525 mm 10: 10 mm	2, 5, 12, 10, 20, 30, 40, 50, 60, 80, 100, 120, 150, 160, 180, 200, 250, 300, 360, 400, 500, 600, 720, 800, 900, 1000, 1024, 1200, 1250, 1500, 1800, 2000, 2048, 2500 P/R	2: AB phase 3: ABZ phase 4: AB+Z high phase	Blank: NPN Voltage C: NPN Open-Collector PP: Push-Pull *L: Line Driver 5Vdc *HL: Line Driver 8~26Vdc	Blank: 8~26Vdc 5V: 5Vdc fixed

HONTKO CO., LTD. ● TEL: +886 2 2226-3867 ● FAX: +886 2 2226-2011 ● E-mail: sales@hontko.com.tw

- **Edge Sensor**

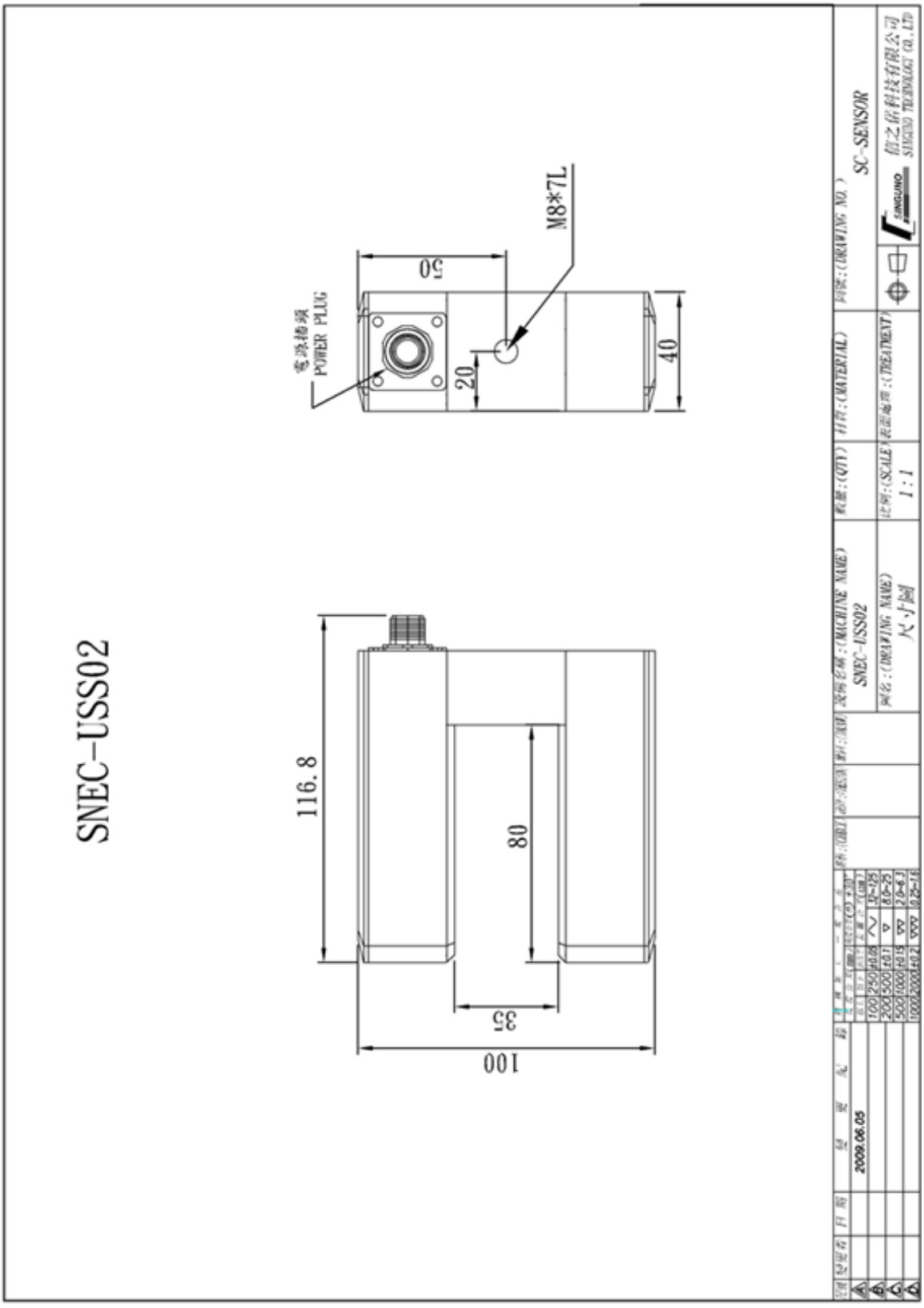
SNEC-USS02
M8*7L
50
20
40
电源插频
POWER PLUG
116.8
80
35
100
SC-SENSOR
SNEC-USS02
2009.06.05

Rewinder Unit:

- **Torque motor**

Torque Motors

●Additional Information●
Technical reference → Page G-1
Safety standards → Page H-2

Torque motors are designed to provide high starting torque and sloping characteristics (torque is highest at zero speed and decreases steadily with increasing speed), and operate over a wide speed range. They also provide stable operation, especially in the low speed range or under a locked rotor condition.

cULus CCC CE RoHS

※For detailed product safety standard information including standards, file number and certification body, please visit www.orientalmotor.com.

Features

●The Speed Can Vary Widely, Depending on the Sloping Characteristics

Torque motors have a high starting torque and sloping characteristics, allowing easy speed control simply by changing the voltage supplied to the motor. (The motor torque varies in proportion to the square of the voltage.)

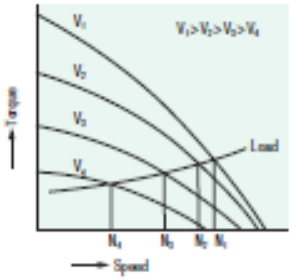

◇Voltage Control of Torque Motors

The method most commonly used to control voltage is by phase control using a triac. As shown in Fig. 1, by changing the phase angle "alpha" at which the triac switches, the input voltage is controlled as represented by the shaded areas of the graph.

※When adjusting the speed or the torque, an external voltage adjuster is necessary.

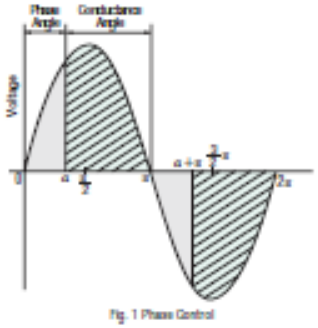

Fig. 1 Phase Control

●Suitable for Winding Applications

In an application where an object is released continuously at a constant speed and wound up with constant tension, the torque must be doubled and the speed must be halved if the diameter of the winding spool is doubled.

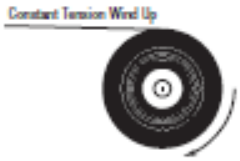

●Locked Rotor Operation is Available

Unlike induction motors or reversible motors, torque motors are designed to provide a stable torque even under locked rotor conditions or at very low speed (nearly locked rotor condition). They are suitable for pushing applications that require static torque, or for loads that are under locked rotor conditions at the end of processes.

Motors of 115 VAC input can operate continuously at 60 VAC. When used at voltages above 60 VAC, these motors have shorter time ratings. They have a 5 minutes rating at 115 VAC.

Note

●When using a motor in a locked rotor operation, the output torque becomes very large. The output torque of the gearhead must be lower than the maximum permissible torque. Also, ensure that the load does not hit an object and stop, since this can cause damage to the gearhead due to the shock.

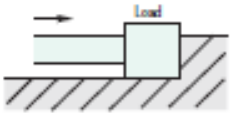

●Use as a Brake

By using the motor in the braking region of the speed – torque characteristics, it can serve as a brake. Constant tension control can be achieved by applying a DC voltage.

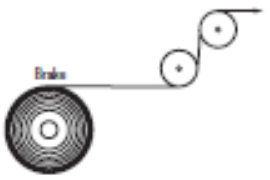

2.1 Electronics component

Arduino Uno Microcontroller

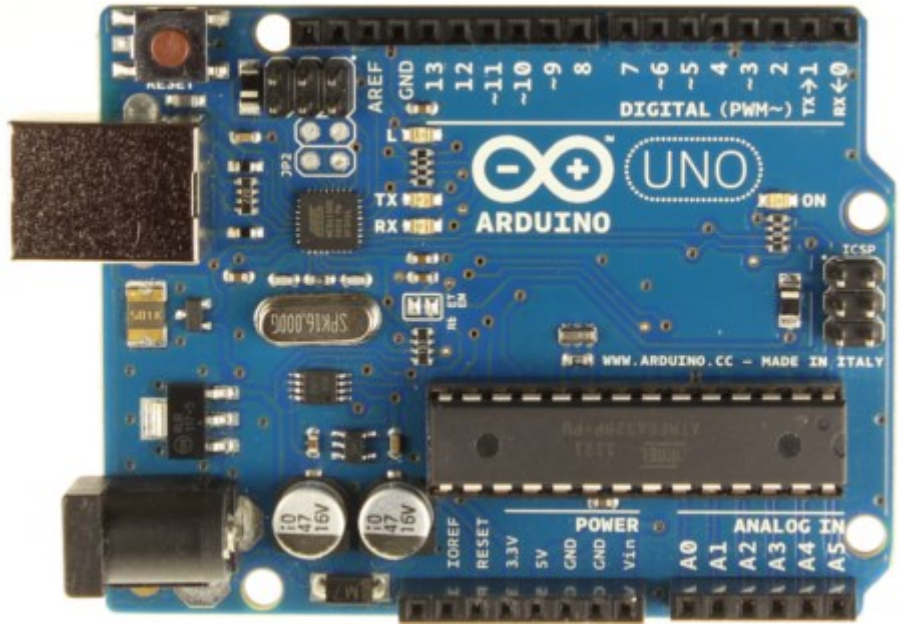

Microcontroller	ATmega328
Operating Voltage	5V
Input Voltage (recommended)	7-12V
Input Voltage (limits)	6-20V
Digital I/O Pins	14 (of which 6 provide PWM output)
Analog Input Pins	6
DC Current per I/O Pin	40 mA
DC Current for 3.3V Pin	50 mA
Flash Memory	32 KB (ATmega328) of which 0.5 KB used by bootloader
SRAM	2 KB (ATmega328)
EEPROM	1 KB (ATmega328)
Clock Speed	16 MHz

Arduino Mega 2560 Microcontroller

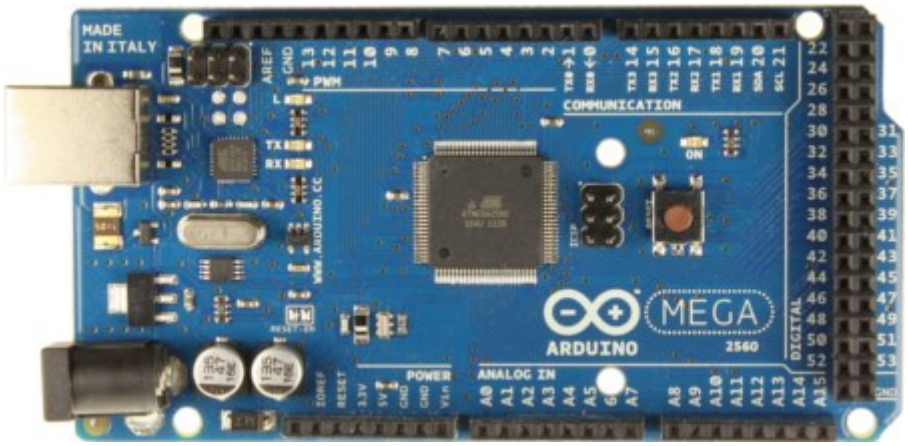

Microcontroller	ATmega2560
Operating Voltage	5V
Input Voltage (recommended)	7-12V
Input Voltage (limits)	6-20V
Digital I/O Pins	54 (of which 15 provide PWM output)
Analog Input Pins	16
DC Current per I/O Pin	40 mA
DC Current for 3.3V Pin	50 mA
Flash Memory	256 KB of which 8 KB used by bootloader
SRAM	8 KB
EEPROM	4 KB
Clock Speed	16 MHz

Signal conditioning circuit and acuator1

Schematics

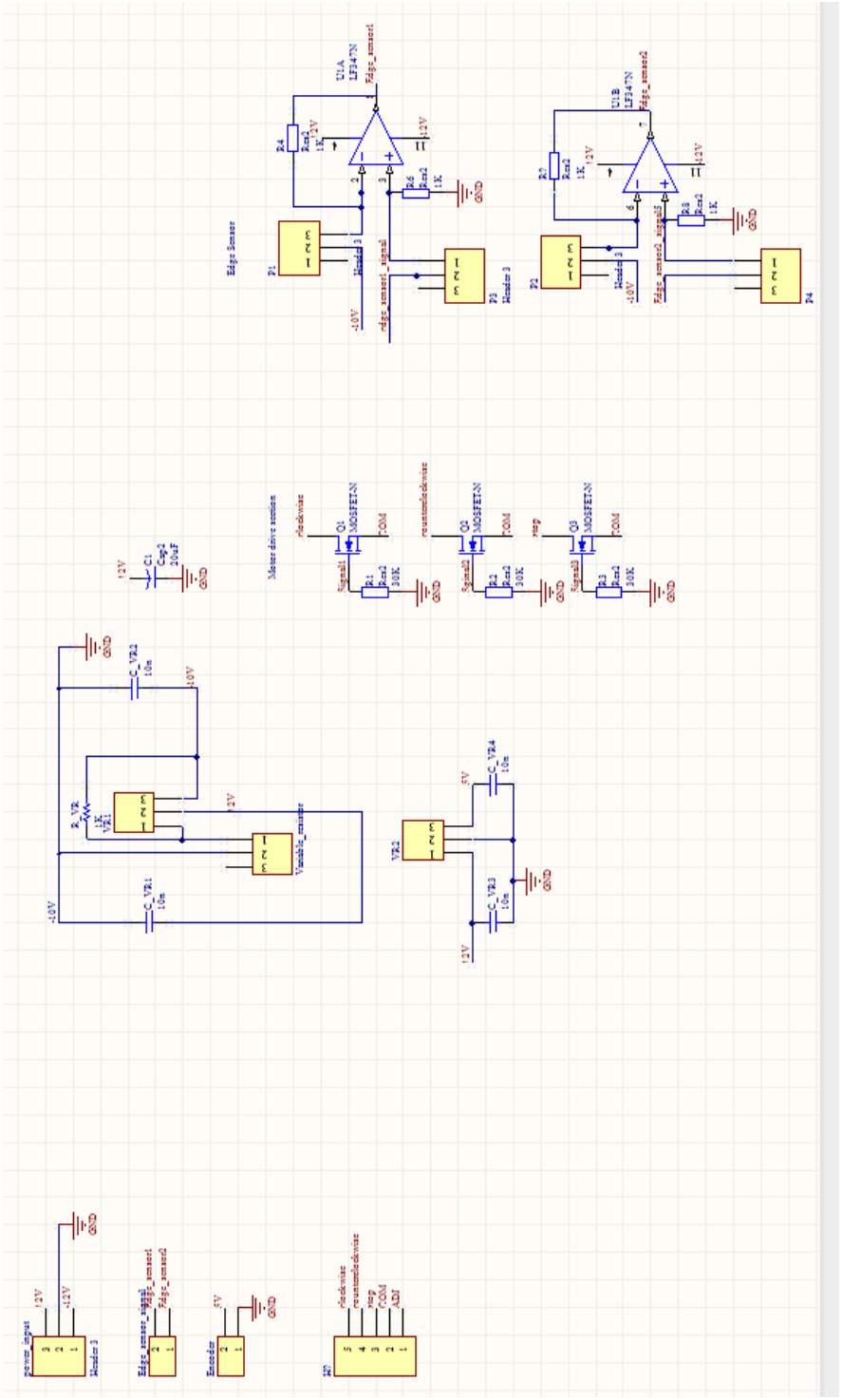

Signal conditioning circuit and acuator1 PCB

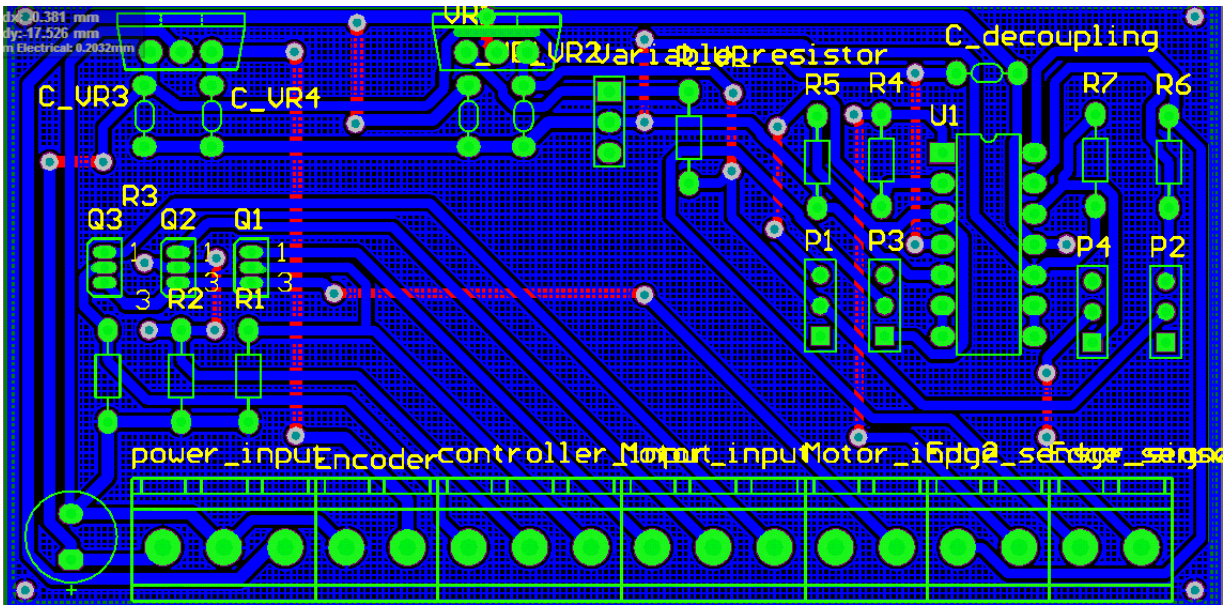

Signal conditioning circuit and acuator2

Schematics

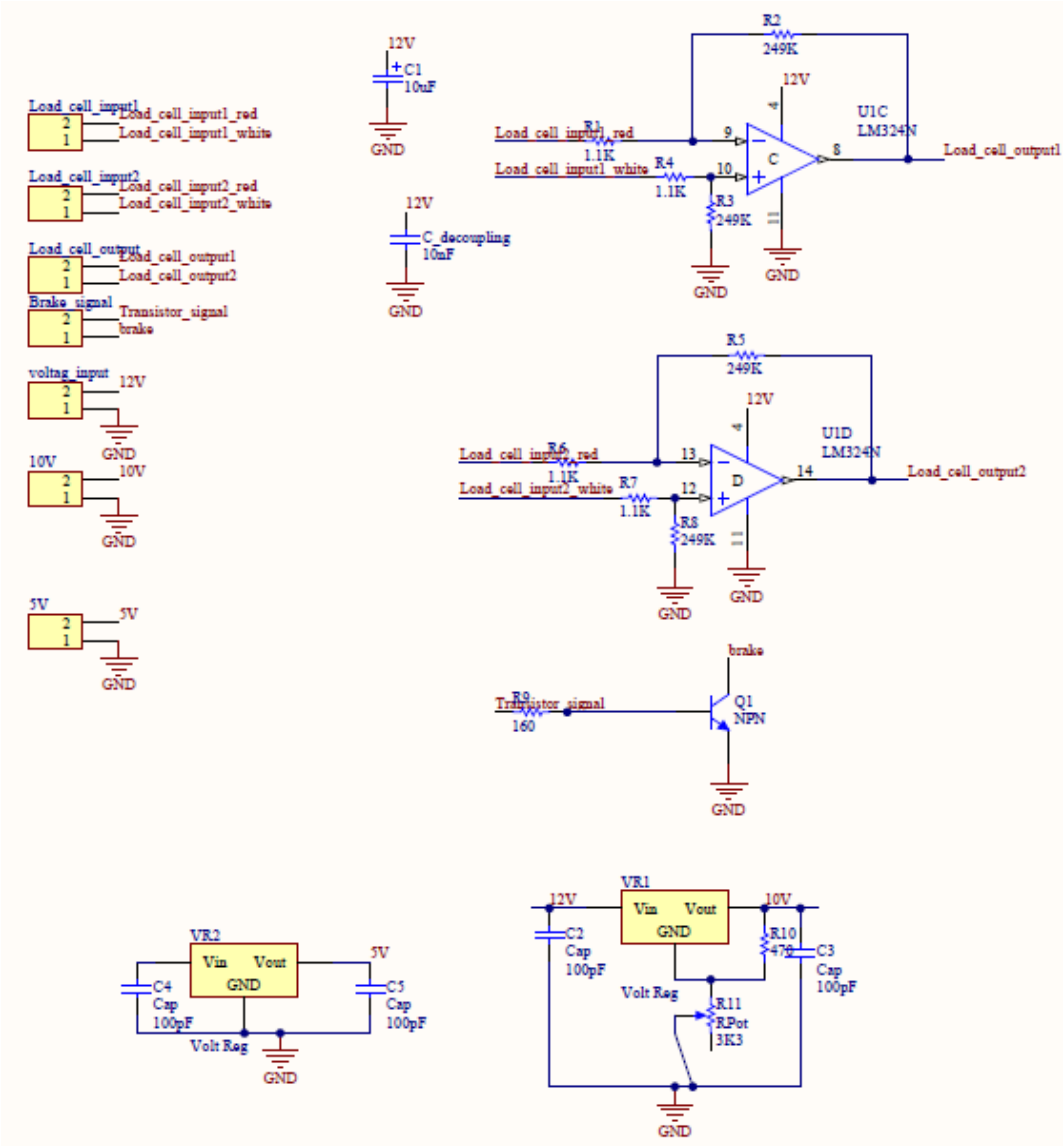

Signal conditioning circuit and acuator2 PCB

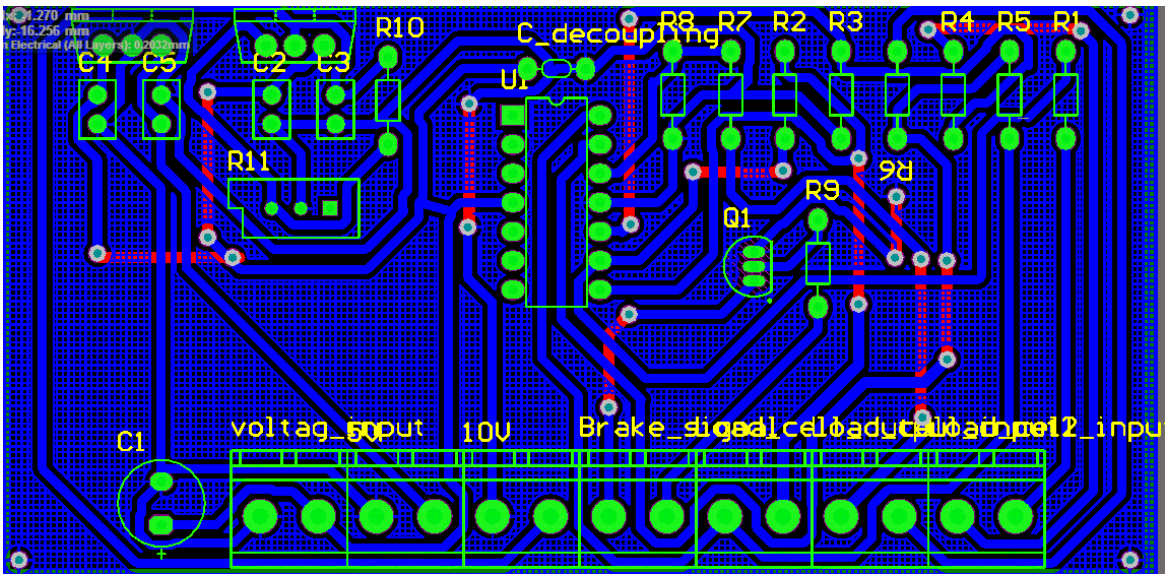

2.2 Simulink

Block Diagram